UNITED STATES DEPARTMENT OF THE INTERIOR

GEOLOGICAL SURVEY

POTENTIAL FOR GENERATION OF NATURAL GAS IN SEDIMENTS OF THE CONVERGENT MARGIN OF THE ALEUTIAN TRENCH AREA

Keith A. Kvenvolden[1]

Roland von Huene[1]

Open-File Report 84-404

The report is preliminary and has not been reviewed for conformity with U.S. Geological Survey editorial standards.

[1] Menlo Park, CA

Table of Contents

Page

List of Tables, Appendices and Plates.....2
List of Figures.....3
Abstract.....4
Introduction.....4
Seismic Surveys.....5
Interpretations of Seismic Records.....6
Geochemical Analyses and Results.....9
Estimate of Geothermal Gradient.....11
Assessment of Potential for Gas Accumulations.....12
Summary.....15
Acknowledgements.....15
References.....16
Tables.....19
Figures.....20
Appendices.....35
Plates.....(Fold out)

List of Tables

Table 1. Summary of Geochemical Results by Sample Sites.....19
Table 2. Results of Analyses of Kerogen.....19
Table 3. Geothermal Gradients in °C/km Determined from Base of Gas Hydrate Reflector (BSR on Marine Seismic Records...19

List of Appendices

Appendix 1. Lithologic Logs of DSDP Cores Showing samples for this report.....35
Appendix 2. Vitrinite Reflectance of Nine Selected Samples.....50

List of Plates

Plate 1. Seismic Line 111 from Grid A showing Progressive Enhancement of Information from Stacked Record to a Migrated Time Record to a Depth Section.
Plate 2. Listing of Geochemical Results.

List of Figures

Figure 1. Plate tectonic map of the Circum-Pacific region showing major plate boundaries including the Aleutian Thrust, the site of the Aleutian Trench subduction zone.....20

Figure 2. Map showing locations of grids A and B of seismic lines and single seismic lines C and D. Seismic lines within grids A and B are indicated at expanded scale.....21

Figure 3. Representative time sections for seismic grid A (Fig. 2)...22

Figure 4. Depth Section of Seismic line 111 from grid A (Fig. 2).....23

Figure 5. Representative time and depth sections for seismic grid B (Fig. 2).....24

Figure 6. Seismic lines C (line 13) and D (Fig. 2).....25

Figure 7. Pyrograms from TEA/FID analyses of 40 samples analyzed in this report.....26

Figure 8a. Profiles with depth of organic geochemical results at site 178.....27

b. Profiles with depth of organic geochemical results at site 180.....28

c. Profiles with depth of organic geochemical results at site 181.....29

d. Profiles with depth of organic geochemical results at site 183.....30

e. Profiles with depth of organic geochemical results at site 192.....31

Figure 9. van Krevelen diagram showing HI (mg HC/g OC) and OI (mg CO_2/g OC) for nine selected samples.....32

Figure 10. Examples of BSR on seismic record 51 from grid B (Fig. 2)..33

Figure 11. Isotherms at temperatures of 50°, 150°, and 250°C based on a constant horizontal and vertical geothermal gradient of 30°C/km and superimposed on seismic line 111 (Fig. 4).....34

Potential for Generation of Natural Gas in Sediments of the Convergent Margin of the Aleutian Trench Area

ABSTRACT

Sediment being subducted in the eastern part of the convergent margin of the Aleutian Trench has a potential to generate large volumes of natural gas, perhaps as much as 2.8 x 10^6 m^3 of methane per km^3 of sediment, even though the content of organic carbon in the sediment is very low, averaging about 0.4%. This high potential for gas generation results primarily from the enormous volume of sediment undergoing subduction. Along the eastern Aleutian Arc-Trench system a 3-km thick sheet of sediment is being subducted at a rate of about 60 km per million years. We estimate, based on considerations of the stability requirements for gas hydrates observed as anomolous reflectors in some of our seismic records, and on one measurement in a deep well, that the geothermal gradient in this region is about 30°C/km. Such a gradient suggests a temperature regime in which the maximum gas generation in the subducting sediment occurs beneath the upper slope. Thus the sediment of the upper slope, as opposed to that of the shelf and lower slope, could be the most prospective for gas accumulation if suitable reservoirs are present.

INTRODUCTION

The theory of plate tectonics provides conceptual models which can be powerful tools in the exploration for oil and gas resources of continental margins of the world's oceans. Continental margins have been broadly classified based on relative movements among crustal plates into passive (divergent) and active (convergent) types. Passive margins generally consist of broad shelves, slopes, and rises and are characterized by lack of seismicity. In contrast, active margins do not always have shelves and are associated with deep trenches, volcanoes, and earthquakes. Although passive or divergent margins have the requisites for the generation and accumulation of significant quantities of oil and gas (Thompson, 1976), the requisites for significant hydrocarbon resources in sediments of active, convergent margins are poorly understood. New information from studies during the last ten years suggests that active margin settings could contain sites of important gas and possibly oil accumulations (Thompson, 1976; Roberts, 1981; Gwilliam, 1982). The peculiar nature of convergent margins, consisting of tectonically complicated subduction complexes, does not lend itself to "conventional" petroleum exploration strategies, and many of the basic tectonic mechanisms operating in subduction zones are only partially understood.

Studies of seismic records and samples from the Deep Sea Drilling Project (DSDP) have established the reality of extensive subduction of sediment along at least six modern convergent margins:

Japan Trench (Scientific Party, 1980)
Nankai Trough (Scientific Party, 1980; Karig, Kagami, et al., in press)
Mariana Trench (Hussong and Uyeda, 1981)
Middle America Trench (Watkins, Moore, et al., 1981; Aubouin, von Huene, et al., 1982; 1983)

Barbados Ridge (Moore, Bijou-Duval, et al., 1981)
Aleutian Trench (von Huene, 1979; von Huene, et al., 1983)

At these margins large volumes of oceanic sediment are being subducted, and the organic matter in the subducting sediment will undergo alterations as this sediment plunges deeper and subsurface temperatures increase. Hydrocarbon gases, particularly methane, are expected to result from these thermogenic alteration processes. Although there are few direct indications of thermal gradients within subduction zones, model studies show that temperatures will eventually reach sufficient levels for the generation of gas (Delong and Fox, 1977). The upward migration of gas from the subducted sediment to traps within the front of the continental margins seems likely considering the Paleogene age of the sediment and the surprising stability of the tectonic environment in many modern convergent margins, ie, the Aleutian, Middle America, and Japan Trenches.

This report summarizes our studies which tested the idea that convergent margins can be the site of significant hydrocarbon gas generation and accumulation. We chose the convergent margin of the Aleutian Trench, at the northern-most edge of the Pacific Plate (Fig. 1), as an appropriate area for investing concepts of gas generation and migration in a subduction zone. Previous DSDP drilling (Kulm, von Huene, et al., 1973; Creager, Scholl, et al., 1973) and extensive geophysical and geological studies (von Huene, 1979; Plafker et al., 1982; von Huene, et al., 1983) provide basic information relevant to this problem. Along the Aleutian Trench, structural styles associated with subduction are diverse ranging from subduction complexes with no accretion (Plafker, et al., 1982) to complexes with extensive accretion as well as sediment subduction (von Huene, 1979; von Huene, et al., 1983). In addition to this basic geological and geophysical information, some geochemical data in the form of organic carbon determinations on sediments of the Aleutian Trench system were available from DSDP Legs 18 and 19 (Bode, 1973a,b). For this report we have done the following:

a. Reprocessed multichannel seismic data from previous U.S.G.S. studies to clarify the tectonic framework of the Aleutian subduction complex, to image deeper parts of the Aleutian subduction zone, and to estimate volumes of sediment involved in subduction.
b. Estimated the thermal gradient from the base of gas hydrate reflector on seismic records, from available drill data, and from generalized information along other convergent margins.
c. Compiled information on organic matter in sediments sampled during DSDP Legs 18 and 19, and in selected dredge samples from U.S.G.S. cruise S-79-WG.
d. Assessed the potential for gas occurrence based on kinds and volumes of sediments, types and amounts of organic matter, geothermal gradients, and the structural framework of the Aleutian subduction complex.

SEISMIC SURVEYS

The seismic records used for this report were taken from two grids (A and B) of seismic lines and two single seismic lines (C and D) across the Aleutian convergent margin near Kodiak Island (Fig. 2). Many records from these grids and lines have been processed to clarify and deepen the seismic information well beyond that of the original, more routinely processed records. Considerable structural variation in the accreted sediment can been seen on these seismic lines (Figs. 3 and 4). An important conclusion from our study of these reprocessed records is that a large amount of sediment is presently

being subducted beneath the accretionary complex. Thus although this portion of the Aleutian convergent margin is truly accretionary at the present time, sediment subduction is an on-going and important process.

Field work. All of the records were shot with the seismic system aboard the RV S.P. LEE during the field seasons of 1976, 1977, and 1981. The seismic system was a tuned array of five air-guns totalling 21.7 liters, a 2,400 m - 24 group streamer, and a GUS 4300 digital recording instrument. In all surveys, shotpoints were located by satellite navigation supplemented by doppler-sonar and Loran-C fixes.

Data processing. The data were processed in two phases. Initial, routine processing was done to general standards for CDP seismic data in records where the structure is relatively simple. In the second phase, the data were reprocessed and enhanced by migration and depth conversions to restore true structural relations.

Seismograph Service Corporation did the initial processing of data collected during 1976; Grant Geophysical Corporation processed data collected during 1977; and the U.S. Geological Survey at Menlo Park processed data from both 1977 and 1981. The processing sequence consisted of demultiplexing, editing, velocity analysis, NMO correction and stacking, deconvolution, filtering, AGC, and display. These data were analyzed and reported in preliminary form in various publications (von Huene, 1979). In this preliminary work many important structural features were masked by diffractions, and more detailed reprocessing including migration was required before these features could be properly resolved. An example of the progressive improvement in information from a stacked record to a migrated time record and ultimately a depth section are shown in Plate 1.

Reprocessing began with a more detailed analysis of the stacking velocities. The improved velocities were then used to restack the data prior to migration, utilizing the Digicon DISCO system at the USGS in Denver, Colorado. Wave equation migration was then applied. Each record was migrated at four or five constant velocities ranging from 1450 m/s to 1850 m/s. This sequence of migrated records was then inspected to determine the best migration velocity of each portion of the record. Migration velocities differed markedly from stacking velocities in areas of complex structure where large changes in dip occur over small distances. Often the best migration velocity for each small area could not be applied to produce a single record because inversion of interval velocity values causes the migration algorithm to fail. Thus, each final migrated record was a compromise and was the best record that could be assembled in one section using the Digicon software, but local complex structures were clearer on some of the constant velocity displays. Where structure was depicted most clearly, we made tracings that comprise the final composite line drawing. Reduced time records from grids A and B are shown on Figures 3 and 4.

INTERPRETATION OF SEISMIC RECORDS

The seismic records were interpreted simultaneously with the processing of each record. The stacked records were studied to identify areas where the clarification of structure and elimination of diffractions would extend the imaging and thereby enhance the information for interpretation of geologic structure. In this manner, each change in velocity and scaling parameters was monitored with respect to the improvement of specific structural features, and a series of interpretations were made on successively improved records.

Generally, migration clarified structures in the first 2 or 3 seconds of

the record but was not as effective in deeper parts of the record. Folds at the beginning of the subduction zone were clearly imaged when masking diffractions were collapsed. The migration velocity that best collapsed diffraction in areas of folding was commonly different from the velocity of the rock measured by seismic refraction or from velocity measurements on DSDP drill cores. Faults were interpreted based on truncations, changes in the dips of reflections, and occasional, shallow fault plane reflections.

The igneous oceanic crust, or basement of the subducting plate, is defined acoustically by high amplitude reflections, low frequency signal returns, and an irregular, diffraction - producing surface. These features give the basement reflection a distinctive character. However, the basement is generally buried by more than 2 km and as much as 4 km of sediment before entering the subduction zone. Thus, down the subduction zone as the overlying sediment rapidly thickens, the basement reflection becomes difficult to follow especially where accoustic dispersal in a complexly deformed overlying sediment sequence has scattered the reflective energy. The maximum depths to which we were able to image the basement are about 7 km, and generally a reasonable record clarity was obtainable at 4-5 km depths; however, relative structural simplicity highly influenced depth and clarity of imaging.

A summary of the main structural features in the records used for this study is shown in Figures 3 through 6. There are differences in the reflections shown between the depth and time presentations because each has a different character even though the original data are the same. This difference is primarily caused by the compression of scale required in the upper, low-velocity part of the sediment sequence during the conversion from time to depth, and by the stretching seen in the lower, high-volecity sediment. It was sometimes difficult to trace exactly the same reflections in both the time and depth presentations.

The seismic records of the eastern Aleutian Trench show considerable subduction of sediment. The thickness of sediment in the trench is from a little more than 2 km (von Huene, 1972) to about 5 km (line 120, Fig. 3) prior to entering the subduction zone. The subduction zone shows a variety of structural styles, and even records only 10-20 km apart are significantly different. Therefore, each grid of lines is discussed separately.

The southwestern most grid (grid A, and Figs. 2, 3, and 4) depicts a part of the trench where sediment is presently from 2.5 to 5 km thick. About 1.5 km of the sediment in the trench is turbidite and hemipelagic fill which is 0.6 million years (m.y.) old at DSDP Site 180, just about 200 km northeast in the trench (von Huene and Kulm, 1973). As the sediment section passes into the trench, the first deformation is marked by small proto-reverse faults that do not reach the surface (Fig. 3). Here, the section is divided into 2 parts; the upper part is scraped off at the deformation front and attached to the front of the margin whereas the lower part is subducted. The depth of this division can vary, and the division is found both above and below the base of the hemipelagic and turbidite sediment filling the trench axis. In record 111 (Figs. 3 and 4) the subducted sediment is 1.2 sec (2.0 km) thick; in records 117 and 120 (Fig. 3) the subducted sediment is 2.5 and 2.6 sec thick; using the same velocity as in record 111, the thickness along records 117 and 120 is 4.2 and 4.3 km, respectively. An average thickness of subducting sediment at the front of the margin in this grid is 2 sec or about 3.7 km. In record 111 (Figs. 3 and 4) the subducted sediment thins slightly with distance landward from the deformation front. Landward of the mid-slope area the slope of the trench steepens, and the structure is mainly monoclinal (Fig. 4). The mid-slope area marks a change in tectonic regime where at least the upper 6 km of

deformed sediment is no longer being extensively tectonized by horizontal compression but is rather being uplifted as a rigid body. The change in tectonic regime may mark a transition from largely ductile deformation of weak, offscrapped sediment with elevated pore-fluid pressure at the front of the margin to a more rigid body being underplated by subducting sediment (von Huene, 1979 and von Huene, et al., 1983). Most pertinent to the the subject of this report is that within the southern grid, which covers a 65 km stretch along the slope of the trench, the thickness of subducted sediment varies between 2.0 and 4.3 km and averages 3.7 km. The subducted sediment here is mainly from a sequence of ocean basin turbidites. At DSDP site 178, this sediment sequence is of Neogene age and contains massive hemipelagic mudstones and some silt and sand turbidites (von Huene and Kulm, 1973).

The segment of the trench surveyed in grid B (Figs. 2 and 5) is also characterized by considerable subduction of sediment; however, because the structural style differs from grid A, the nature of the sediment being subducted may also differ. In fact, it has been suggested that considerable trench fill and even slope sediment may be subducted along this segment of the trench (von Huene, 1979). This previous structural interpretation has been modified, however, based on the more recent processing results. The four records studied from grid B (Fig. 5) show a variable structural style but each demonstrates subduction of a sediment section that varies in thickness from 1.2 to 3.3 km at the front of the margin. In records 71 and 72/62, the subduction involves both the trench fill and the underlying ocean basin sediment sequence; the zone of sediment subduction appears to break through the lower slope and could involve some slope sediment. Landward of the deformation front the maximum thickness on a subducting sediment section is about 4 km in record 71. An average thickness of all lines in the grid is 2.75 km, and can vary from 1.2 km to 4.0 km.

One record at line C (Fig. 2), equivalent to record 13 (Fig. 6), shows a very thick accreted section, and no subducting sediment is obvious; however, the basement surface was not imaged. Thus, we cannot determine how much sediment is subducted along record 13, and whether record 13 is representative of the area.

In contrast to line C, nearby line D, (Fig. 2 and 6) shows subduction of the complete sediment section (Plafker et al., 1982). Although the seismic record does not show a well-developed decollement, the age relation required by the stratigraphy of a well on the shelf compels such an interpretation. On the shelf, the drill hole off Middleton Island penetrated a sediment sequence of at least lowest Eocene age (Rau, et. al., 1977, Keller, et al., in press). The Oligocene/Miocene time horizon can be clearly followed from the drill hole to the base of the trench slope; the position of the base of the Eocene is inferred from its depth in the drill hole. From DSDP hole 180 the Quaternary section is traced to the base of the slope and must pass beneath the front of the margin (Plafker et al., 1982). If this record is representative of a segment of the trench, there is a 2.7 km thick sediment section being subducted which includes the uppermost trench sediment. This seismic record shows that the subduction of sediment may involve the total section in the trench as has also been demonstrated in the Middle America Trench off Guatemala (Aubouin et al., 1984). The proximity of line D to line C (Fig. 2), which failed to record sediment subduction, emphasizes the variability possible from total sediment subduction to total sediment accretion.

GEOCHEMICAL ANALYSES AND RESULTS

The organic matter in sediment associated with the area of the Aleutian Trench can provide a guide to the organic matter that is being subducted beneath the present convergent margin. Forty samples have been studied in order to ascertain the content and properties of the organic matter in sediment postulated to be involved in one way or the other in the subduction process. Thirty four of these samples came from five DSDP sites (178, 180, 181, 183, and 192), and six samples came from two USGS dredge sites (2 and 4). Figure 2 shows the location of these sampling sites relative to the seismic grids which were discussed previously. The basinal sediments at sites 178, 180, and 183 are believed to be equivalent to sediments currently undegoing subduction at this active margin. Sediments sampled at Site 181 are lower slope deposits which may have been accreted during the subduction. Site 192 is on a seamount where the sediment cover may be representative of basinal sediments involved in subduction at the western end of the Aleutian Trench. Dredge samples 2 and 4 came from outcrops on the upper slope. These samples may be lithified equivalents of older sediments undergoing subduction.

DSDP samples. Selection of 34 samples from the DSDP repository was guided by the following considerations: samples from DSDP Leg 18 were chosen from Sites 178, 180, and 181; samples from DSDP Leg 19 were chosen from Sites 183 and 192. These sites were selected because the sediments at these sites appear to be equivalent to sediments currently involved in some stage of subduction. Individual samples were selected on the basis of position in the core, organic carbon content, and on availability, with the samples containing the highest amount of organic carbon being preferentially collected. Approximately 40 cc of sediment were removed for each sample. Weights of samples ranged from 62 to 114 g. Appendix 1 shows the location within each DSDP core where samples were recovered. The lithologies and ages of the samples are given in Appendix 1 and on Plate 2.

USGS samples. Six dredge samples from U.S.G.S. cruise S-79-WG were analyzed (Plate 2). Five samples, including three mudstone and two dolomites were obtained from site 2, and one sample, a massive limestone was used from site 4. These upper slope, outcrop samples ranged in age from middle Eocene to early Pleistonce. The water depths at sites 2 and 4 are 1800 and 2200 m, respectively.

Organic carbon. For the 34 DSDP samples used in this study, an estimate of the organic carbon content (Plate 2) was available through compilations by Bode (1973a,b) which contain organic carbon values for equivalent core samples. Our determinations by high temperature oxidation techniques, utilizing a LECO analyzer, are listed in Plate 2 and are in remarkable agreement with the values obtained by Bode (1973a,b). This close agreement establishes a high level of confidence in the reported organic carbon values.

Total carbon. Total carbon determinations were made on 40 samples (Plate 2). The results show that all but three samples contain only small (less than 0.37%) carbonate carbon. Three dredge samples contain 6.3 to 9.1% total carbon, and these samples are classified as dolomite or limestone.

Pyrolysis. All 40 samples were analyzed by a temperature programmed pyrolysis technique (Thermal Evolution Analysis or TEA) in which the products of pyrolysis are measured by a flame ionization detector (FID), and the temperature of maximum pyrolysis yield is determined (Claypool and Reed, 1976). Pyrograms of the 40 samples are shown in Figure 7. In general the patterns are rather non-descript and lack distinctive peaks. The patterns signal that the organic matter in many samples is somewhat unstructured and

likely immature . This pyrolysis method provides information on total hydrocarbon yield (measured in percent of organic carbon), volatile hydrocarbons (measured in parts per million of the total hydrocarbon yield), and Tmax in degrees C representing the temperature at which the maximum amount of organic matter is thermally decomposed. "Live carbon" is a measure of the content of "hydrocarbon-prone" organic matter and is obtained by dividing the total hydrocarbon yield by the amount of organic carbon. "Live carbon" is considered to be the carbon that will, upon thermal evolution, still yield additional hydrocarbon products such as methane gas.

Discussion. The results of our organic geochemical analyses are listed in Plate 2. These results show that all of the samples analyzed contain low amounts (less than 1%) of organic carbon (OC). The total hydrocarbon yield is also low and ranges between 0.03 and 0.10%. With the exception of four samples, the amounts of "live carbon" are less than 25%. Those four samples with "live carbon" exceeding 25% are samples with the least amount of organic carbon. The volatile hydrocarbon content is always less than 200 ppm. Tmax ranges from 398 to 523°C, but the pyrograms (Fig. 7) from which these data are taken are so indistinctive that the results are generally considered unreliable for interpretive purposes. Profiles with depth of our geochemical results for the five DSDP sites are shown in Figure 8a-e. These profiles emphasize the low amounts of the various geochemical parameters. Organic carbon decreases irregularly with depth at site 178, 181, and 192. Significant trends of other parameters are not obvious. The highest amount of organic carbon (0.9%) was found at a 220 m subbottom depth at site 183. This amount of organic carbon is interesting from the point of view of source-rock evaluation, but the low total hydrocarbon yield makes the amount of "live carbon" very low (8%) thus decreasing the potential of this sediment for hydrocarbon generation.

Table 1 summarizes our results. The low amounts of organic carbon, total hydrocarbon yield, "live carbon", and volatile hydrocarbons suggest that the sediments we have sampled and analyzed are poor potential source sediments for petroleum, both oil and gas. The average amount of organic carbon is equal to or less than 0.6%, a value considered near the lower limit for potential sources of hydrocarbons (Hunt, 1979). The amount of "live carbon", i.e., the carbon available for future hydrocarbon generation, is less than 30% which indicates, according to work by Magoon and Claypool (1981), that the organic matter is prone to gas generation rather than oil generation.

Nine samples were selected for detailed examination of organic matter type (Table 2). These samples were chosen because they appeared to be richest in organic carbon, and there was sufficient sample on which to carry out the analyses. These samples were subjected to a specialized pyrolytic technique called Rock-Eval (Tissot and Welte, 1978). In addition, our analyses consisted of vitrinite reflectance measurements, visual kerogen analyses by both transmitted and incident light, and evaluation of the thermal alteration index (TAI).

Rock-Eval analyses provided an independent measurement of organic carbon and Tmax. In all cases the Rock-Eval organic carbon value is larger than the value obtained by TEA (Plate 2). Tmax is significantly higher in the Rock-Eval analysis of all DSDP samples, but Rock-Eval Tmax is lower than Tmax from TEA for two dredge samples (Plate 2). The Rock-Eval measurements for these two parameters are considered less reliable than TEA measurements and therefore are not considered further. Rock-Eval analyses yield hydrogen indices (HI) and oxygen indices (OI) from which a van Krevelen diagram can be constructed (Table 2). For the most part all of the samples lie along the

Type III pathway of this diagram (Fig. 9). Type III organic matter is generally considered to be of terrestrial origin and gas-prone (Tissot and Welte, 1978).

Vitrinite reflectance (R_o) values of primary vitrinite range from 0.36 to 0.50% (Table 2). Recycled vitrinite of greater R_o values is also present in all samples. Appendix 2 gives detailed descriptions of vitrinite reflectance readings. TAI evaluations range from 1.5 to 2.6 (Table 2). Both vitrinite reflectance and TAI values indicate that the organic matter of these samples is immature with respect to oil or gas generation and shows strong indications of reworking. Visual kerogen analyses (Table 2) indicate that, in addition to vitrinite and recycled vitrinite, the samples also contain exinite, inertinite, recycled sporinite, and amorphous material. The distribution of these kerogen macerals suggests that most of the organic matter is terrestrial in origin, and the position of these samples on the diagram indicates immaturity.

Taken together our geochemical analyses show the following: The amount of organic carbon in the samples is small and approaches the lower limit as a potential source of hydrocarbons. The presence of inertinite further reduces the hydrocarbon potential of these samples. The organic matter is mainly from terrestial sources, is gas prone, and is immature with respect to gas generation. Upon thermal evolution the samples are expected to generate only small amounts of gas.

ESTIMATION OF GEOTHERMAL GRADIENT

To determine the region where gas is generated in the subduction complex of the Aleutian Trench requires some knowledge of the geothermal regime. Information regarding this regime in the Aleutian Trench is minimal, and direct readings of geothermal temperatures have been made at only one place. A temperature log from a well drilled just offshore of Middleton Island on the edge of the shelf showed an average temperature gradient of 28°C/km.

An innovative approach to the determination of regional geothermal gradients has been described by Yamano et al. (1982) for areas where gas hydrates are present and are manifest on seismic records as an anomalous bottom-simulating reflector or BSR. From the depth of the BSR, the geothermal gradients are estimated using the phase relations of the gas hydrate system. This method has been successfully applied to data from the Nankai Trough offshore Japan, around Central America including the Middle America Trench, and along the Blake Outer Ridge. Geothermal gradients in the Nankai Trough ranged from 41.5 to 65.8°C/km, and along the Middle America Trench they ranged from 35.1 to 28.2°C/km. Both of these areas are convergent margins as is the Aleutian Trench. MacLeod (1982), using the same methods, estimated the geothermal gradient in sediment of the Gulf of Alaska to be 27.8°C/km.

BSRs can be seen on some seismic records from the upper slope of the Aleutian Trench (Fig. 10). Depths to the BSR were obtained using a seismic velocity of 2.0 km/sec. Five depths to BSRs were calculated at five positions with different water depths. This information was applied to the phase diagram for gas hydrates given by Kvenvolden and McMenamin (1980) for five different bottom-water temperatures to obtain estimates of the geothermal gradient (Table 3). In addition, on Table 3 are geothermal gradients estimated from hydrate stability curves given by Macleod (1982). There are several reasons for the difference in gradients. Kvenvolden and McMenamin assume a pure methane - pure water, gas-hydrate system whereas Macleod uses a pure methane - Arctic seawater, gas-hydrate system. Also the latter system

assumes bottom-water temperatures that vary with depth of water and are all less than 1°C.

Our estimates for the geothermal gradient on the upper slope of the Aleutian Trench area, based on the depth of the BSR, range from 28 to 36°C/km (Table 3) with a best estimate for bottom-water temperatures near 1°C of about 30°C/km. This number agrees reasonably well with the geothermal gradient from the Middleton Island well of 28°C/km and with the estimate of MacLeod (1982) of 27.8°C/km for sediment of the Gulf of Alaska.

A geothermal gradient of about 30°C/km for the upper slope of the Aleutian Trench is significantly lower than the average gradient of 53°C/km in the Nankai Trough but nearly the same as the average gradient of 32°C/km along the Middle America Trench and the 24°-32°C/km gradient for the Japan Trench (Langseth and Burch, 1980). All of these areas are convergent margins at the edge of the Pacific Plate (Fig. 1). The Nankai Trough is exceptional in that it is a convergent margin where back-arc crust of the Philippine Plate is being subducted, and thus its thermal structure is unusual. Because of the uncertainties in the use of gas hydrate BSRs to estimate geothermal gradients, the accuracy of the estimates is not high, but the values obtained are consistent with those measured by conventional means and sufficient for our purposes.

Temperature distribution across active margins is characteristically complex (cf Watanabe, et al., 1977). The uncertainties derive not only from the subduction of cool oceanic crust but also from the fluid flux and differential rates of tectonic transport as well. Most investigators model a zone of temperature reversal along the principal slip plane of a subduction zone. Our temperature information is so rudimentary that any attempts to account for such variations is overshadowed by the uncertainties of sparse observations. Thus, for our estimates of thermal structure, we simply assume a linear vertical gradient but are aware of the imprecision this assumption incorporates.

ASSESSMENT OF POTENTIAL FOR NATURAL GAS GENERATION

An assessment of the potential of the Aleutian Trench subduction zone for natural gas generation requires basic geologic information, some of which has been obtained for this report. We now have preliminary ideas about the amount and nature of carbon in some of the sediments involved in the subduction process. Our seismic surveys show the tectonic framework of the area from which we can estimate subducted sediment thicknesses and assume sediment volumes. Finally, we have estimated a geothermal gradient based on considerations of gas hydrates and a measurement in a well. We can now put this geochemical, geophysical, and geothermal information together to estimate the amount of natural gas generated by thermogenic processes. For our subduction model we have chosen to use average values of our data, and to extrapolate these averages for the eastern Aleutian Trench subduction complex.

Our geochemical studies show that the average organic carbon content of the samples analyzed is 0.44% and that an average of 15% of this carbon is "live", that is, able to thermally react further to produce hydrocarbons. These average values were calculated from Table 2. Because the kerogen in these samples is Type III, we assume an H/C ratio of about 1. However, the H/C ratio of methane is 4; therefore, we assume that only about one fourth of this produced hydrocarbon can be methane gas, because of the deficiency of hydrogen in the kerogen. This assumption leads to maximum values of potential generation of natural gas. The actual amount of methane possible could be two

or three orders of magnitude lower. These average values coupled with the following assumptions led to a calculated potential methane content of these sediments of about 5.5 x 10^8 cubic meters of methane per cubic kilometer of sediment (m^3/km^3): (1) 12 g of "live carbon" equals 1 mole of "live carbon"; (2) 1 mole of "live carbon" equals 22.4 liters (l) of methane; and (3) the density of sediments is 1.8 g/cc. A value of 5.5 x 10^8 m^3 of methane/km^3 of sediment represents the maximum amount of methane disperesed in the sediment. Estimates of the ratio of dispersed and dissolved gas to reservoir gas in sedimentary basins in general range from 10 - 200 to 1 (Hunt, 1979). Because we saw little evidence for reservoir-type sediment, that is, sediment with good porosity and permeability, during our sampling (Appendix 1), we selected the larger value of this ratio to apply in our estimate. Thus the amount of reservoired methane in each km^3 of sediment is estimated to be about 2.8 x 10^6 m^3.

Thicknesses of sediment involved in the subduction process of the Aleutian Trench area can be estimated from the seismic sections of the two grids and two lines described previously.

Grid/Line	Thickness (k)	Comment
A	3.7	lower section only
B	2.75	including trench and slope(?) sediment
C	0	accretionary sediment only
D	2.7	whole trench section

The average thickness of subducting sediment is about 3 km. If we consider an element of sediment measuring 1 km by 1 km of areal extent and 3 km thick, the volume of this element is, of course, 3 km^3. If the rate of subduction is about 60 km/m.y. (Fig. 1) then in that time period , 60 of these sediment elements would have been subducted equaling a volume of subducted sediment of 180 km^3. The amount of reservoired methane to be expected from this volume of sediment is therefore 180 x 2.8 x 10^6 = 5.0 x 10^8 m^3. If this number is extrapolated over the length of the eastern Aleutian Trench of 600 km, then the amount of expected, thermally generated, reservoired methane per million years in this province is about 0.3 x 10^{12} m^3 or, in 20 million years, about 6 x 10^{12} m^3. This number is about 9% of the current world reserves of natural gas of 66.4 x 10^{12} m^3 (Rice and Claypool, 1981).

Other studies support the idea that thermally produced gases are present in sediments of the Aleutian Trench area, but none of these studies provides quantitive assessments of the amount of gas. For example, Claypool, et al. (1973) suggested that active thermal generation of gases was taking place at depths as shallow as 250 m in this area. Some of the gas represents early thermal generation as opposed to peak generation. On the basis of spore-coloration data, Grayson and LaPlante (1973) indicated that the level of maturation of a sample from DSDP Site 181 from a subbottom depth of about 340 m was equivalent to an overburden depth in the Gulf Coast of about 2,600 m. Dow (1978) calculated an equivalent R_o = 0.3% for this sample. Our measured R_o values for shallower sediments at the same site equal 0.46 and 0.47% (Table 2). The calculated and measured R_o values indicate that the samples currently are at lower termperatures than required for gas generation; however, as we have shown, these samples may eventually be included in the subduction complex and be exposed to temperatures at which the organic matter will be transformed to methane.

There are large uncertainties in our estimate of 0.3 x 10^{12} m^3 of potential, reservoired methane generated each million years of subduction. Our calculated value results from extensive extrapolations and assumes that

the methane becomes reservoired and is not lost from the system either downward into the subduction zone or upward into the atmosphere. Our model requires that the generated methane somehow migrates from the subducting sediments where it formed into the overlying, non-subducted sediments where it becomes trapped. We have no direct evidence relating to conduits for gas migration or for traps of suitable size for exploration. Also our estimates represent a maximum and could easily be two orders of magnitude smaller if, for example, only one percent of the "live carbon" is transformed thermally into methane. Our large number estimate results not from the richness of organic matter in these sediments but rather from the enormous volumes of sediment involved in the subduction process. In fact, the amount of organic matter is very small and, by itself, would indicate only a poor potential for significant gas generation.

Our calculations have not taken into account biogenically produced methane which was present in the modern sediments associated with the Aleutian Trench. Kulm, von Huene et al. (1973) and Creager, Scholl, et al. (1973) refer to the gassy nature of sediment cores recovered during DSDP Legs 18 and 19, although no quantitative measure of the total amount of gas was made. Claypool et al. (1973) showed that the carbon isotopic composition of methane from DSDP Site 180 (one of the sample sites used in this report) ranged from -72.6 to -80.8 per mil relative to the PBD standard. This range of values is well within the range diagnostic of biogenic gas (Fuex, 1979). Also we have not considered the gas volume consequences of the presence of gas hydrates observed in some of our seismic records. In spite of the low measured concentrations of organic matter in the sediments of the Aleutian Trench area, our study suggests that very large concentrations of both biogenic and thermogenic methane can be formed during sedimentation and subsequent subduction. A major unknown is where the gas is now. We still lack sufficient data on preservation, migration, and trapping to draw firm conclusions at this time. Clues from onshore geology (Fisher, 1980) indicate both poor reservior and source potential at least for the area of the Kodiak shelf.

If we accept the idea that significant quantities of methane can be thermally generated in the subduction zone of the Aleutian Trench, we can determine, based on the geothermal gradient, in what region of the subduction complex the gas might be present. Figure 11 shows the geologic section for seismic line 111 of Grid A. Superimposed on this section are isothermal lines for 50°, 150°, and 250°C based on our estimated, constant vertical geothermal gradient of 30°C/km. The three isothermal temperature lines represent the temperatures for the gas ceiling, maximum gas generation, and the gas floor, respectively. Of these three temperatures, the gas floor is the most uncertain and is likely a higher temperature than 250°C (Barker, 1982). A 3 km-thick section of marine sediment involved in subduction would pass through the temperature of maximum gas generation somewhere beneath upper slope sediment. Thus, if our ideas are correct, the region below upper slope sediment would be most prospective for future gas exploration if reservoirs and traps are present. This is the same region that was predicted by Thompson (1976), based on a thrust-fault-controlled model, for petroleum accumulation in the Aleutian Trench area.

Besides the possible existence of gas in deep, upper slope sediments, gas may also be present in the deep basins associated with the Aleutian convergent margin. Except for the great depth of water, these basins are similar to basins of the shelves and require conventional strategies for evaluation of petroleum prospects. Hedberg et al. (1979) concluded that deep ocean basins,

including those associated with convergent margins, are potential sites for petroleum accumulation. We have not considered these kinds of basins in our assessment. If in the Aleutian Trench area both the basins, as suggested by Hedberg et al. (1979), and the upper slope sediments, as suggested by Thompson (1976) and ourselves, are prospective for petroleum gas, then this vast area may become an important exploration target in the future.

SUMMARY

This report provides preliminary data addressed to the question of the potential of subducted sediment within the Aleutian Trench convergent margin to generate significant quantities of natural gas. Our results suggest that even though the content of organic carbon in sediments of the ocean basin is low, averaging about 0.4%, the volume of sediment involved in subduction is so large, having an average thickness of 3 km, that, indeed, significant quantities of gas can be thermally generated. We calculate that as much as 6×10^{12} m^3 of natural gas could have been generated and stored during the last 20 million years of subduction. This number is equal to 9% of the currently known world reserves of natural gas. To this number can also be added an as yet unknown, but probably large quantity, of biogenically derived methane which is present in the sediments even before they undergo subduction. In addition, there is an unknown amount of natural gas in basins associated with this convergent margin. Our estimate of potential gas generation during subduction has great uncertainties, but because of the large volumes of sediment involved, a significant amount of generated gas is possible even though the content of organic matter in the sediment is small. A large unknown is where the gas migrates and is currently stored. Our model assumes that the gas is not lost through subduction or through diffusion to the atmosphere. We have no direct evidence for migration pathways or for traps of suitable size for exploration. Our results, based in part on consideration of our estimated geothermal gradient of 30°C/km, suggest that, if significant quantities of natural gas can migrate upward above the area of maximum gas generation, then this gas would likely be found in sediment of the upper slope of the Aleutian Trench and not in shelf or lower slope deposits.

ACKNOWLEDGEMENTS

Samples from DSDP Legs 18 and 19 were supplied by the Deep Sea Drilling Project through the assistance of the U.S. National Science Foundation. Geochemical analyses were provided by GeoChem Research Laboratories of Houston, Texas, and by Clark Geological Services of Fremont, California. We greatly appreciate the help of John Miller in processing the seismic data. This work was partially funded by the Morgantown Energy Technology Center under U.S. Geological Survey - Department of Energy Interagency Agreememt No. DE-A121-83MC20422.

REFERENCES

Aubouin, J., von Huene, R., et al., 1982, Initial Reports of the Deep Sea Drilling Project, v. 67: Washington (U.S. Gov't. Printing Office), 799 p.

Aubouin, J., von Huene, R., et al., 1983, Leg 84 of the Deep Sea Drilling Project, Subduction without accretion: Middle America Trench off Guatemala: Nature, v. 297, p. 458-460.

Barker, C., 1982, Methane generation and survival in the deep subsurface: In Gwilliam, W.J., ed., Deep Source Gas Workshop Technical Proceedings, DOE/METC/82-50, UC-92a, p. 86-107.

Bode, G.W., 1973a, Carbon and carbonate analyses, Leg 18: In Kulm, L.D., von Huene, R., et al., Initial Reports of the Deep Sea Drilling Project, v. 18: Washington (U.S. Gov't. Printing Office), p. 1069-1076

Bode, G.W., 1973b, Carbon - carbonate: In Creager, J.S., Scholl, D.W., et al., Initial Reports of the Deep Sea Drilling Project, v. 19: Washington (U.S. Gov't. Printing Office), p. 663-665.

Claypool, G.E., and Reed, P.R., 1976, Thermal analysis technique for source-rock evaluation: quantitative estimate of organic richness and effects of lithologic variation: Am. Assoc. Petroleum Geologists Bull., v. 60, p. 608-626.

Claypool, G.E., Presley, B.J., and Kaplan, IR., 1973, Gas analyses in sediment samples from Legs 10, 11, 13, 14, 15, 18, and 19: In Creager, J.S., Scholl, D.W., et al., Initial Reports of the Deep Sea Drilling Project v. 19: Washington (U.S. Gov't. Printing Office), p. 879-884.

Creager, J.S., Scholl, D.W., et al., 1973, Initial Reports of the Deep Sea Drilling Project, v. 19: Washington (U.S. Gov't Printing Office), 913 p.

Delong, S.E., and P.J. Fox, 1977, Geological consequences of ridge subduction: In Talwani, M., and Pittman, W.C., eds., Island Arc, Deep Sea Trenches, and Back-Arc Basins: Maurice Ewing Series 1, Am. Geophysical Union, Washington, D.C., p. 221-228.

Dow, W.D., 1978, Petroleum source beds on continental slopes and rises: Am. Assoc. Petroleum Geologists Bull., v. 62, p. 1584-1606.

Fisher, M.A., 1980, Petroleum geology of Kodiak shelf, Alaska: Am. Assoc. Petroleum Geologists Bull., v. 64, p. 1140-1157.

Fuex, N, 1977, The use of stable isotopes in hydrocarbon exploration. Jour. Geochemical Exploration, v. 7, p. 155-188.

Grayson, J., and LaPlante, R.E., 1973, Estimated temperature history in the lower part of hole 181 from carbonization measurements: In Kulm, L.D., von Huene, R., et al., Initial Reports of the Deep Sea Drilling Project, v. 18: Washington (U.S. Gov't. Printing Office), p. 1077.

Gwilliam, W.J., 1982, Subducted organic origin gas hypothesis for deep source methane: In Gwilliam, W.J., ed., Deep Source Gas Workshop Technical Proceedings, DOE/METC/82-50, UC-92a, p. 140-161.

Hedberg, H.D., Moody, J.D., and Hedberg, R.M., 1979, Petroleum prospects of the deep offshore: Am. Assoc. Petroleum Geologists Bull., v. 63, p. 286-300.

Hunt, J.M., 1979, Petroleum Geochemistry and Geology: San Francisco (W.H. Freeman), 617 p.

Hussong, D.M., and Uyeda, S., 1981, Tectonics in the Mariana Arc: results of recent studies including DSDP Leg 60: Oceanologica Acta, No. SP of v. 4, p. 203-212.

Karig, D.E., Kagami, H., et al., in press, Initial Reports of the Deep Sea Drilling Project, v. 87: Washington (U.S. Gov't. Printing Office).

Keller, G., von Huene, R., McDougall, K., and Bruns, T.R., in press, Paleoclimatic evidence for Cenozoic migration of Alaskan terrances: Tectonics.

Kulm, L.D., von Huene, R., et al., 1973, Initial Reports of the Deep Sea Drilling Project, v. 18: Washington (U.S. Gov't. Printing Office), 1077 p.

Kvenvolden, K.A., and McMenamin, M.A., 1980, Hydrates of natural gas: a review of their geologic occurrence: U.S. Geol. Survey Circular 825, 11 p.

Langseth, M., and Burch, T., 1980, Geothermal observations of the Japan Trench transect: In Scientific Party, Initial Reports of the Deep Sea Drilling Project, v. 56, 57, pt 2, Washington (U.S. Gov't. Printing Office), p. 1207-1210.

Macleod, M.K., 1982, Gas hydrates in ocean bottom sediments: Am. Assoc. Petroleum Geologists Bull., v. 66, p. 2649-2662.

Magoon, L.B., and Claypool, G.E., 1981, Petroleum geology of Cook Inlet Basin, Alaska - An exploration model: Am. Assoc. Petroleum Geologists Bull., v. 65, p. 355-374.

Moore, G.W., 1982, Plate-tectonic map of the Circum-Pacific region -- explanatory notes: Am. Assoc. Petroleum Geologists, Tulsa, OK., 14 p.

Moore, J.C., Bijou - Duval, B., 1981, Near Barbados Ridge scraping off subduction scrutinized: Geotimes, v. 26, n. 10, p. 24-26.

Plafker, G., Bruns, T.R., Winkler, G.R., and Tysdal, R.G., 1982, Cross-section of the eastern Aleutian arc, from Mount Spurr to the Aleutian Trench near Middleton Island, Alaska: Geological Society of America, map and chart series MC-28-P.

Rau, W.W., Plafker, G., and Winkler, G.R., 1977, Preliminary foraminiferal biostratigraphy and correlation of selected stratigraphic sections and wells in the Gulf of Alaska Tertiary Province: U.S. Geological Survey, Open-File Report 77-747, 54 p.

Rice, D.D., and Claypool, G.W., 1981, Generation, accumulation, and resource potential, of biogenic gas: Am. Assoc. Petroleum Geologists Bull., v. 65, p. 5-25.

Roberts, D.G., 1981, Geological issues in offshore hydrocarbon exploration: In the Future of Offshore Petroleum, New York (McGraw Hill), p. 27-79.

Scientific Party, 1980, Initial Reports of the Deep Sea Drilling Project, v. 56 and 57: Washington (U.S. Gov't. Printing Office), 1417 p.

Thompson, T.L., 1976, Plate tectonics in oil and gas exploration of continental margins: Am. Assoc. Petroleum Geologists Bull., v. 60, p. 1463-1501.

Tissot, B., and Welte, D., 1978, Petroleum Formation and Occurrence: New York (Springer-Verlag) 538 p.

von Huene, R., 1972, Structure of the continental margin and tectonism at the eastern Aleutian Trench: Geol. Soc. Am. Bull., v. 83, p. 3613-3626.

von Huene, R., 1979, Structure of the outer continental margin off Kodiak Island, Alaska, from multichannel seismic records; In Watkins, J., and Montadert, L., eds., Geological Investigations of Continenetal Margins: Am. Assoc. Petroleum Geologists, Memoir 29, p. 261-272.

von Huene, R., and Kulm, L.D., 1973, Tectonic summary of Leg 18: In Kulm, L.D., von Huene, R., et al., Initial Reports of the Deep Sea Drilling Project, v. 18: Washington (U.S. Gov't Printing Office), p., 1069-1076

von Huene, R., Miller, J., Fisher, M., and Smith, G., 1983, An eastern Aleutian Trench seismic record: In Bally, A.W., ed., Seismic Expression of Structural Styles - A Picture and Work Atlas: Am. Assoc. Petroleum Geologists, Studies in Geology, n. 15, v. 3.

Watanabe, T., Langseth, M.G., and Anderson, R.N., 1977, Heat flow in back-arc basins of the western Pacific: In Talwani, M., and Pittman, W.C., eds., Island Arcs, Deep Sea Trenches, and Back-Arc Basins: Maurice Ewing Series 1, Am. Geophysical Union, Washington, D.C., p. 137-161.

Watkins, J.S., Moore, J.C., et al., 1981, Initial Reports of the Deep Sea Drilling Project, v. 66: Washington (U.S. Gov't. Printing Office), 864 p.

Yamano, M. Uyeda, S., Aoki, Y., and Shipley, T.H., 1982, Estimates of heat flow derived from gas hydrates: Geology, v. 10, p. 339-343.

Table 1. Summary of Geochemical Results by Sample Sites

Site	Number of Samples	OC (%)	Hydrocarbon Yield (%)	"Live Carbon" (%)	Volatile Hydrocarbons (ppm)	Tmax (°C)
178	12	0.36 ± 0.16	0.05 ± 0.01	18 ± 13	49 ± 21	464 ± 39
180	5	0.62 ± 0.08	0.06 ± 0.01	9 ± 2	88 ± 43	462 ± 30
181	6	0.61 ± 0.17	0.05 ± 0.01	8 ± 1	70 ± 17	464 ± 20
183	6	0.46 ± 0.27	0.07 ± 0.02	20 ± 17	119 ± 64	448 ± 11
192	5	0.21 ± 0.13	0.04 ± 0.01	31 ± 28	91 ± 36	439 ± 47
2	5	0.50 ± 0.23	0.04 ± 0.01	10 ± 4	52 ± 28	441 ± 9
4	1	0.30	0.03	10	76	443

Table 2. Results of Analyses of Kerogen

Sample No.	HI (mgHc/gOC)	OI ($mgCO_2$/gOC)	Ro (%)	TAI	Exinite (%)	Vitrinite (%)	Inertinite (%)	Recycled Vitrinite (%)	Recycled Sporinite (%)	Other Amorphous (%)
6	270	202	0.40	--	4	32	26	24	4	10
14	95	92	0.40	2.0	1	13	7	68	7	6
16	223	136	0.45	1.5	-	12	6	62	--	20
17	130	50	0.36	2.0	4	38	13	40	5	--
19	156	91	0.47	2.0-2.3	3	39	4	32	18	4
21	119	53	0.46	2.4-2.6	-	13	--	18	7	2
27	245	105	0.45	2.0-2.3	2	14	10	28	--	48
38	160	71	0.50	2.0-2.4	5	20	5	30	10	30
39	122	111	0.38	2.3-2.5	7	15	--	24	16	40

Table 3. Geothermal Gradients in °C/km Determined from Base of Gas Hydrate Reflector (BSR) on Marine Seismic Records

Water Depth (m)	Sediment Depth (m)	Total Depth (m)	Bottom Water Temperatures (°C) 1.0	1.5	2.0	2.5	3.0	Temperature Gradient from Macleod (1982)
2085	648	2733	32.5	31.8	31.1	30.3	29.6	29
1928	567	2495	35.9	35.0	34.0	33.1	32.2	32
2325	648	2973	33.9	33.2	32.4	31.7	30.9	30
1830	666	2496	30.8	30.1	29.3	28.6	27.8	28
1575	612	2187	31.5	30.7	30.0	29.2	28.4	28

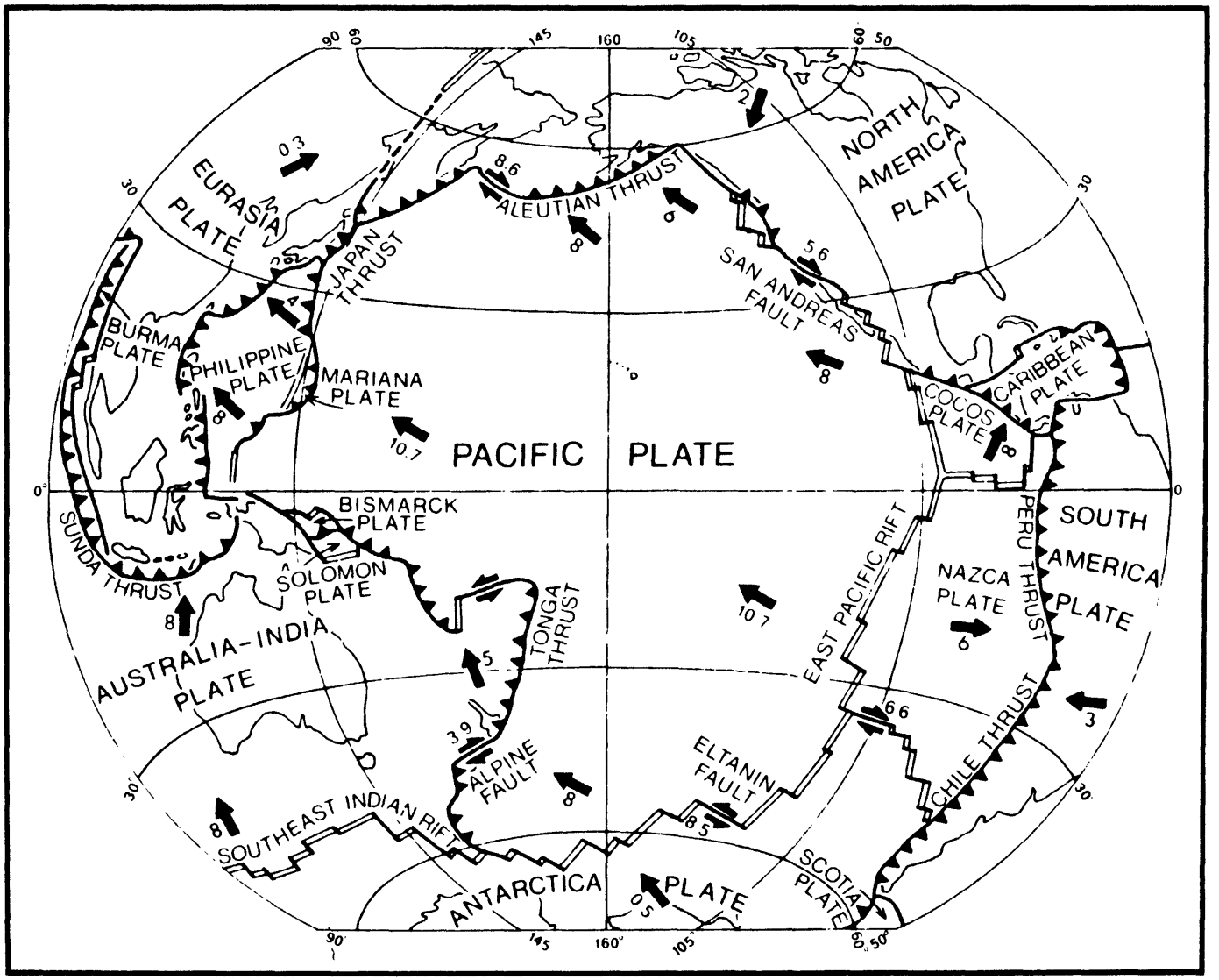

Figure 1. Plate tectonic map of the Circum-Pacific region showing major plate boundaries including the Aleutian Thrust, the site of the Aleutian Trench subduction zone. Numbers and arrows indicate rates (centimeters per year) and directions of plate movements. The Cocos Plate is the site of the Middle America Trench; the Japan Thrust is the site of the Japan Trench. (Modified after Moore, 1982.)

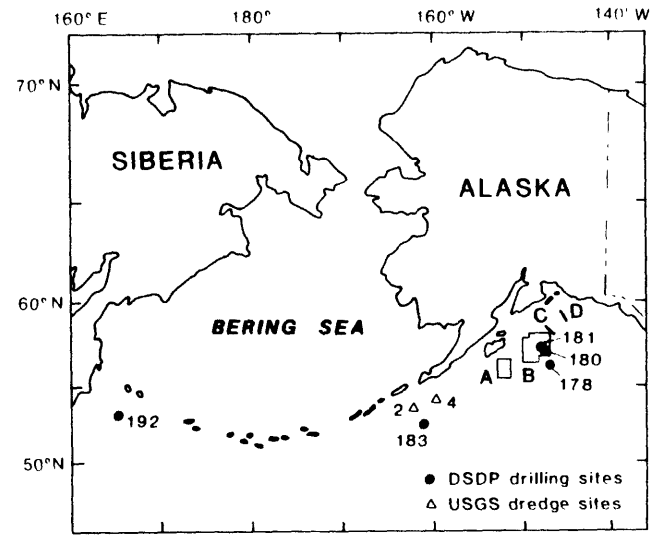

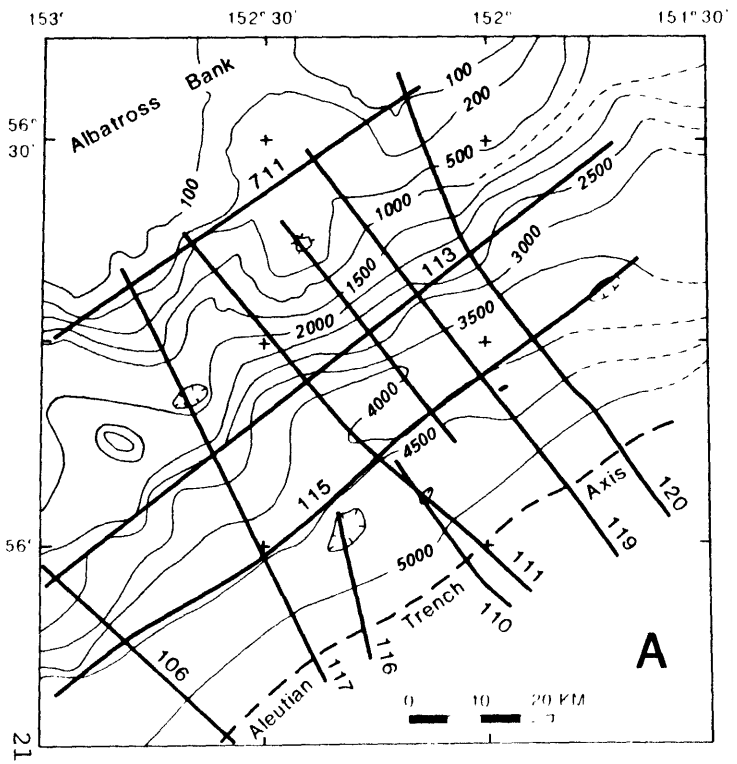

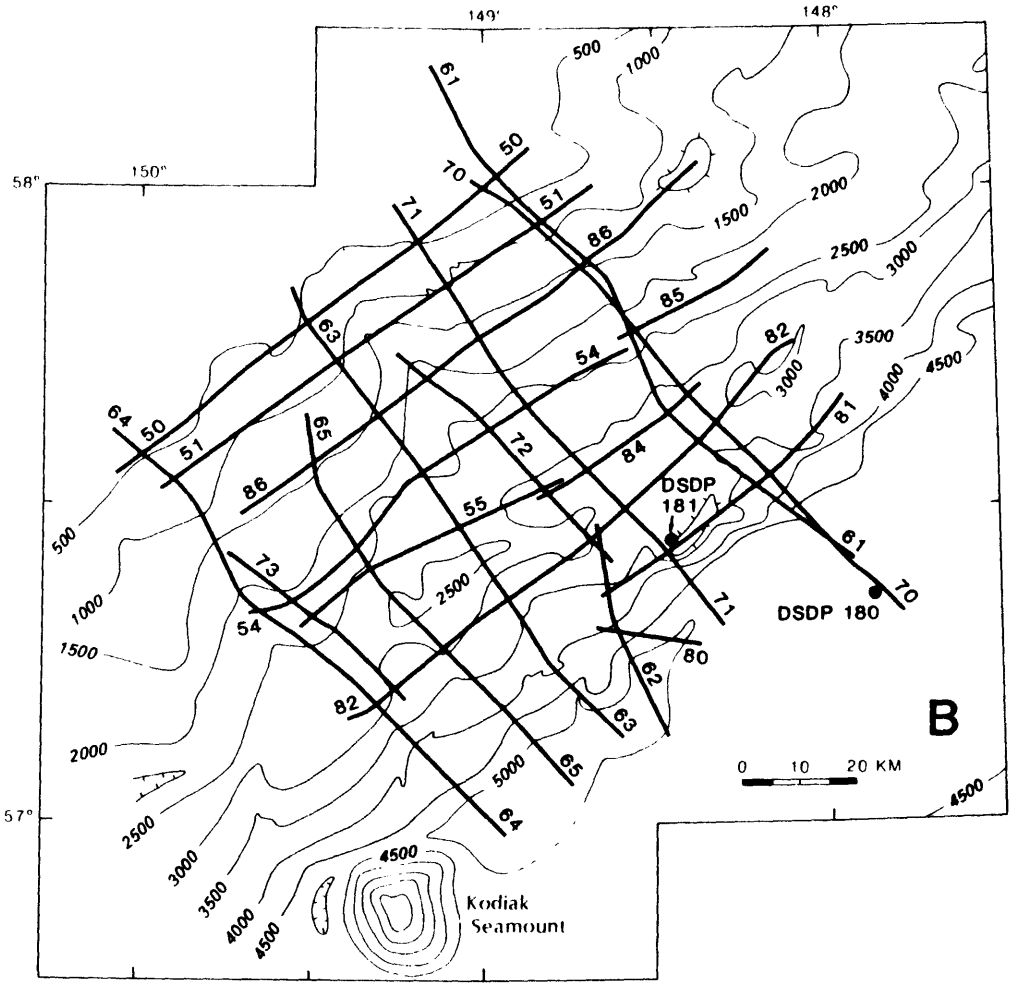

Figure 2. Locations of seismic-survey grids A and B with positions of multichannel seismic lines in the grids shown at expanded scale. Locations of single seismic lines C and D are also shown. In addition, DSDP sample sites 178, 180, 181, 183. and 192 (•) and USGS dredge sites 2 and 4 (△) are indicated.

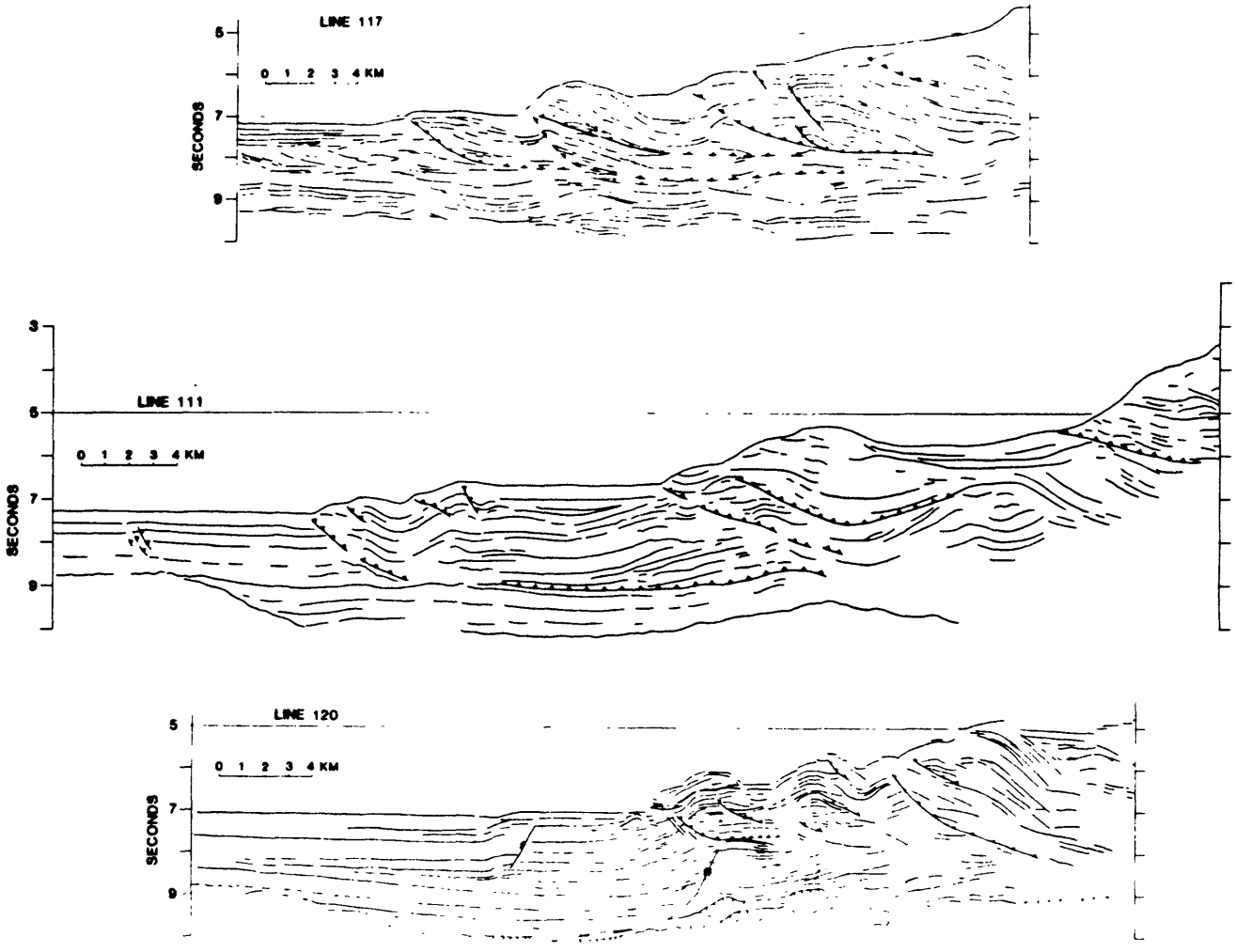

Figure 3. Time-sections of lines 111, 117, and 120 from seismic grid A (Fig. 2).

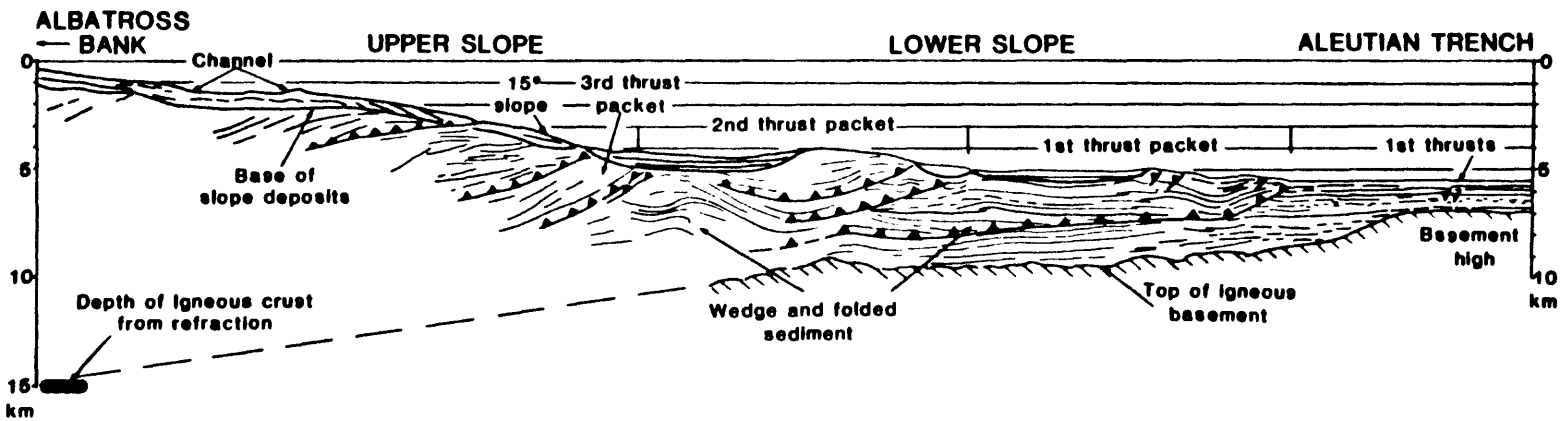

Figure 4. Depth section of seismic line 111 from grid A (Fig. 2) (after von Huene, et al., 1983).

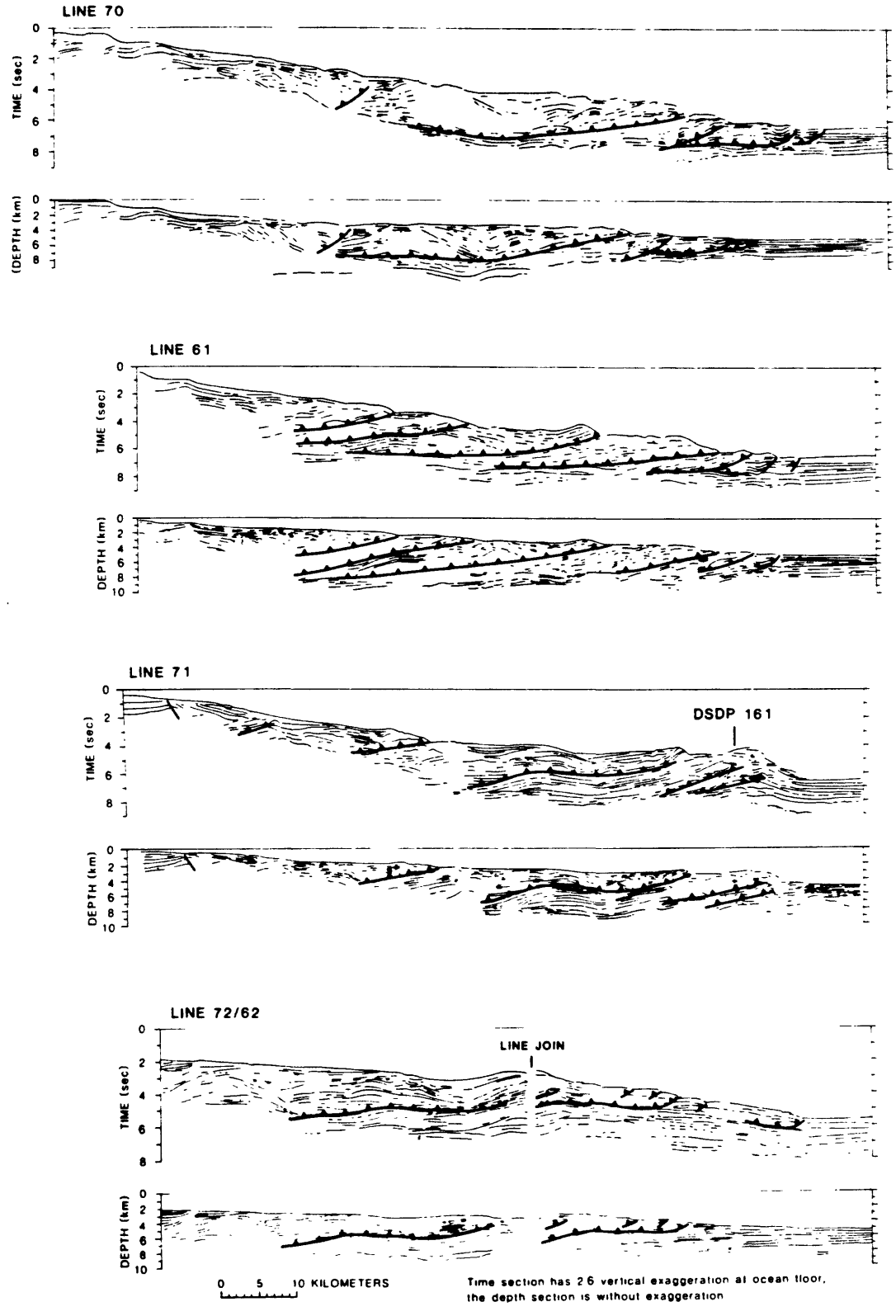

Figure 5. Time and depth sections of seismic lines 61, 70, 71, and 72/62 from seismic grid B (Fig. 2).

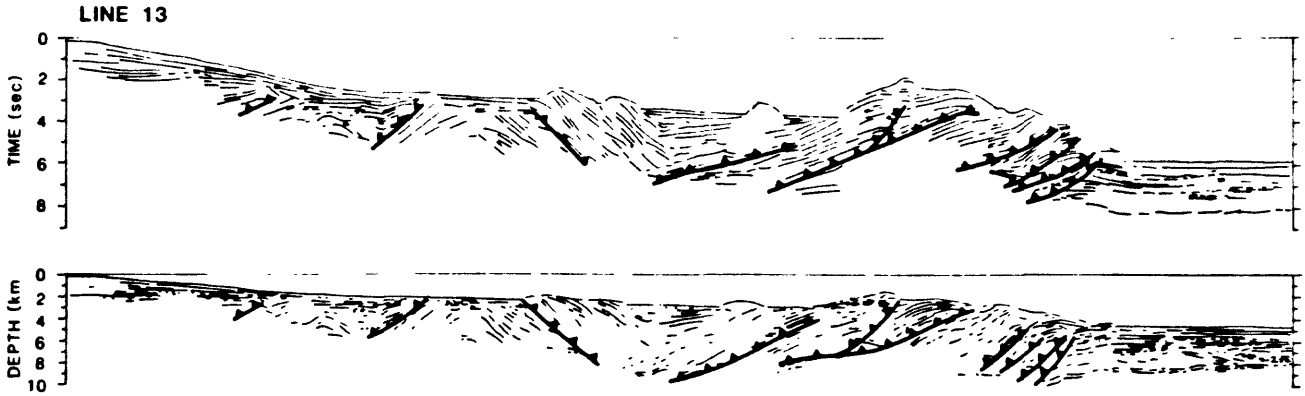

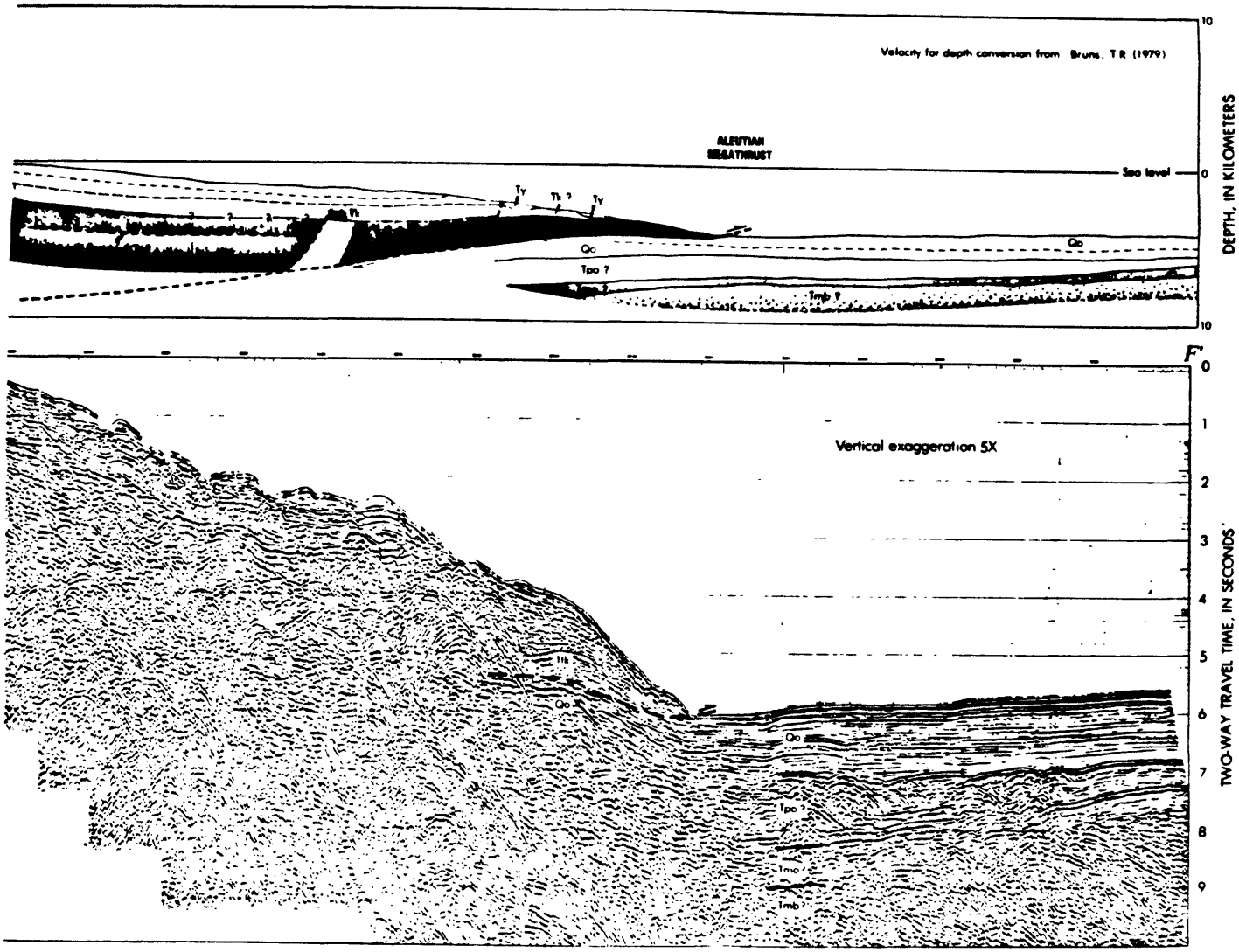

Figure 6. (Top) Time and depth sections of seismic line 13 which is the same as line C (Fig. 2).
(Bottom) Depth and time sections of seismic line D (Fig. 2) from Plafker, et al. (1982).

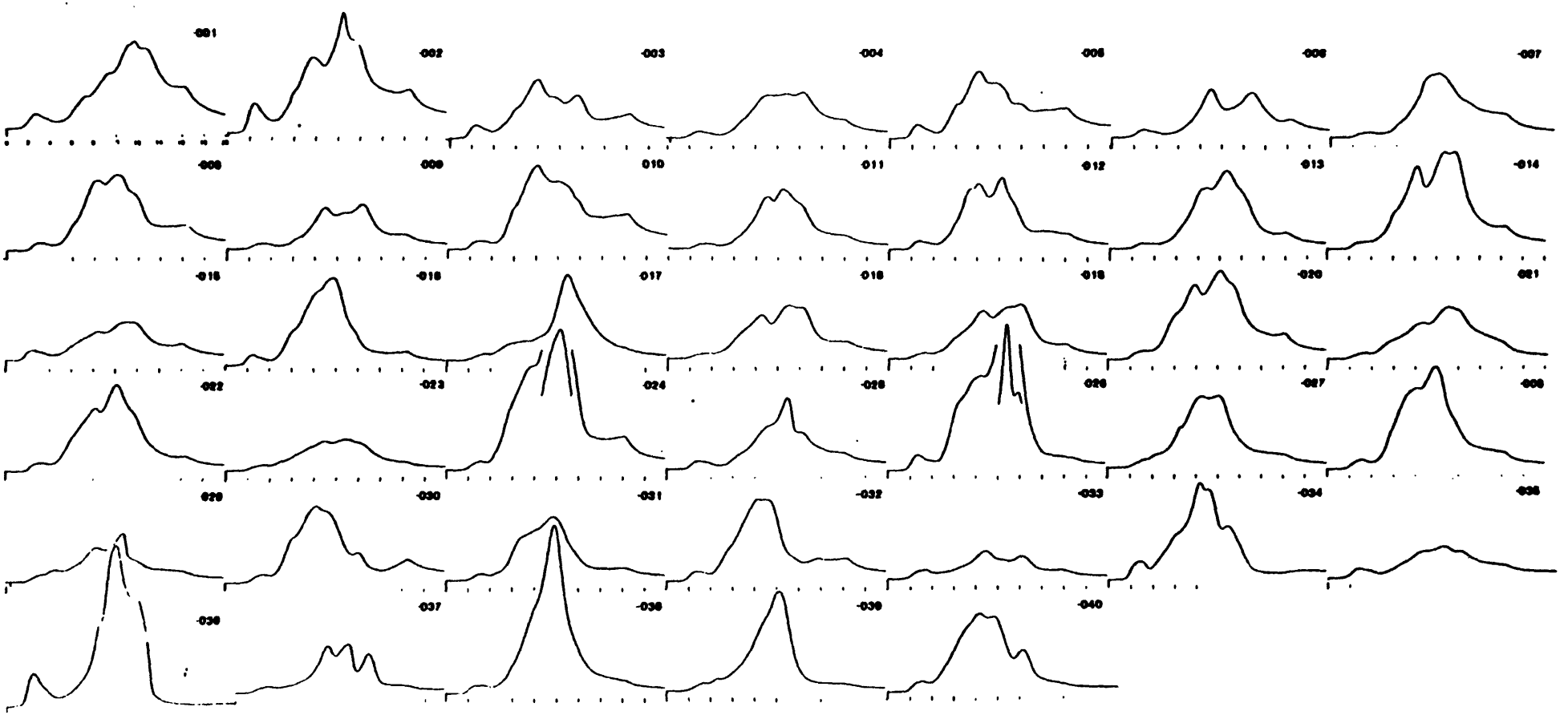

Figure 7. Pyrograms from TEA/FID analyses of 40 samples used in this report. The curves show the profile of the release of volatile material as temperature is increased during pyrolysis. Temperature increases to the right on the horizontal axis; amount of released volatiles increases upward on the vertical axis.

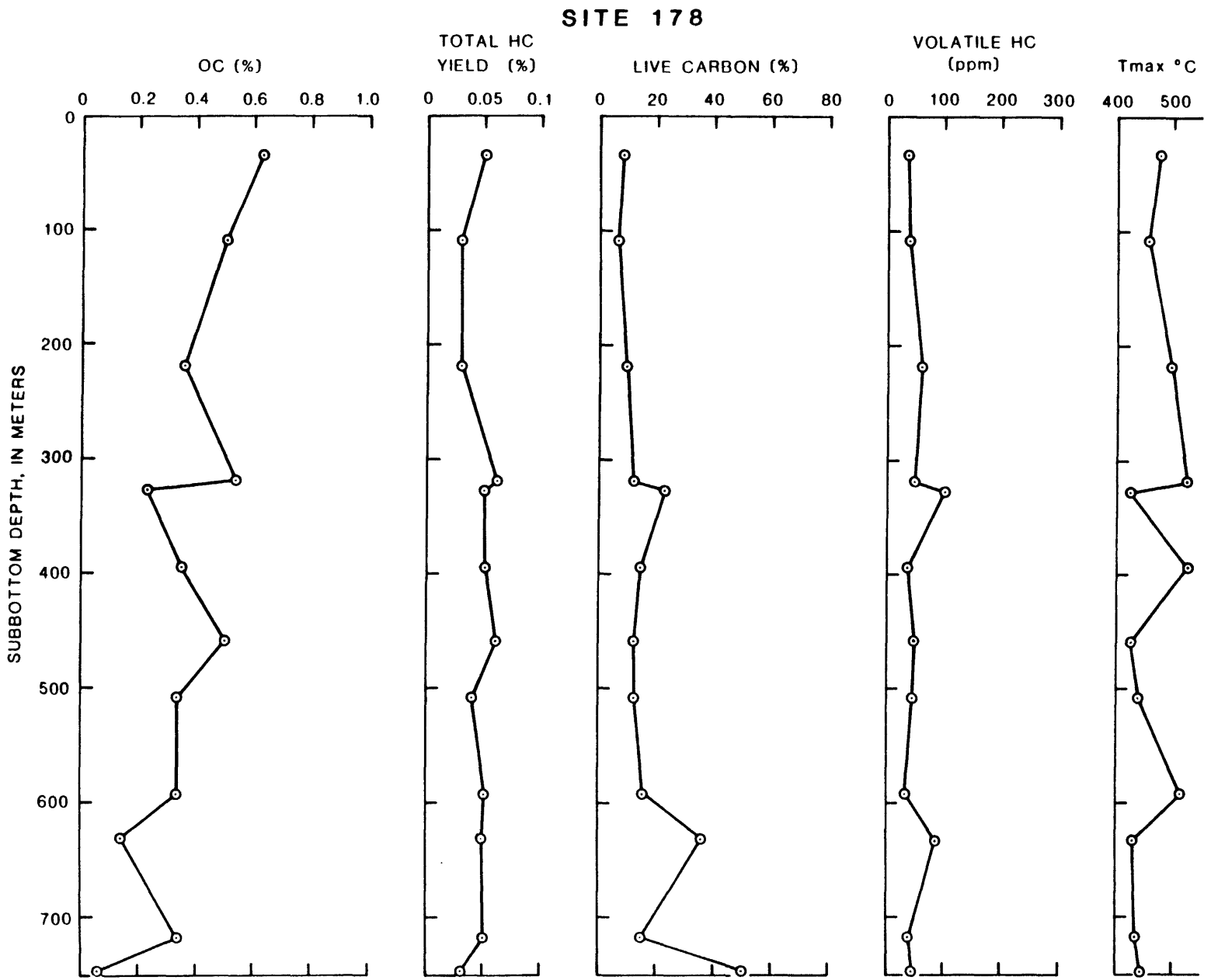

Figure 8a. Profiles with depth of organic geochemical results [organic carbon (OC); total hydrocarbon (HC) yield; live carbon; volatile hydrocarbons; temperature at maximum yield of pyrolysis products (Tmax)] for DSDP site 178.

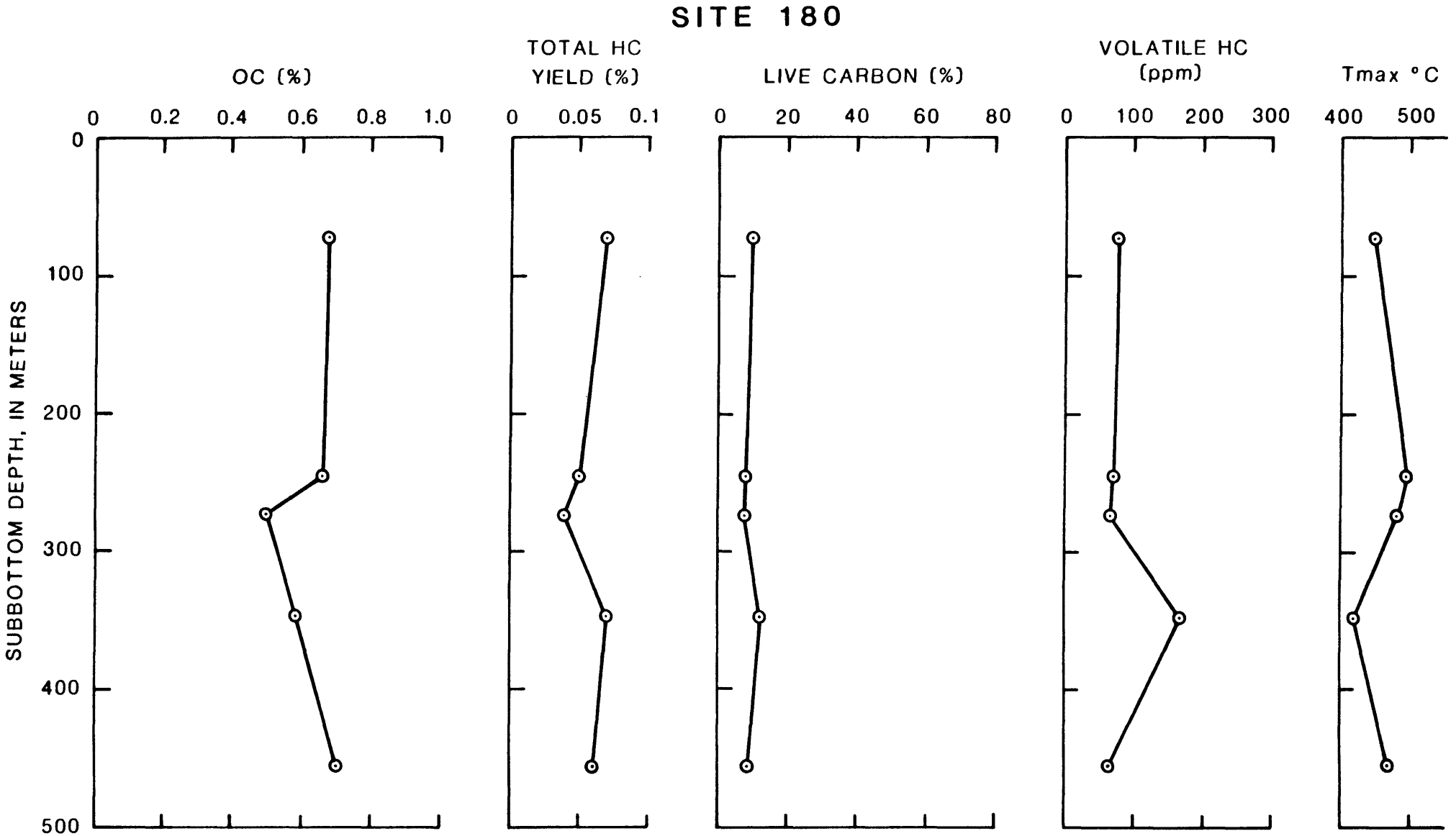

Figure 8b. Profiles with depth of organic geochemical results [organic carbon (OC); total hydrocarbon (HC) yield; live carbon; volatile hydrocarbons; temperature at maximum yield of pyrolysis products (Tmax)] for DSDP site 180.

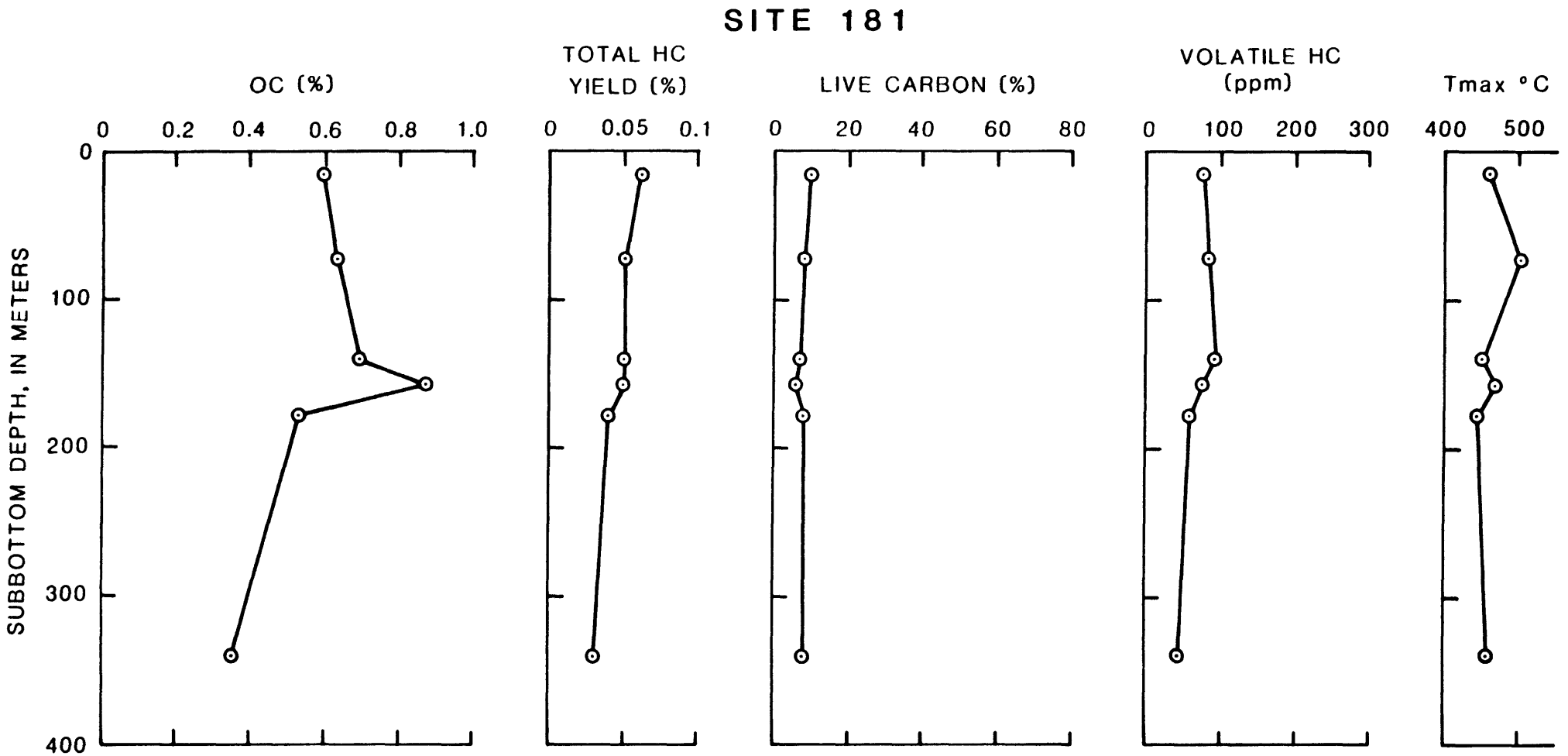

Figure 8c. Profiles with depth of organic geochemical results [organic carbon (OC); total hydrocarbon (HC) yield; live carbon; volatile hydrocarbons; temperature at maximum yield of pyrolysis products (Tmax)] for DSDP site 181.

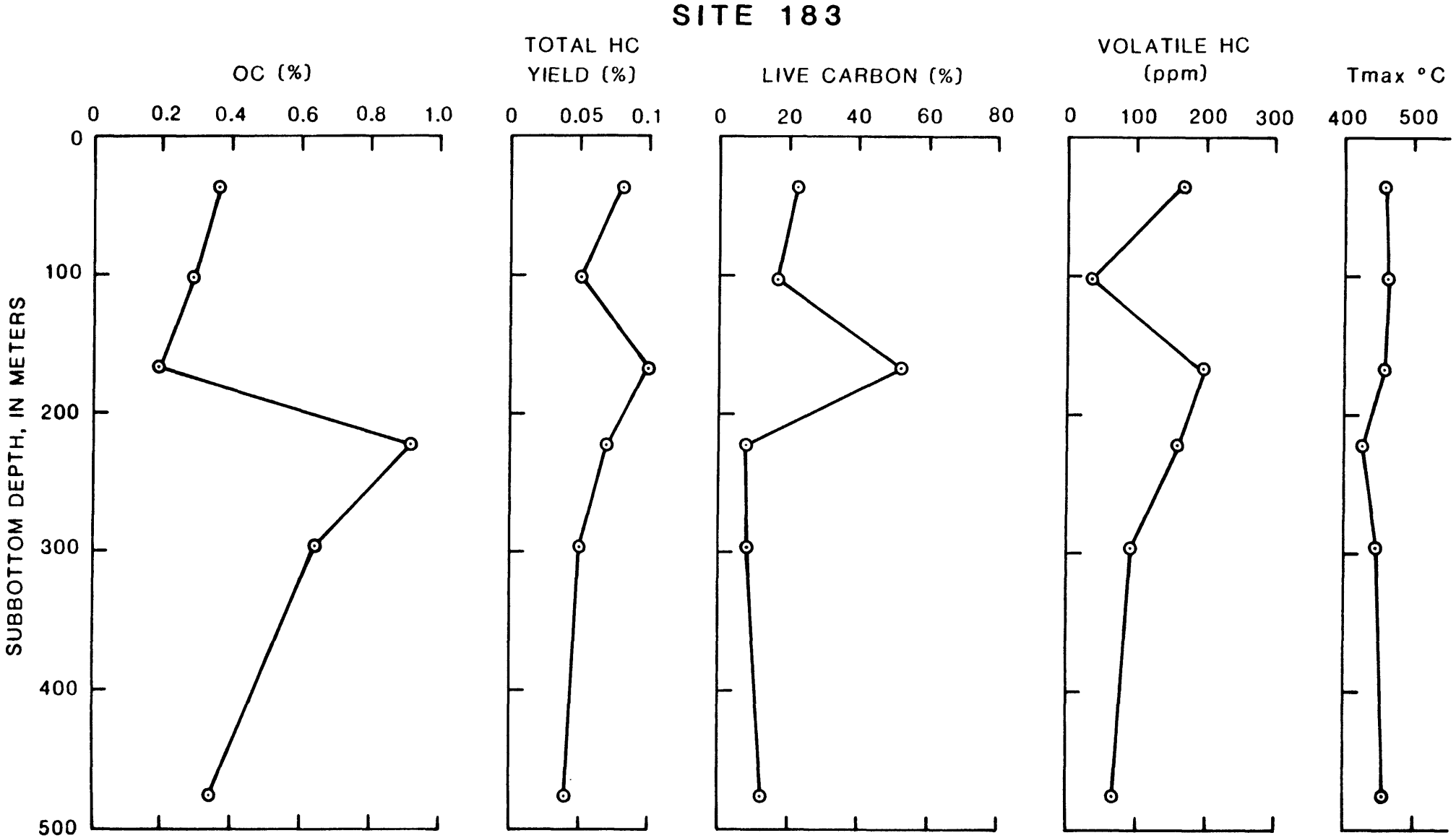

Figure 8d. Profiles with depth of organic geochemical results [organic carbon (OC); total hydrocarbon (HC) yield; live carbon; volatile hydrocarbons; temperature at maximum yield of pyrolysis products (Tmax)] for DSDP site 183.

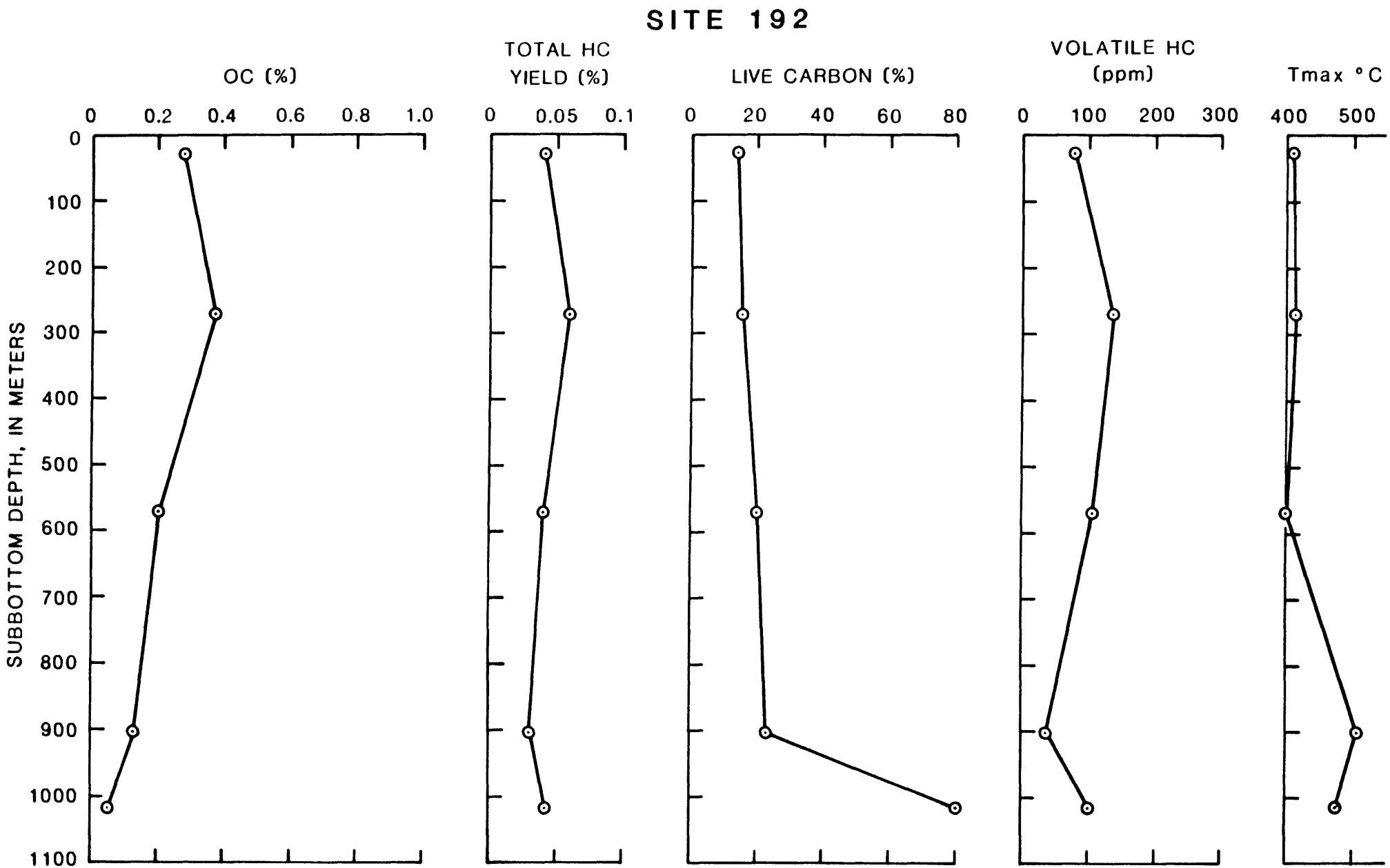

Figure 8c. Profiles with depth of organic geochemical results [organic carbon (OC); total hydrocarbon (HC) yield; live carbon; volatile hydrocarbons; temperature at maximum yield of pyrolysis products (Tmax)] for DSDP site 192.

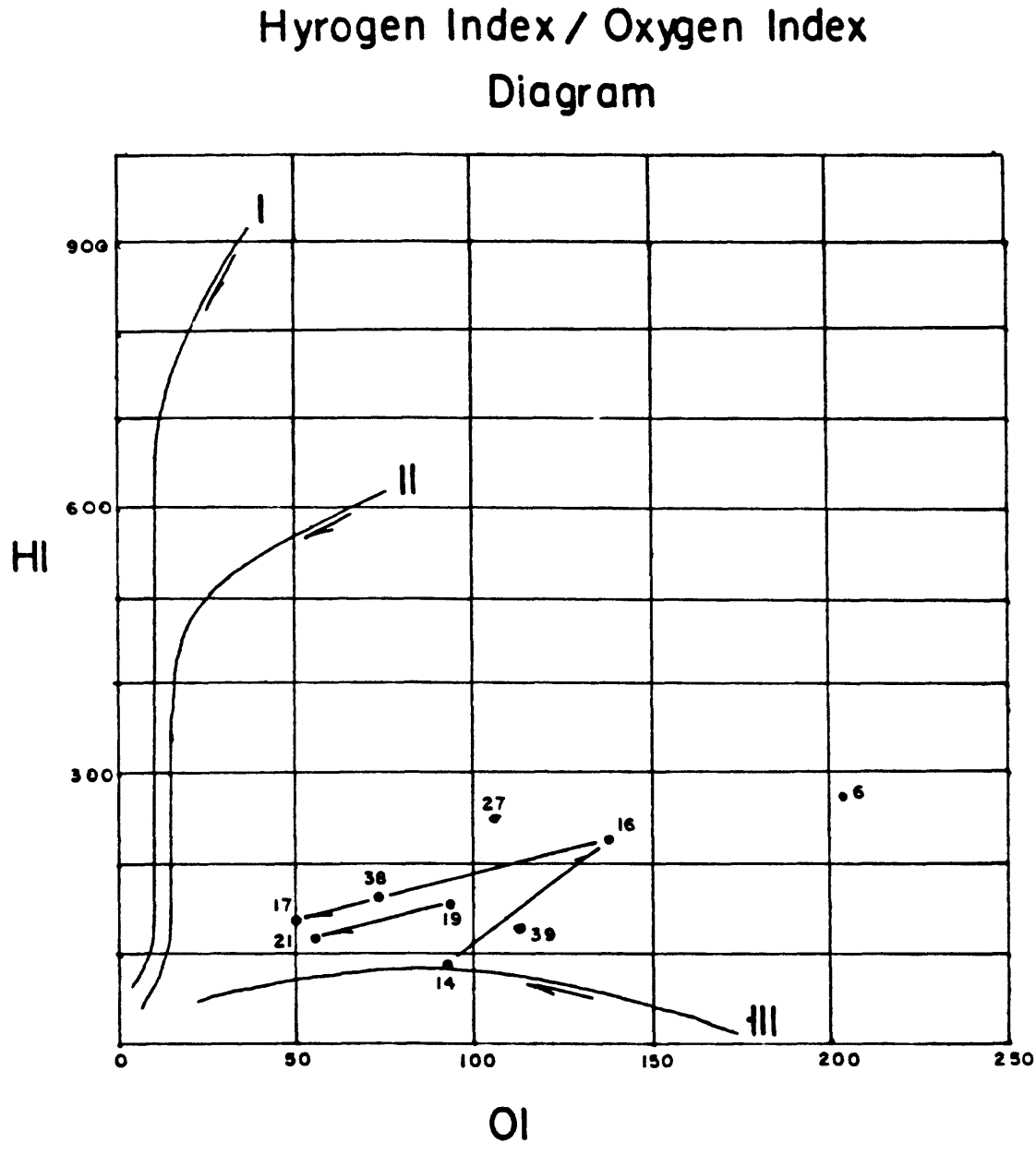

Figure 9. van Krevelen diagram showing the hydrogen index (HI) in mg HC/g OC and the oxygen index (OI) in mg CO_2/g OC for nine selected samples (Table 2). Results fall in the region of type III organic matter.

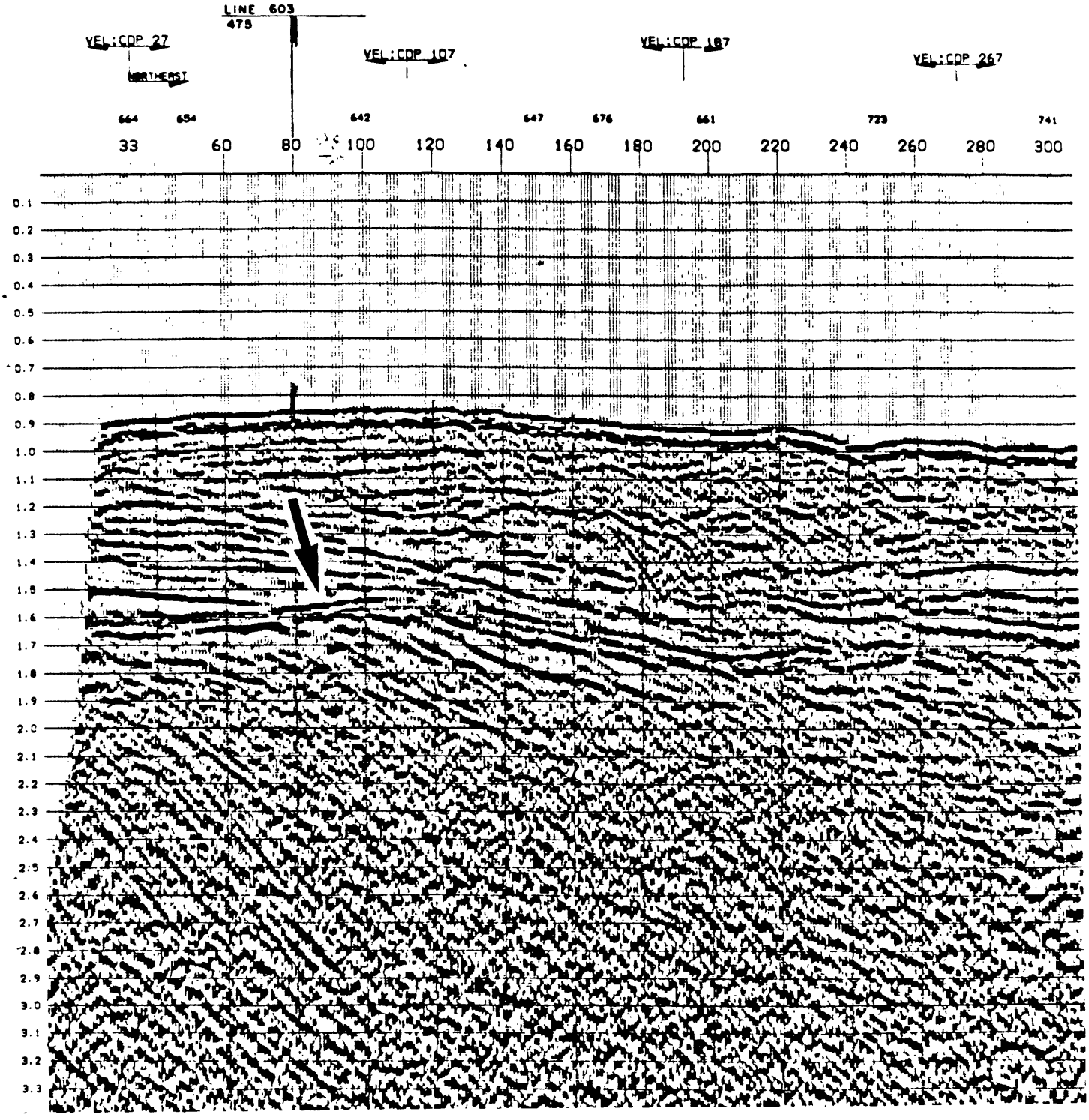

Figure 10. Example of a BSR (arrow) on seismic record 51 from grid B (Fig. 2).

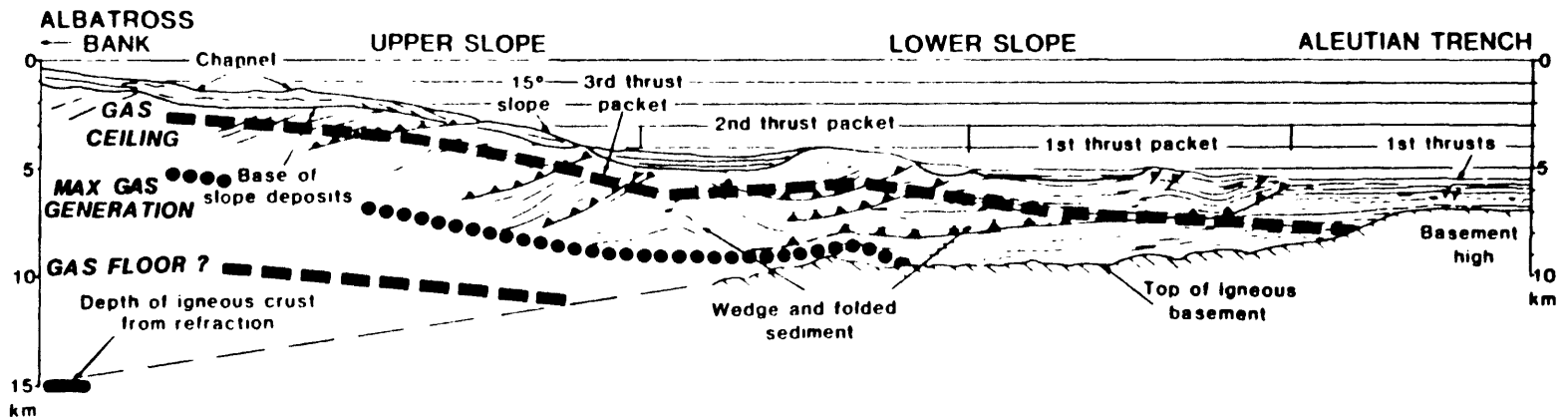

Figure 11. Isotherms at temperatures of 50°C (gas ceiling, i.e., the lowest temperature for gas generation), 150°C (temperature of maximum gas generation), and 250°C (gas floor, i.e., the highest temperature for gas generation) superimposed on seismic line 111 Fig. 4) based on a constant geothermal gradient of 30°C/km.

APPENDIX 1. Lithologic Logs of DSDP Cores Showing Samples (■) Used in This Report. Logs Were Reproduced from The Initial Reports of the Deep Sea Drilling Project, Volumes 18 and 19.

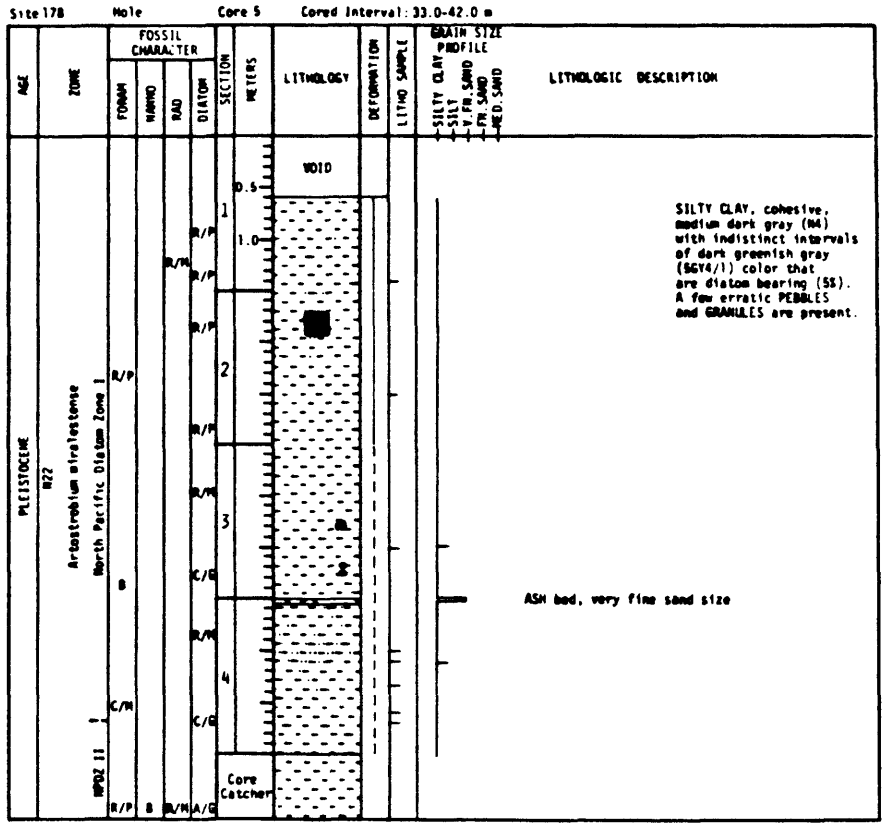

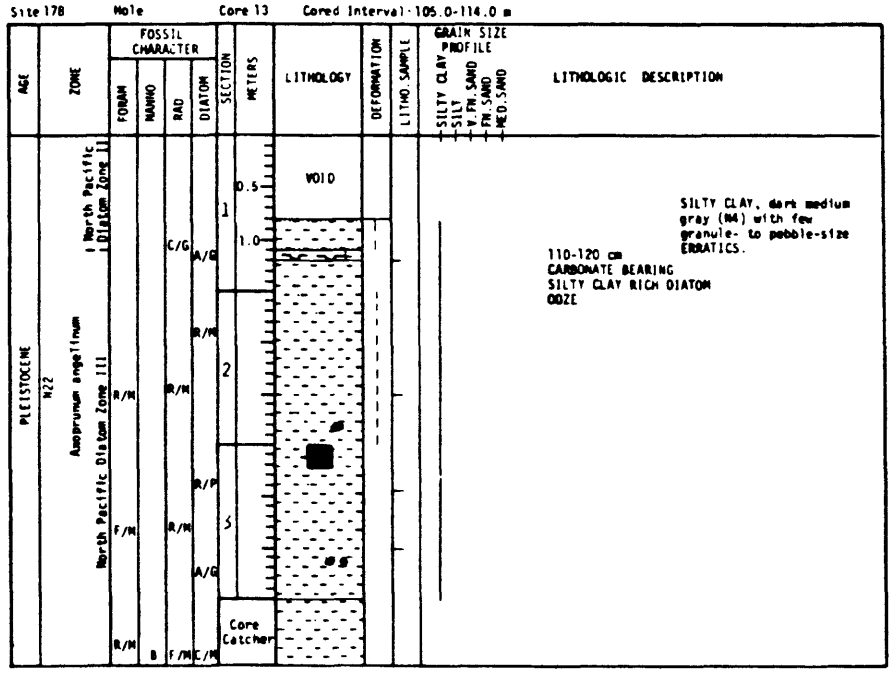

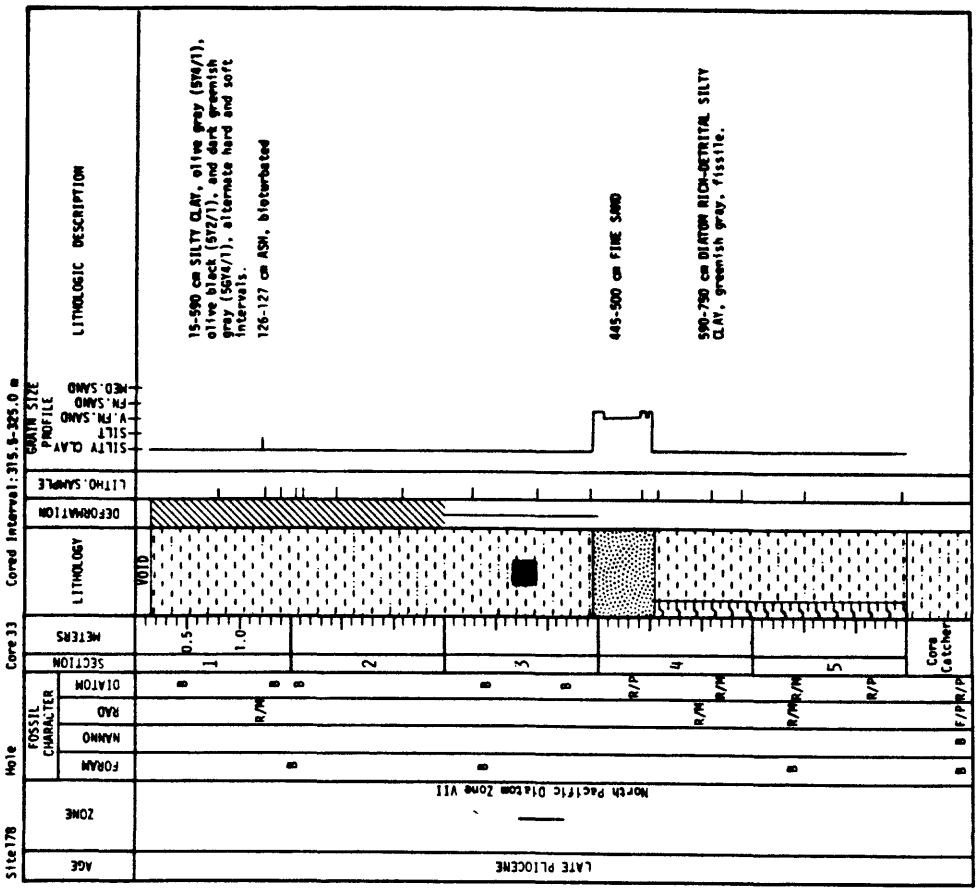
Site 178
Hole
Core 33
Cored Interval: 315.5-325.0 m
AGE
ZONE
FOSSIL CHARACTER
DIATOM
RAD
NANNO
FORAM
SECTION
METERS
LITHOLOGY
DEFORMATION
LITHO. SAMPLE
GRAIN SIZE PROFILE
SILTY CLAY
SILT
V. FN. SAND
FN. SAND
MED. SAND
LITHOLOGIC DESCRIPTION
LATE PLIOCENE
North Pacific Diatom Zone VII
VOID
15-590 cm SILTY CLAY, olive gray (5Y4/1), olive black (5Y2/1), and dark greenish gray (5GY4/1), alternate hard and soft intervals.
126-127 cm ASH, bioturbated
445-500 cm FINE SAND
590-790 cm DIATOM RICH-DETRITAL SILTY CLAY, greenish gray, fissile.
Core Catcher

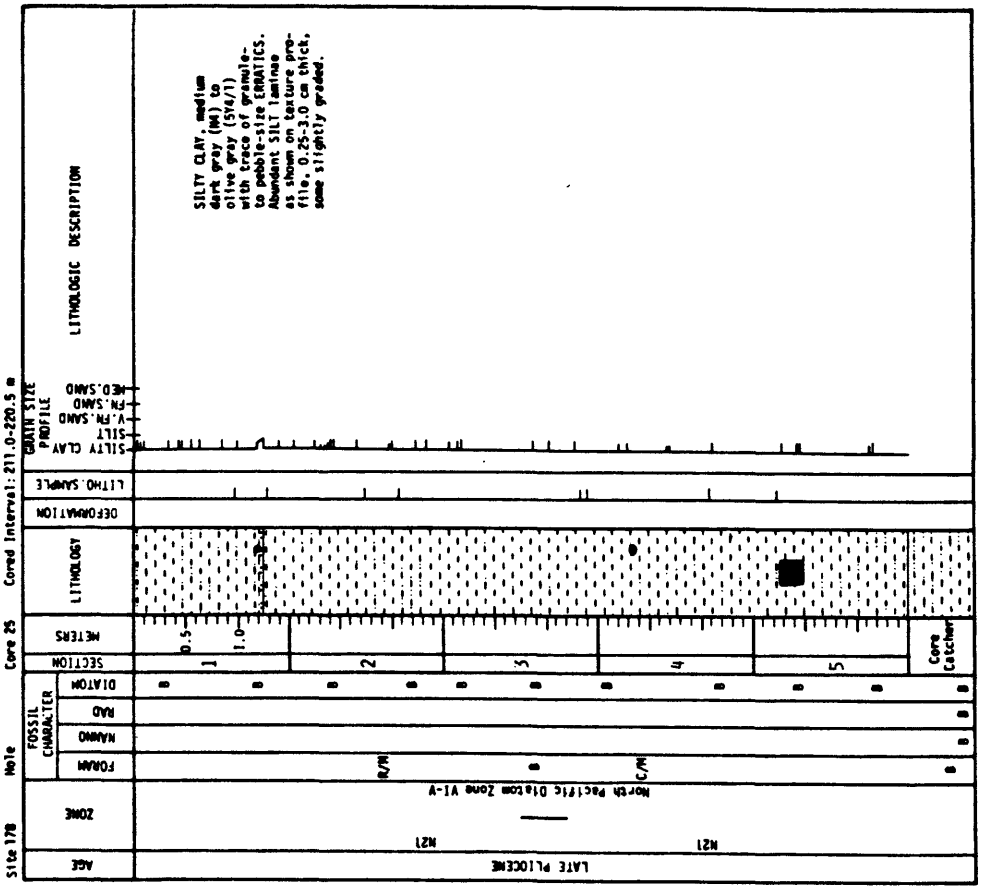
Site 178
Hole
Core 25
Cored Interval: 211.0-220.5 m
AGE
ZONE
FOSSIL CHARACTER
DIATOM
RAD
NANNO
FORAM
SECTION
METERS
LITHOLOGY
DEFORMATION
LITHO. SAMPLE
GRAIN SIZE PROFILE
SILTY CLAY
SILT
V. FN. SAND
FN. SAND
MED. SAND
LITHOLOGIC DESCRIPTION
LATE PLIOCENE
N21
North Pacific Diatom Zone VI-V
SILTY CLAY, medium dark gray (N4) to olive gray (5Y4/1) with trace of granule- to pebble-size ERRATICS. Abundant SILT laminae as shown on texture profile, 0.25-3.0 cm thick, some slightly graded.
Core Catcher

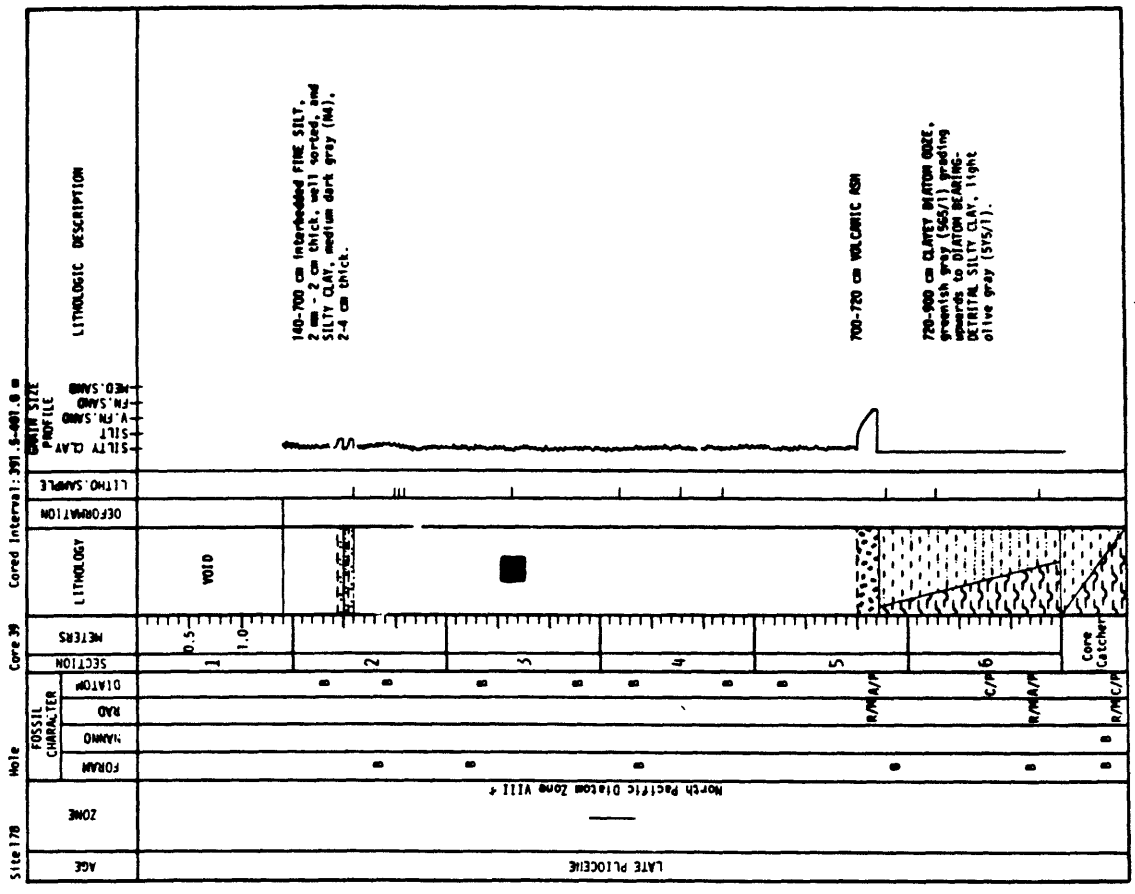
Site 178
Hole
Core 39
Cored Interval: 391.5-401.0 m
AGE
ZONE
FOSSIL CHARACTER
FORAM
NANNO
RAD
DIATOM
SECTION
METERS
LITHOLOGY
DEFORMATION
LITHO. SAMPLE
GRAIN SIZE PROFILE
SILTY CLAY
SILT
V.FN.SAND
FN.SAND
MED.SAND
LITHOLOGIC DESCRIPTION
LATE PLIOCENE
North Pacific Diatom Zone VII +
VOID
140-700 cm interbedded FINE SILT, 2 mm - 2 cm thick, well sorted, and SILTY CLAY, medium dark gray (N4), 2-4 cm thick.
700-720 cm VOLCANIC ASH
720-900 cm CLAYEY DIATOM OOZE, greenish gray (5G6/1), grading upwards to DIATOM BEARING-DETRITAL SILTY CLAY, light olive gray (5Y5/1).
Core Catcher

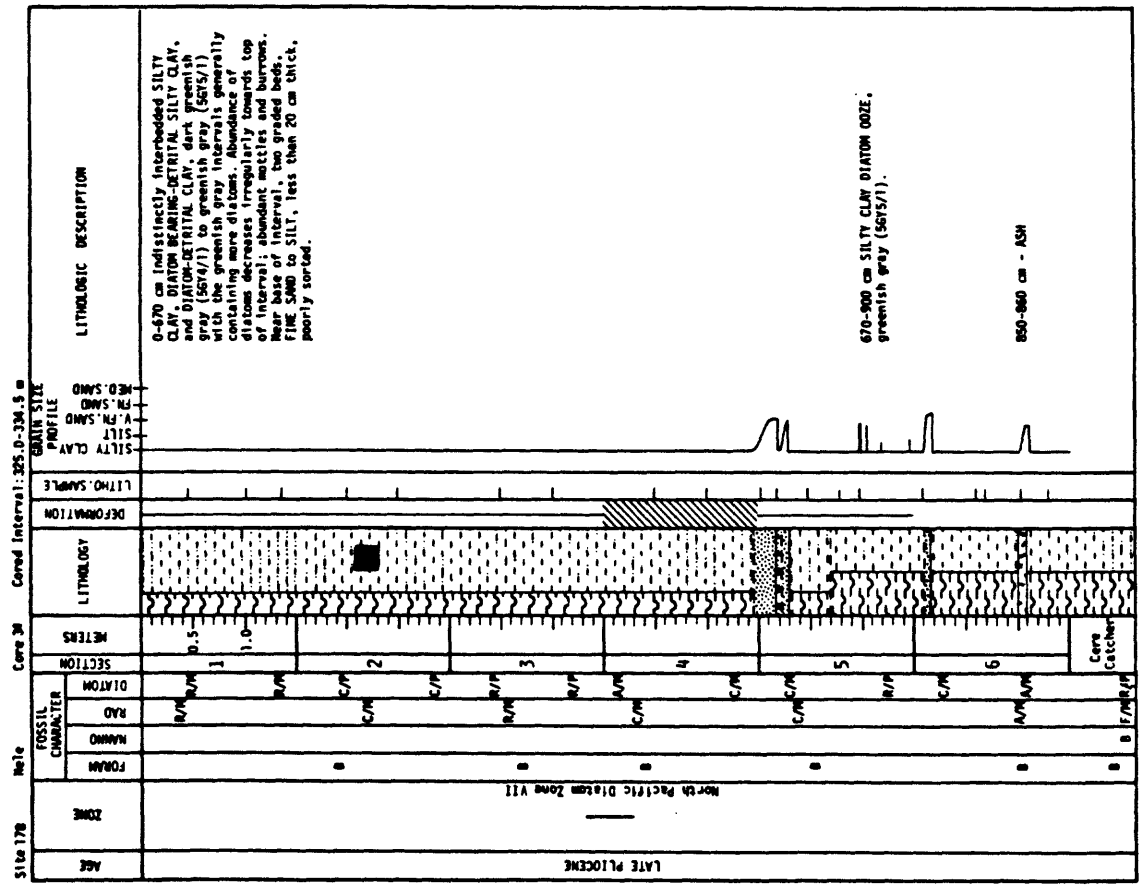
Site 178
Hole
Core 38
Cored Interval: 325.0-334.5 m
AGE
ZONE
FOSSIL CHARACTER
FORAM
NANNO
RAD
DIATOM
SECTION
METERS
LITHOLOGY
DEFORMATION
LITHO. SAMPLE
GRAIN SIZE PROFILE
SILTY CLAY
SILT
V.FN.SAND
FN.SAND
MED.SAND
LITHOLOGIC DESCRIPTION
LATE PLIOCENE
North Pacific Diatom Zone VII
0-670 cm indistinctly interbedded SILTY CLAY, DIATOM BEARING-DETRITAL SILTY CLAY, and DIATOM-DETRITAL CLAY, dark greenish gray (5G4/1) to greenish gray (5G5/1) with the greenish gray intervals generally containing more diatoms. Abundance of diatoms decreases irregularly towards top of interval; abundant mottles and burrows. Near base of interval, two graded beds. FINE SAND to SILT, less than 20 cm thick, poorly sorted.
670-900 cm SILTY CLAY DIATOM OOZE, greenish gray (5G5/1).
850-860 cm - ASH
Core Catcher

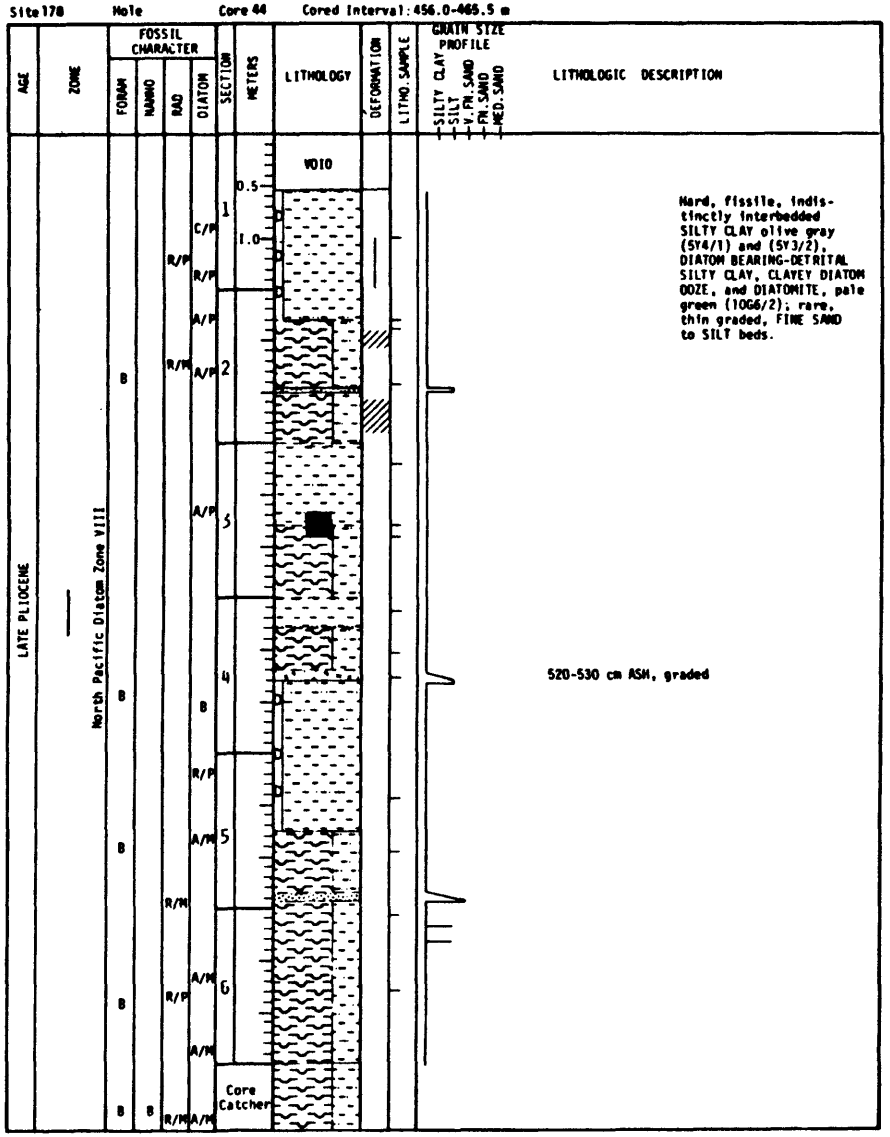
Site 178
Hole
Core 44
Cored Interval: 456.0-466.5 m
AGE
ZONE
FOSSIL CHARACTER
FORAM
NANNO
RAD
DIATOM
SECTION
METERS
LITHOLOGY
DEFORMATION
LITHO. SAMPLE
GRAIN SIZE PROFILE
SILTY CLAY
SILT
V. FN. SAND
FN. SAND
MED. SAND
LITHOLOGIC DESCRIPTION
LATE PLIOCENE
North Pacific Diatom Zone VIII
VOID
Core Catcher
Hard, fissile, indistinctly interbedded SILTY CLAY olive gray (5Y4/1) and (5Y3/2), DIATOM BEARING-DETRITAL SILTY CLAY, CLAYEY DIATOM OOZE, and DIATOMITE, pale green (10G6/2); rare, thin graded, FINE SAND to SILT beds.
520-530 cm ASH, graded

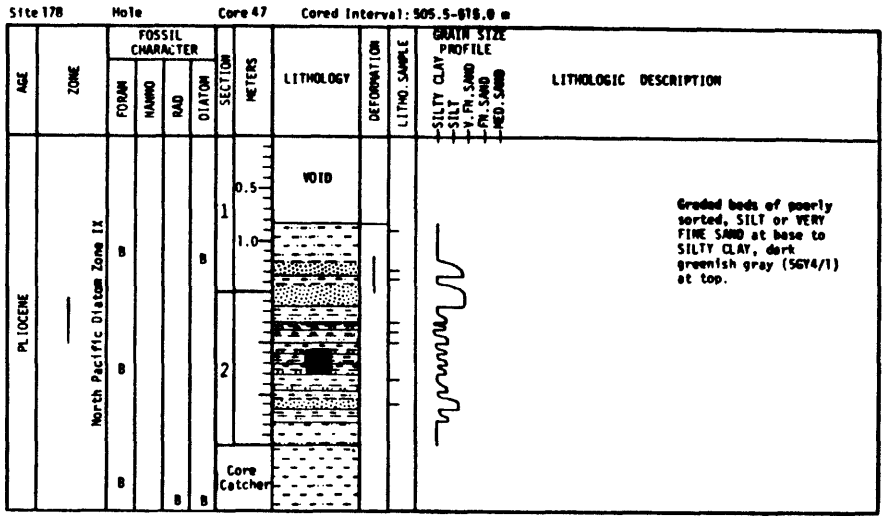
Site 178
Hole
Core 47
Cored Interval: 505.5-515.0 m
AGE
ZONE
FOSSIL CHARACTER
FORAM
NANNO
RAD
DIATOM
SECTION
METERS
LITHOLOGY
DEFORMATION
LITHO. SAMPLE
GRAIN SIZE PROFILE
SILTY CLAY
SILT
V. FN. SAND
FN. SAND
MED. SAND
LITHOLOGIC DESCRIPTION
PLIOCENE
North Pacific Diatom Zone IX
VOID
Core Catcher
Graded beds of poorly sorted, SILT or VERY FINE SAND at base to SILTY CLAY, dark greenish gray (5GY4/1) at top.

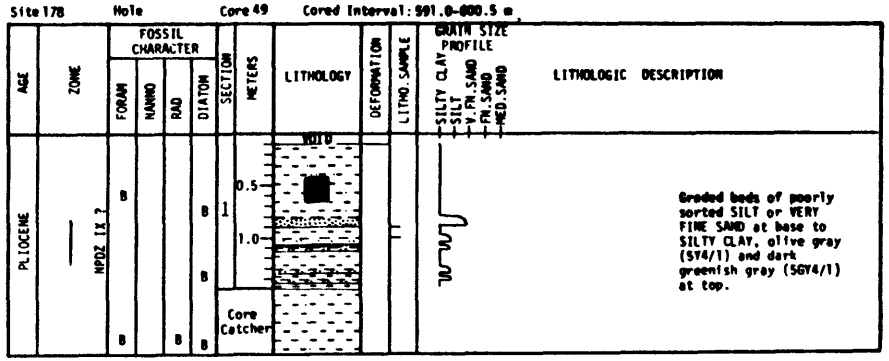
Site 178
Hole
Core 49
Cored Interval: 991.0-600.5 m
AGE
ZONE
FOSSIL CHARACTER
FORAM
NANNO
RAD
DIATOM
SECTION
METERS
LITHOLOGY
DEFORMATION
LITHO. SAMPLE
GRAIN SIZE PROFILE
SILTY CLAY
SILT
V. FN. SAND
FN. SAND
MED. SAND
LITHOLOGIC DESCRIPTION
PLIOCENE
NPDZ IX ?
VOID
Core Catcher
Graded beds of poorly sorted SILT or VERY FINE SAND at base to SILTY CLAY, olive gray (5Y4/1) and dark greenish gray (5GY4/1) at top.

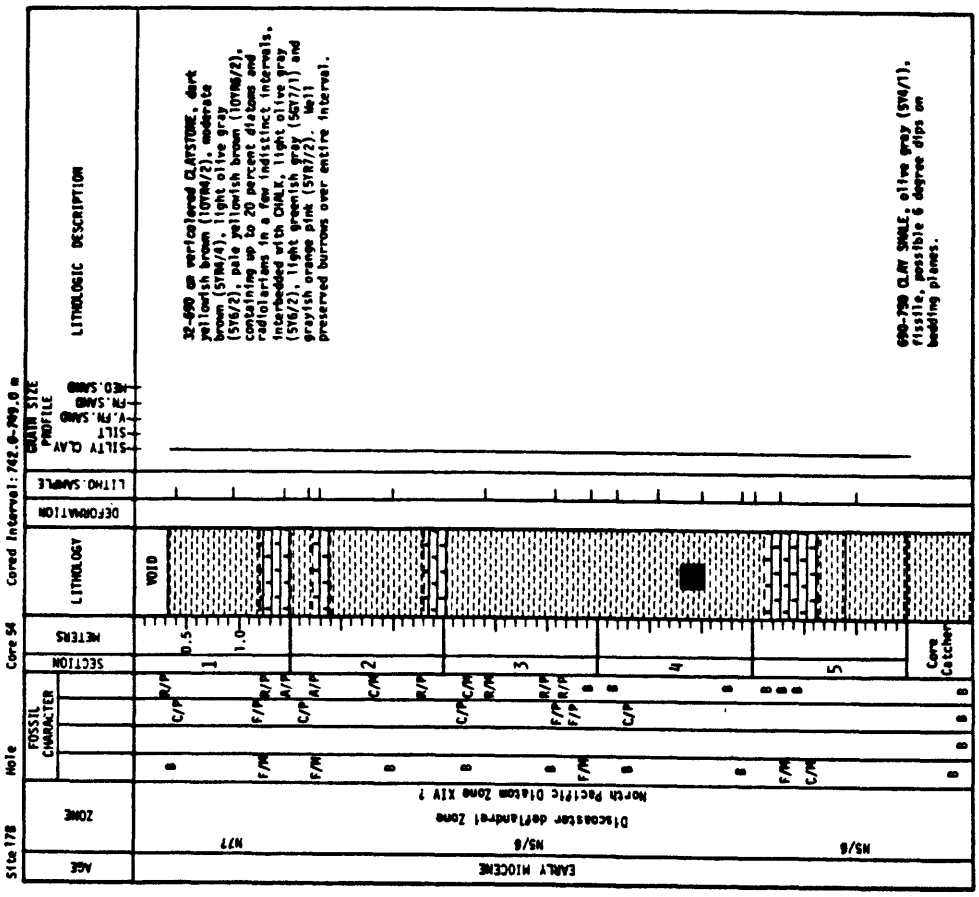
Site 178
Hole
Core 54
Cored Interval: 742.0-799.0 m
AGE
EARLY MIOCENE
ZONE
Discoaster deflandrei Zone
North Pacific Diatom Zone XIV ?
FOSSIL CHARACTER
SECTION
METERS
LITHOLOGY
VOID
DEFORMATION
LITHO. SAMPLE
GRAIN SIZE PROFILE
SILTY CLAY
SILT
V.FN. SAND
FN. SAND
MED. SAND
LITHOLOGIC DESCRIPTION
32-680 cm variegated CLAYSTONE, dark yellowish brown (10YR4/2), moderate brown (5YR4/4), light olive gray (5Y6/2), pale yellowish brown (10YR6/2), containing up to 20 percent diatoms and radiolarians in a few indistinct intervals, interbedded with CHALK, light olive gray (5Y6/2), light greenish gray (5GY7/1) and grayish orange pink (5YR7/2). Well preserved burrows over entire interval.
680-799 CLAY SHALE, olive gray (5Y4/1), fissile, possible 6 degree dips on bedding planes.
Core Catcher
N77
N5/6
N5/6

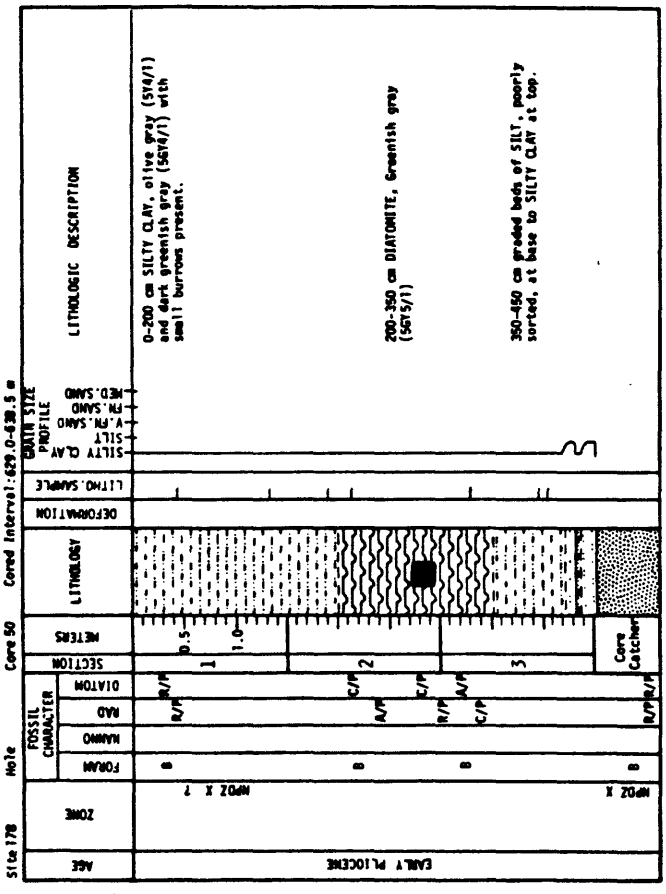
Site 178
Hole
Core 50
Cored Interval: 629.0-638.5 m
AGE
EARLY PLIOCENE
ZONE
NPOZ X ?
NPOZ X
FOSSIL CHARACTER
FORAM
NANNO
RAD
DIATOM
SECTION
METERS
LITHOLOGY
DEFORMATION
LITHO. SAMPLE
GRAIN SIZE PROFILE
SILTY CLAY
SILT
V.FN. SAND
FN. SAND
MED. SAND
LITHOLOGIC DESCRIPTION
0-200 cm SILTY CLAY, olive gray (5Y4/1) and dark greenish gray (5GY4/1) with small burrows present.
200-350 cm DIATOMITE, Greenish gray (5GY5/1)
350-450 cm graded beds of SILT, poorly sorted, at base to SILTY CLAY at top.
Core Catcher

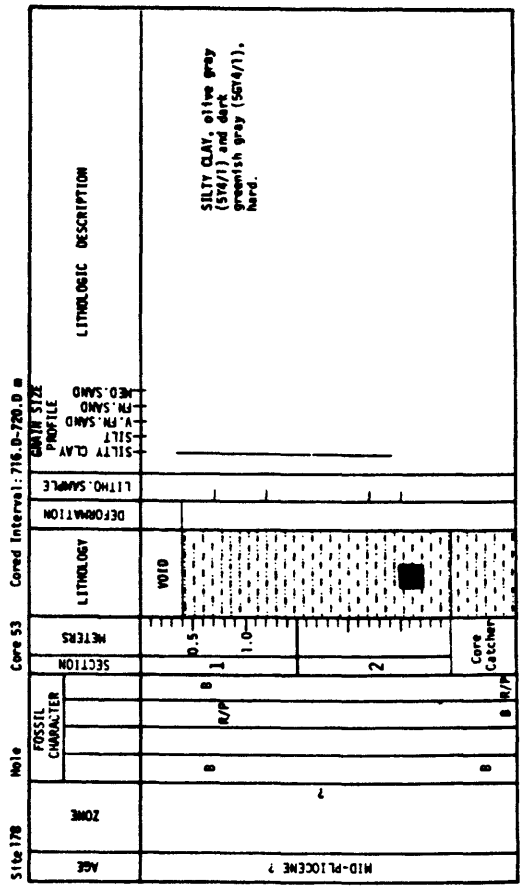
Site 178
Hole
Core 53
Cored Interval: 716.0-720.0 m
AGE
MID-PLIOCENE ?
ZONE
?
FOSSIL CHARACTER
SECTION
METERS
LITHOLOGY
VOID
DEFORMATION
LITHO. SAMPLE
GRAIN SIZE PROFILE
SILTY CLAY
SILT
V.FN. SAND
FN. SAND
MED. SAND
LITHOLOGIC DESCRIPTION
SILTY CLAY, olive gray (5Y4/1) and dark greenish gray (5GY4/1). Hard.
Core Catcher

Site 180 Hole Core 8 Cored Interval: 66.5-76.0 m

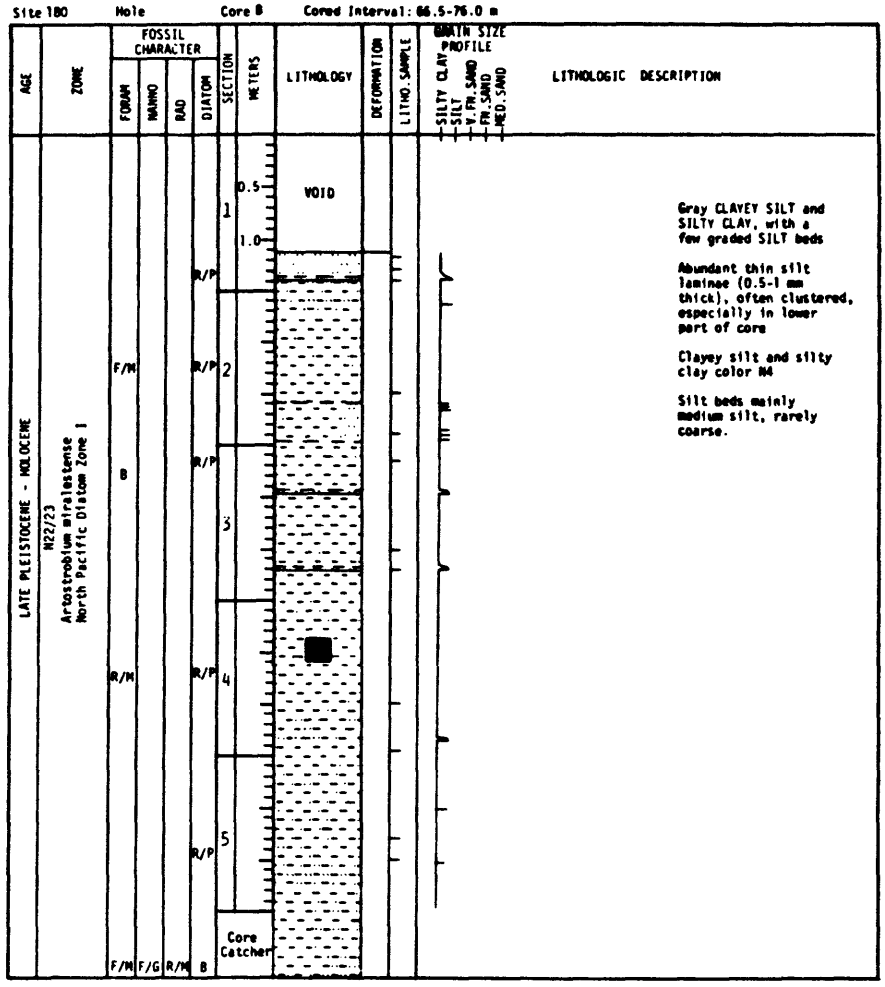

Site 180 Hole Core 15 Cored Interval: 242.5-252.0 m

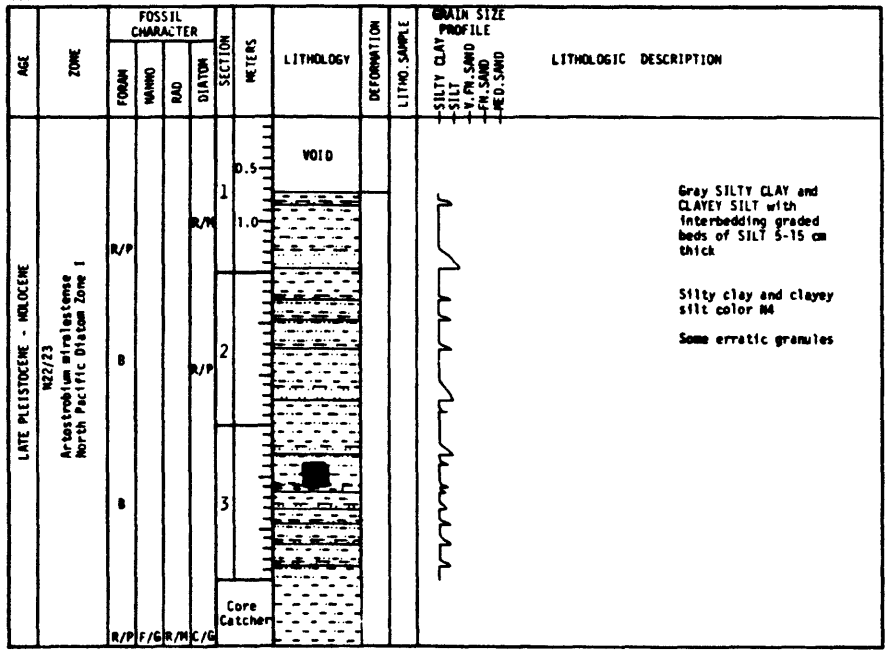

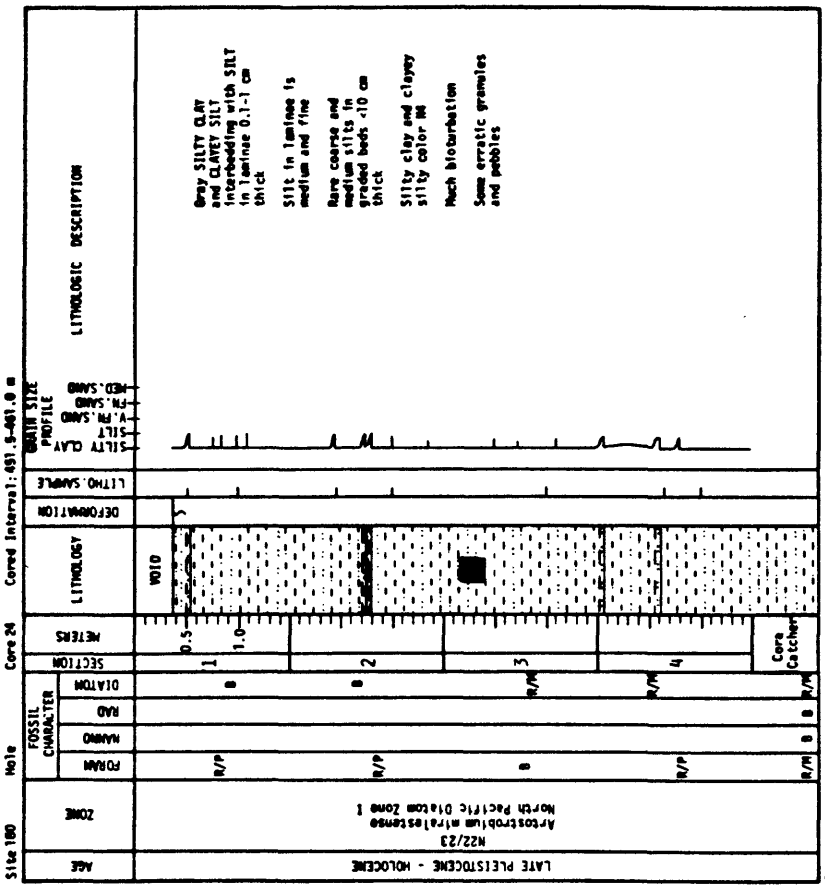
Site 180
Hole
Core 24
Cored Interval: 451.5-461.0 m
AGE
ZONE
FOSSIL CHARACTER
FORAM
NANNO
RAD
DIATOM
SECTION
METERS
LITHOLOGY
DEFORMATION
LITHO. SAMPLE
GRAIN SIZE PROFILE
SILTY CLAY
SILT
V.FN.SAND
FN.SAND
MED.SAND
LITHOLOGIC DESCRIPTION
LATE PLEISTOCENE - HOLOCENE
NZ22/23
Artostrobium mirabilostense
North Pacific Diatom Zone 1
VOID
Gray SILTY CLAY and CLAYEY SILT interbedding with SILT in laminae 0.1-1 cm thick
Silt in laminae is medium and fine
Rare coarse and medium silts in graded beds <10 cm thick
Silty clay and clayey silty color N4
Much bioturbation
Some erratic granules and pebbles
Core Catcher

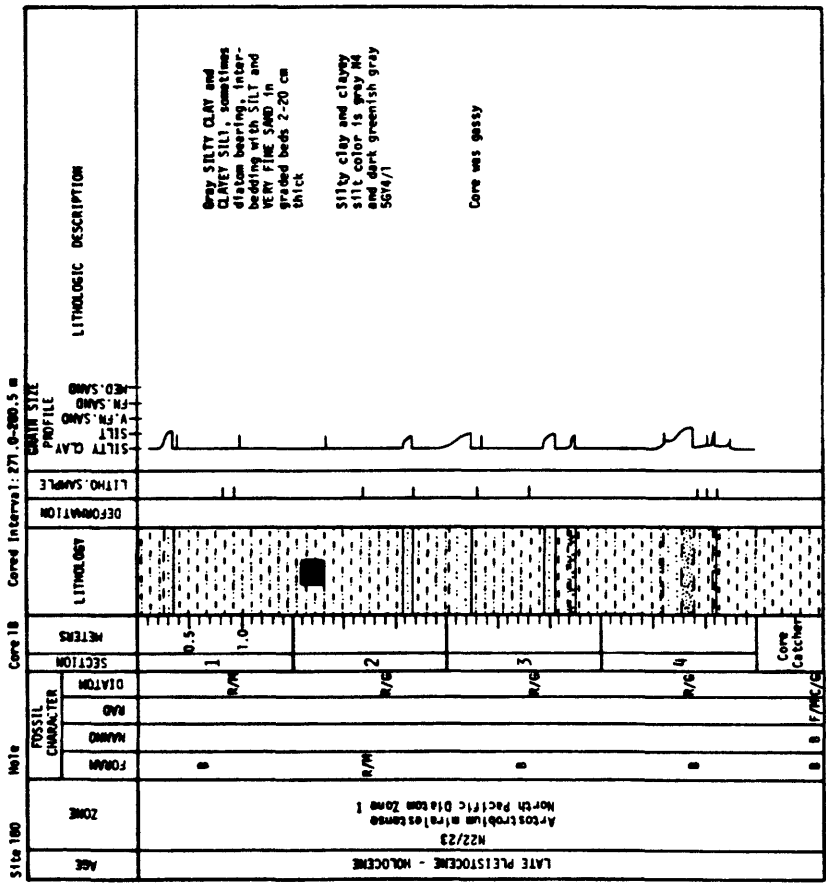
Site 180
Hole
Core 18
Cored Interval: 271.0-280.5 m
AGE
ZONE
FOSSIL CHARACTER
FORAM
NANNO
RAD
DIATOM
SECTION
METERS
LITHOLOGY
DEFORMATION
LITHO. SAMPLE
GRAIN SIZE PROFILE
SILTY CLAY
SILT
V.FN.SAND
FN.SAND
MED.SAND
LITHOLOGIC DESCRIPTION
LATE PLEISTOCENE - HOLOCENE
NZ22/23
Artostrobium mirabilostense
North Pacific Diatom Zone 1
Gray SILTY CLAY and CLAYEY SILT sometimes diatom bearing, interbedding with SILT and VERY FINE SAND in graded beds 2-20 cm thick
Silty clay and clayey silt color is gray N4 and dark greenish gray 5GY4/1
Core was gassy
Core Catcher
Site 180
Hole
Core 19
Cored Interval: 347.0-356.5 m
AGE
ZONE
FOSSIL CHARACTER
FORAM
NANNO
RAD
DIATOM
SECTION
METERS
LITHOLOGY
DEFORMATION
LITHO. SAMPLE
GRAIN SIZE PROFILE
SILTY CLAY
SILT
V.FN.SAND
FN.SAND
MED.SAND
LITHOLOGIC DESCRIPTION
LATE PLEISTOCENE - HOLOCENE
NZ22/23
Artostrobium mirabilostense
North Pacific Diatom Zone 1
Gray SILTY CLAY and CLAYEY SILT with interbedding SILT and VERY FINE SAND in graded beds 2-20 cm thick
Silty clay and clayey silt color N4
Silt and sand poorly sorted
Core Catcher

Site 181 Hole Core 2 Cored Interval: 9.0-18.5 m

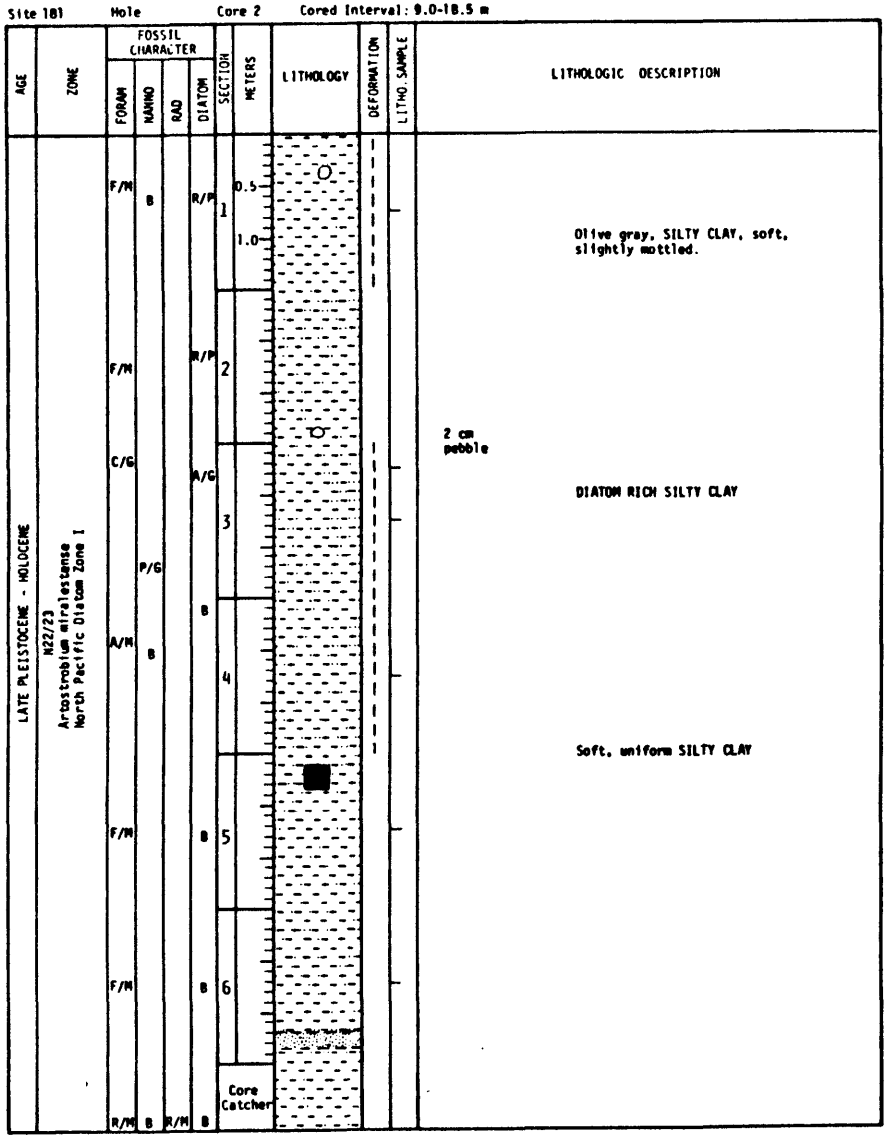

Site 181 Hole Core 8 Cored Interval: 66.6-75.5 m

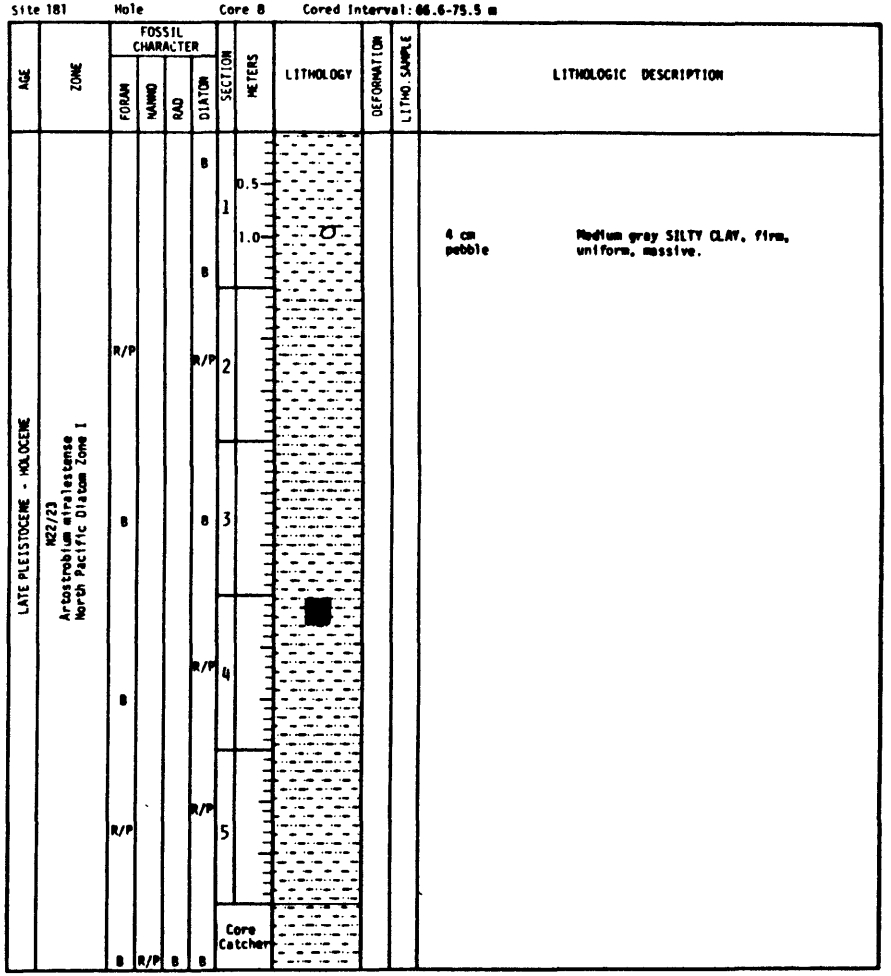

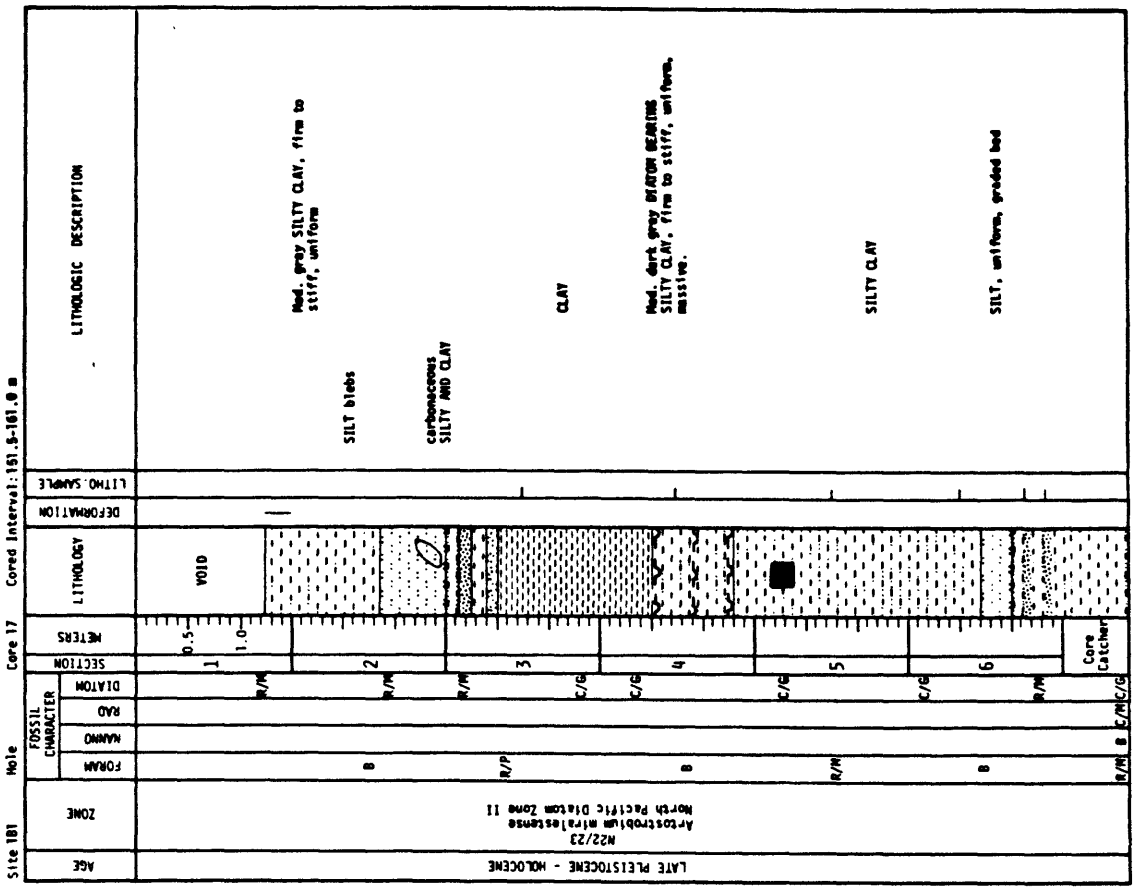
Site 181
Hole
Core 17
Cored Interval: 151.5-161.0 m
AGE
ZONE
FOSSIL CHARACTER
FORAM
NANNO
RAD
DIATOM
SECTION
METERS
LITHOLOGY
DEFORMATION
LITHO. SAMPLE
LITHOLOGIC DESCRIPTION
LATE PLEISTOCENE - HOLOCENE
N22/23
Arctostrobilum miralestense
North Pacific Diatom Zone II
VOID
Mod. gray SILTY CLAY, firm to stiff, uniform
SILT blebs
carbonaceous SILTY AND CLAY
CLAY
Mod. dark gray DIATOM BEARING SILTY CLAY, firm to stiff, uniform, massive.
SILTY CLAY
SILT, uniform, graded bed
Core Catcher

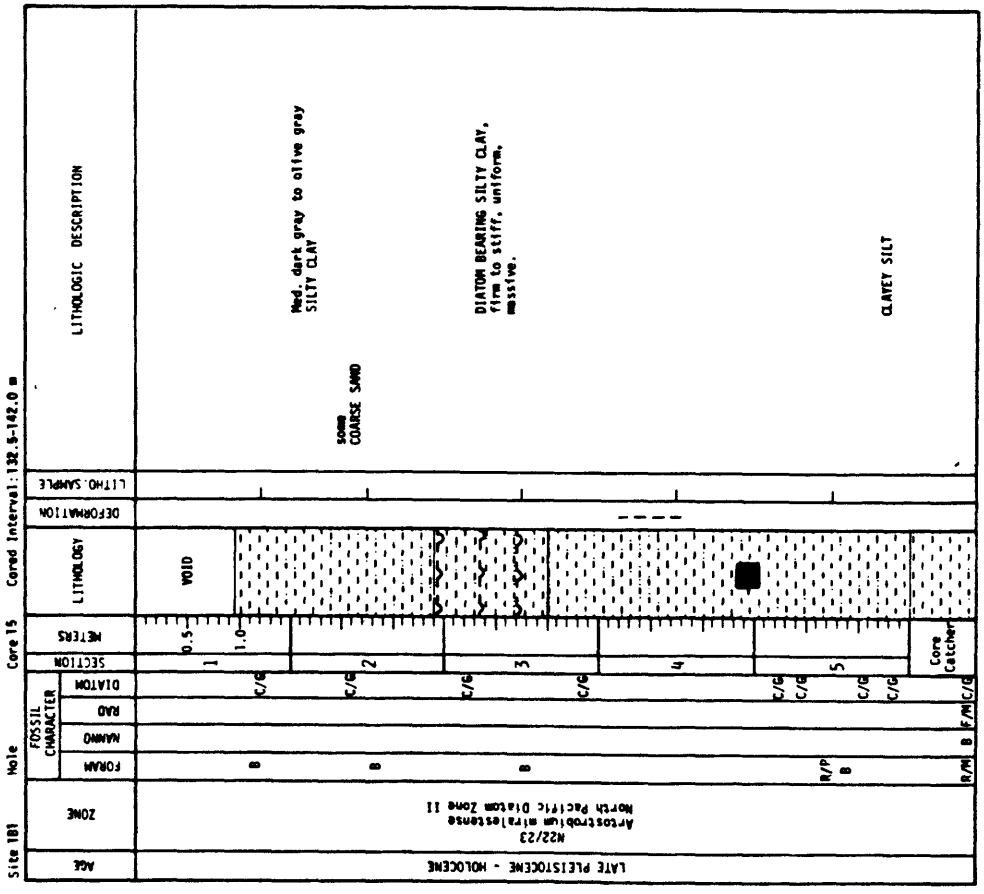
Site 181
Hole
Core 15
Cored Interval: 132.5-142.0 m
AGE
ZONE
FOSSIL CHARACTER
FORAM
NANNO
RAD
DIATOM
SECTION
METERS
LITHOLOGY
DEFORMATION
LITHO. SAMPLE
LITHOLOGIC DESCRIPTION
LATE PLEISTOCENE - HOLOCENE
N22/23
Arctostrobilum miralestense
North Pacific Diatom Zone II
VOID
Mod. dark gray to olive gray SILTY CLAY
SAND COARSE SAND
DIATOM BEARING SILTY CLAY, firm to stiff, uniform, massive.
CLAYEY SILT
Core Catcher

Site 181 Hole Core 20 Cored Interval: 177.0-186.5 m

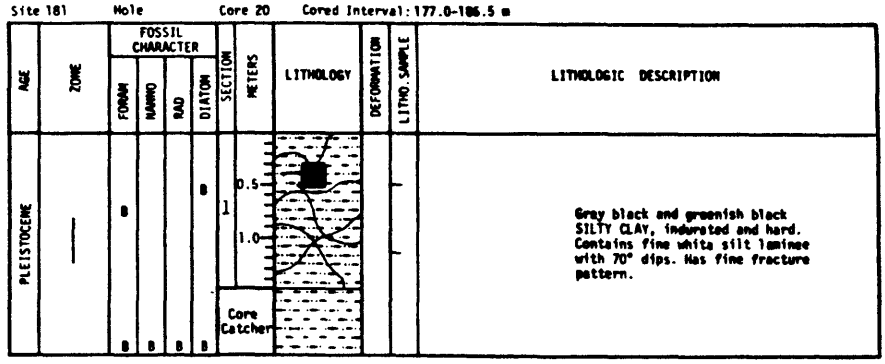

Site 181 Hole Core 29 Cored Interval: 337.5-340.5 m

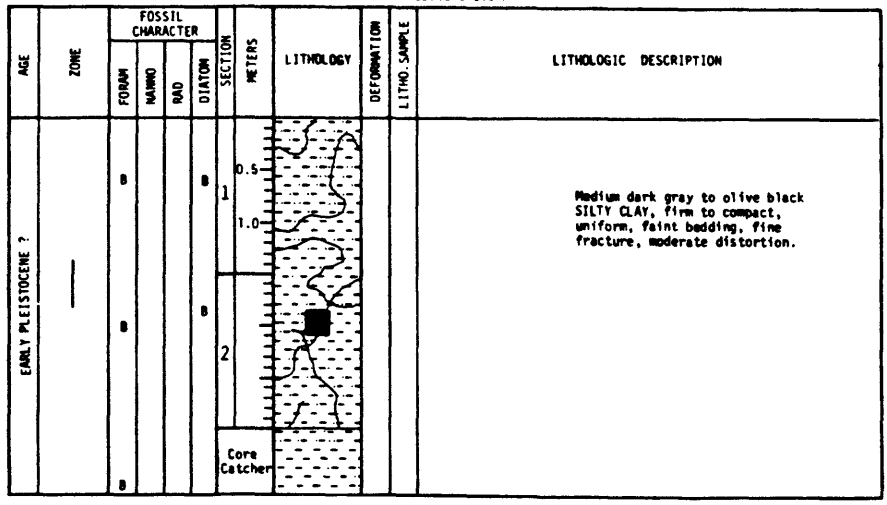

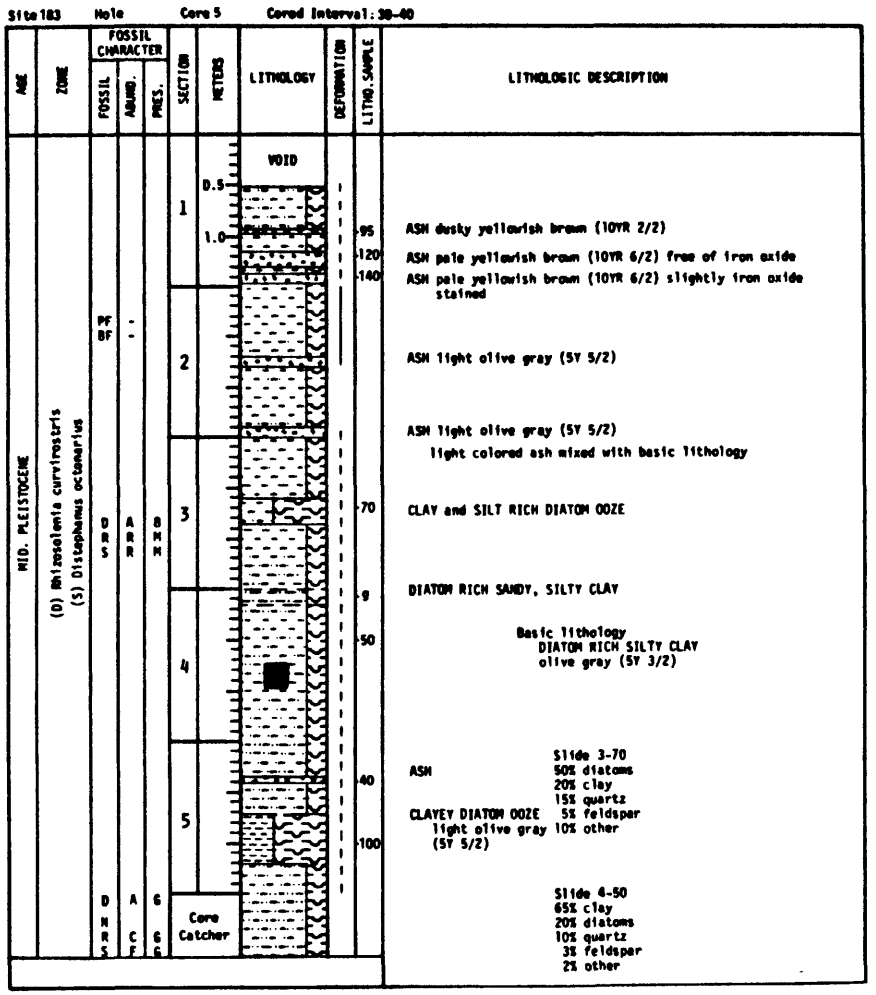
Site 183 Hole Core 5 Cored Interval: 38-48
AGE
ZONE
FOSSIL CHARACTER
FOSSIL
ABUND.
PRES.
SECTION
METERS
LITHOLOGY
DEFORMATION
LITHO. SAMPLE
LITHOLOGIC DESCRIPTION
MID. PLEISTOCENE
(D) Rhizosolenia curvirostris
(S) Distephanus octonarius
VOID
0.5
1.0
1
2
3
4
5
Core Catcher
PF
BF
D
S
A
C
G
95
120
140
70
9
50
40
100
ASH dusky yellowish brown (10YR 2/2)
ASH pale yellowish brown (10YR 6/2) free of iron oxide
ASH pale yellowish brown (10YR 6/2) slightly iron oxide stained
ASH light olive gray (5Y 5/2)
ASH light olive gray (5Y 5/2)
light colored ash mixed with basic lithology
CLAY and SILT RICH DIATOM OOZE
DIATOM RICH SANDY, SILTY CLAY
Basic lithology
DIATOM RICH SILTY CLAY
olive gray (5Y 3/2)
ASH
CLAYEY DIATOM OOZE
light olive gray (5Y 5/2)
Slide 3-70
50% diatoms
20% clay
15% quartz
5% feldspar
10% other
Slide 4-50
65% clay
20% diatoms
10% quartz
3% feldspar
2% other

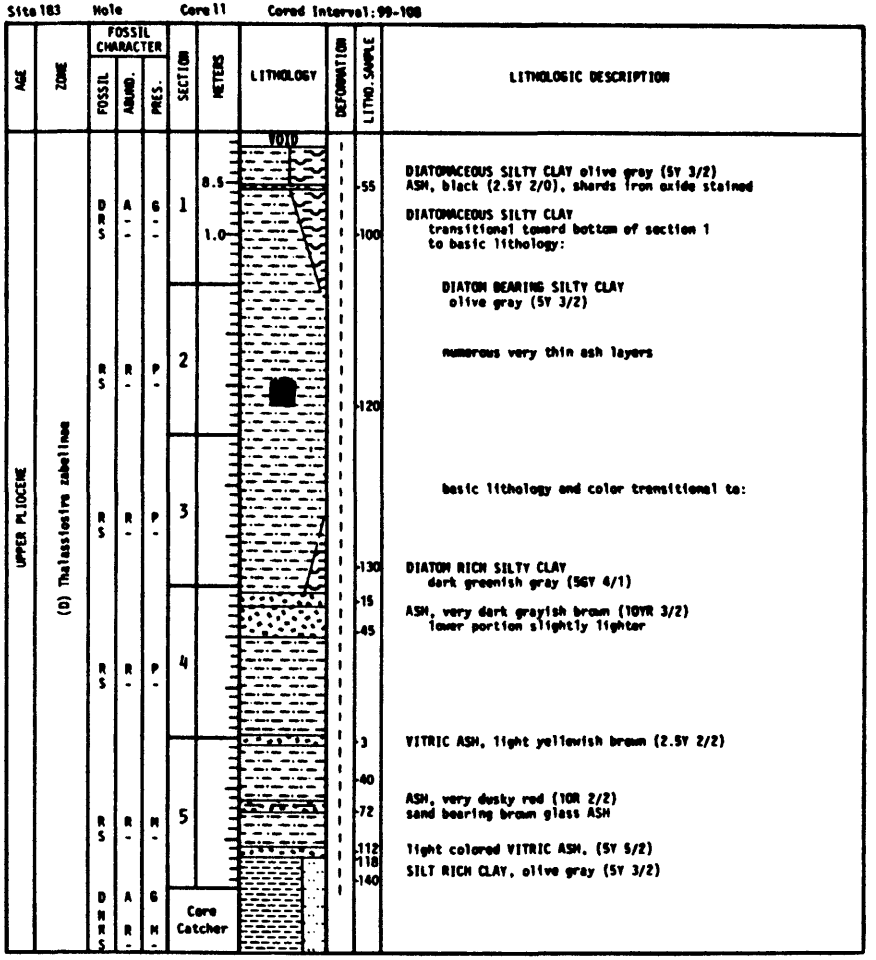
Site 183 Hole Core 11 Cored Interval: 99-108
AGE
ZONE
FOSSIL CHARACTER
FOSSIL
ABUND.
PRES.
SECTION
METERS
LITHOLOGY
DEFORMATION
LITHO. SAMPLE
LITHOLOGIC DESCRIPTION
UPPER PLIOCENE
(D) Thalassiosira zabelinae
VOID
8.5
1.0
1
2
3
4
5
Core Catcher
D
S
A
C
G
55
100
120
130
15
45
3
40
72
112
118
140
DIATOMACEOUS SILTY CLAY olive gray (5Y 3/2)
ASH, black (2.5Y 2/0), shards iron oxide stained
DIATOMACEOUS SILTY CLAY
transitional toward bottom of section 1
to basic lithology:
DIATOM BEARING SILTY CLAY
olive gray (5Y 3/2)
numerous very thin ash layers
basic lithology and color transitional to:
DIATOM RICH SILTY CLAY
dark greenish gray (5GY 4/1)
ASH, very dark grayish brown (10YR 3/2)
lower portion slightly lighter
VITRIC ASH, light yellowish brown (2.5Y 2/2)
ASH, very dusky red (10R 2/2)
sand bearing brown glass ASH
light colored VITRIC ASH, (5Y 5/2)
SILT RICH CLAY, olive gray (5Y 3/2)

Site 183 Hole Core 17 Cored Interval: 164-173

AGE	ZONE	FOSSIL CHARACTER: FOSSIL	FOSSIL CHARACTER: ABUND.	FOSSIL CHARACTER: PRES.	SECTION	METERS	LITHOLOGY	DEFORMATION	LITHO. SAMPLE	LITHOLOGIC DESCRIPTION
UPPER MIOCENE	(D) Denticulina kamtschatica (S) Distephanus speculum var. pentagonus	D R S	A R C	G X N	1	0.5 1.0			75	
		R S	R F	N N	2				76 96 106	VITRIC ASH, light gray (N7)
		D R S	A R F	G X N	3					Basic lithology DIATOM OOZE light yellowish brown (2.5Y 6/4)
		R S	R F	N N	4				145	average composition 95 - 100% diatoms 5% silt and clay locally contains up to 15% glass
		R S	R C	N N	5					streaks and pods of grayish brown (2.5Y 3/2) ASH and SILTY CLAY
		R S	R C	N N	6					
		D R S	A C F	G N N	Core Catcher					

Site 183 Hole Core 23 Cored Interval: 220-229

AGE	ZONE	FOSSIL CHARACTER: FOSSIL	FOSSIL CHARACTER: ABUND.	FOSSIL CHARACTER: PRES.	SECTION	METERS	LITHOLOGY	DEFORMATION	LITHO. SAMPLE	LITHOLOGIC DESCRIPTION
					1	0.5 1.0			84 90	
					2					CLAYEY SILT and CLAY alternating bands of: olive gray (5Y 4/1) and greenish gray (5G 6/1)
					3					Slides 1-84, 1-90: 95 - 100% clay TR diatoms and rods (very rare) lab grain size analysis, sect. 2, 120 cm: 56% silt, 44% clay
					4					
					5					sections 5 and 6 injected
					6					
					Core Catcher					Core Catcher: D - R - R - S - PF - BF -

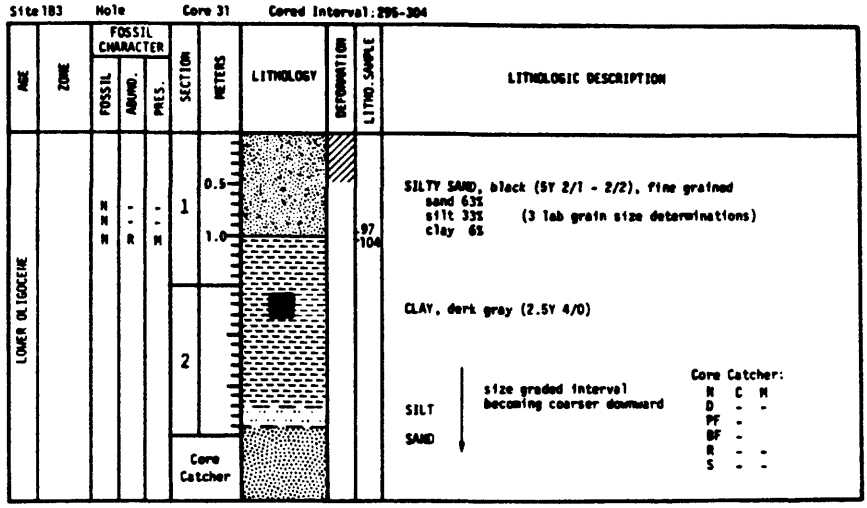
Site 183 Hole Core 31 Cored Interval: 296-304
AGE
ZONE
FOSSIL CHARACTER
FOSSIL
ABUND.
PRES.
SECTION
METERS
LITHOLOGY
DEFORMATION
LITHO. SAMPLE
LITHOLOGIC DESCRIPTION
LOWER OLIGOCENE
0.5
1.0
1
2
Core Catcher
97
104
SILTY SAND, black (5Y 2/1 - 2/2), fine grained
sand 63%
silt 33%
clay 6%
(3 lab grain size determinations)
CLAY, dark gray (2.5Y 4/0)
SILT
SAND
size graded interval
becoming coarser downward
Core Catcher:
N C M
D - -
PF -
BF -
R - -
S - -

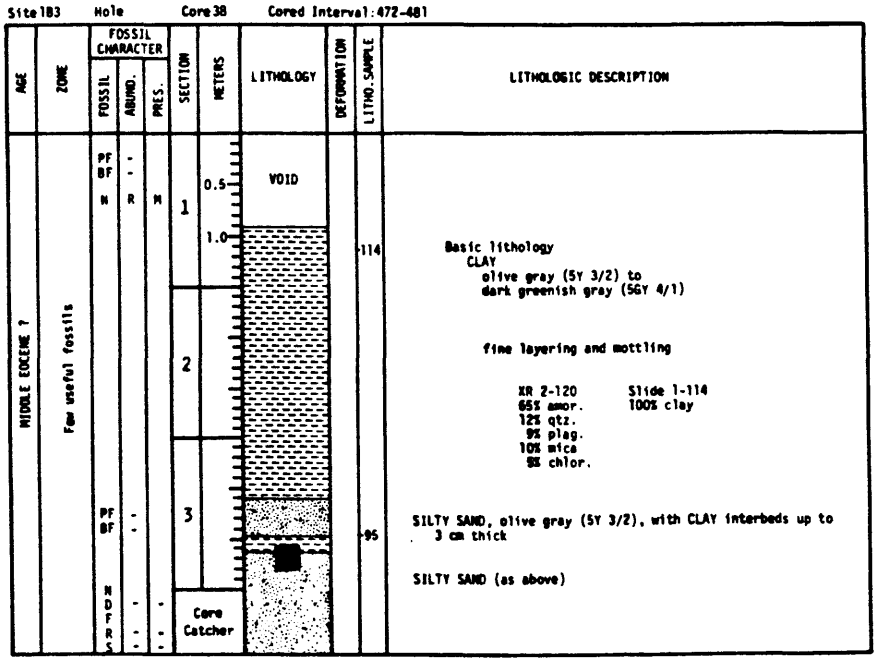
Site 183 Hole Core 38 Cored Interval: 472-481
AGE
ZONE
FOSSIL CHARACTER
FOSSIL
ABUND.
PRES.
SECTION
METERS
LITHOLOGY
DEFORMATION
LITHO. SAMPLE
LITHOLOGIC DESCRIPTION
MIDDLE EOCENE ?
Few useful fossils
PF
BF
N
R
M
0.5
1.0
1
2
3
Core Catcher
VOID
114
95
Basic lithology
CLAY
olive gray (5Y 3/2) to
dark greenish gray (5GY 4/1)
fine layering and mottling
XR 2-120
65% amor.
12% qtz.
9% plag.
10% mica
9% chlor.
Slide 1-114
100% clay
SILTY SAND, olive gray (5Y 3/2), with CLAY interbeds up to 3 cm thick
SILTY SAND (as above)

Site 192 Hole Core 4 Cored Interval: 19-28

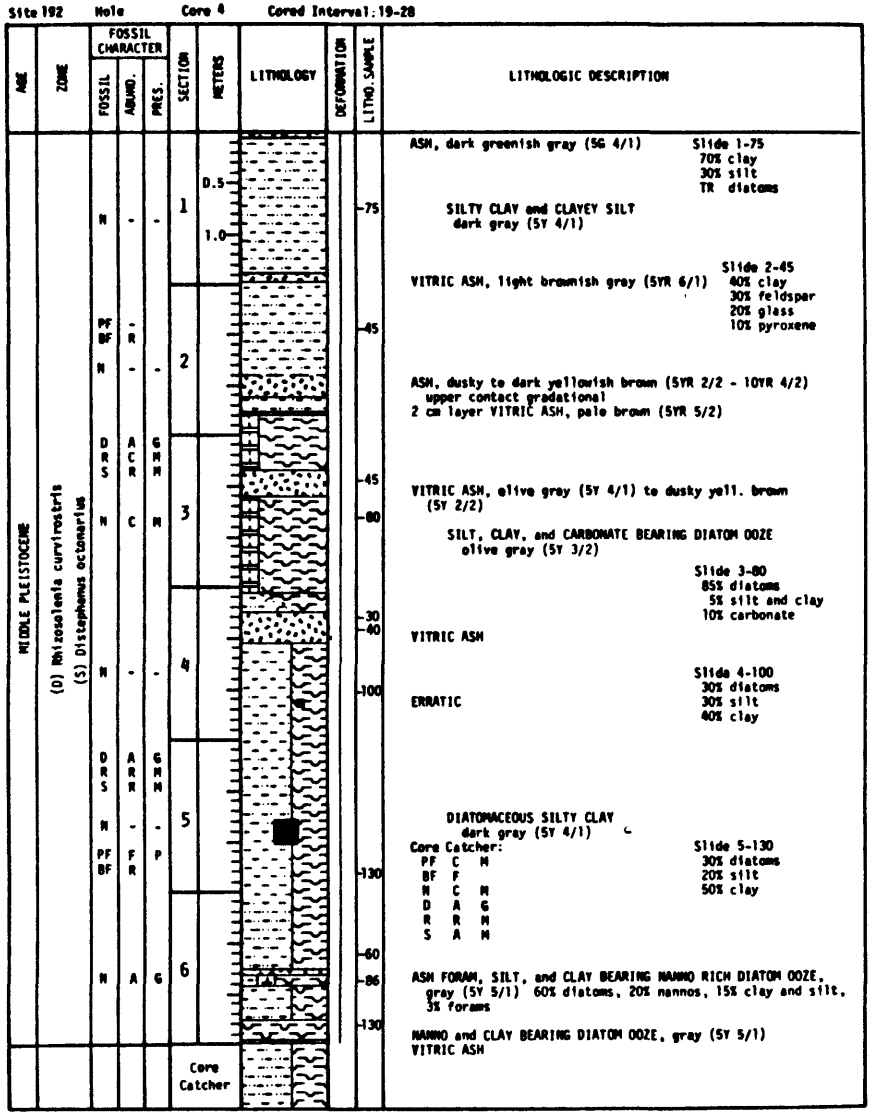

Site 192 Hole Core 15 Cored Interval: 269-278

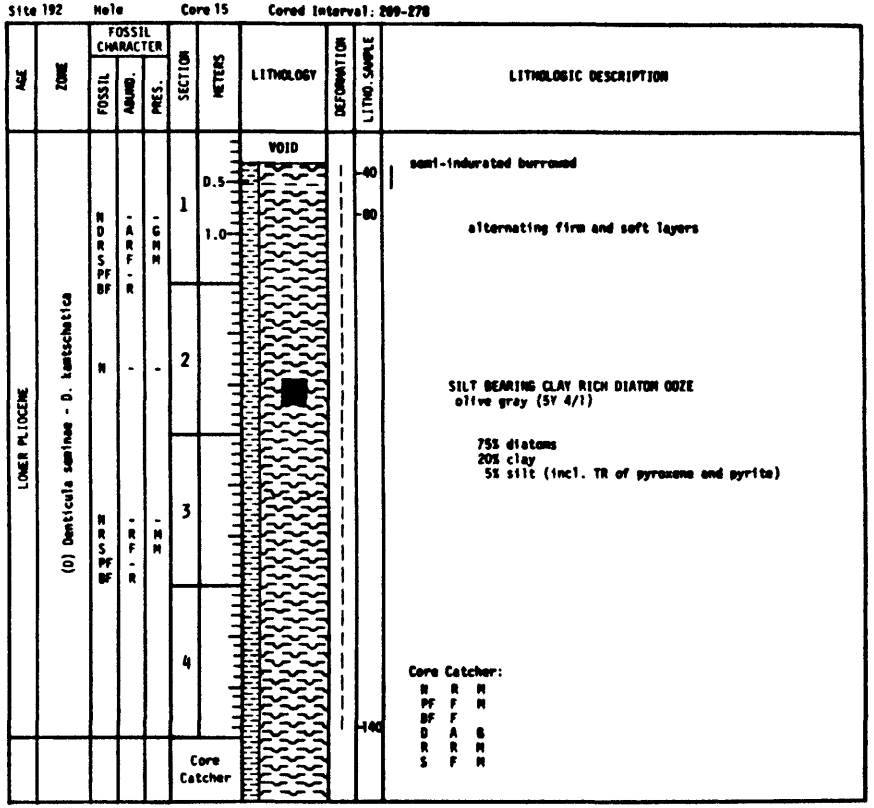

Site 192 Hole Core 23 Cored Interval: 569-578

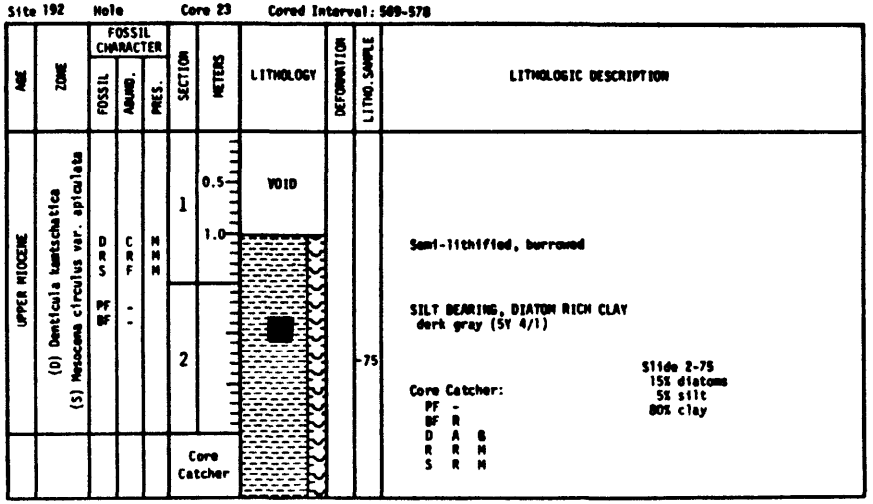

Site 192 Hole Core 32 Cored Interval: 906-912

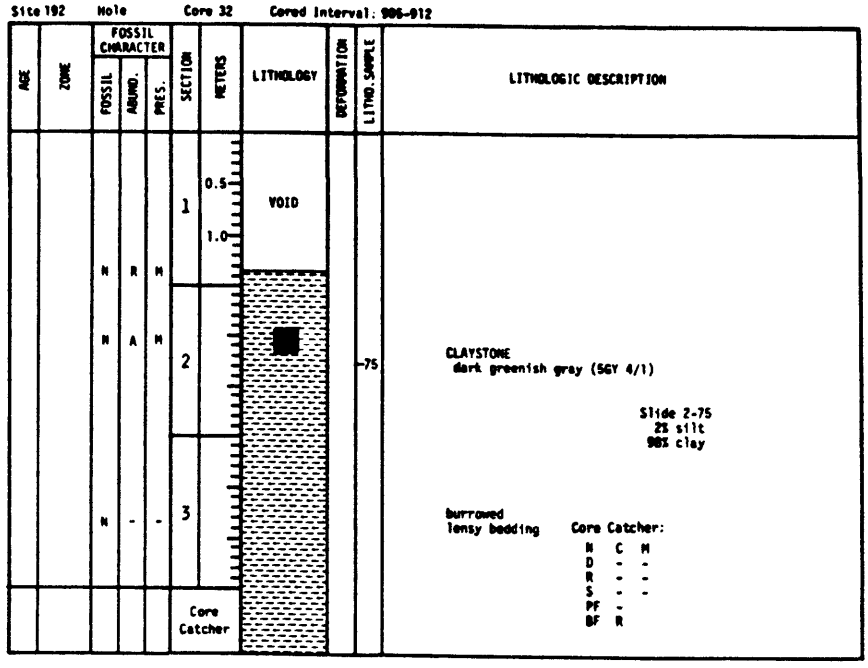

Site 192 Hole A Core 4 Cored Interval: 1018-1027

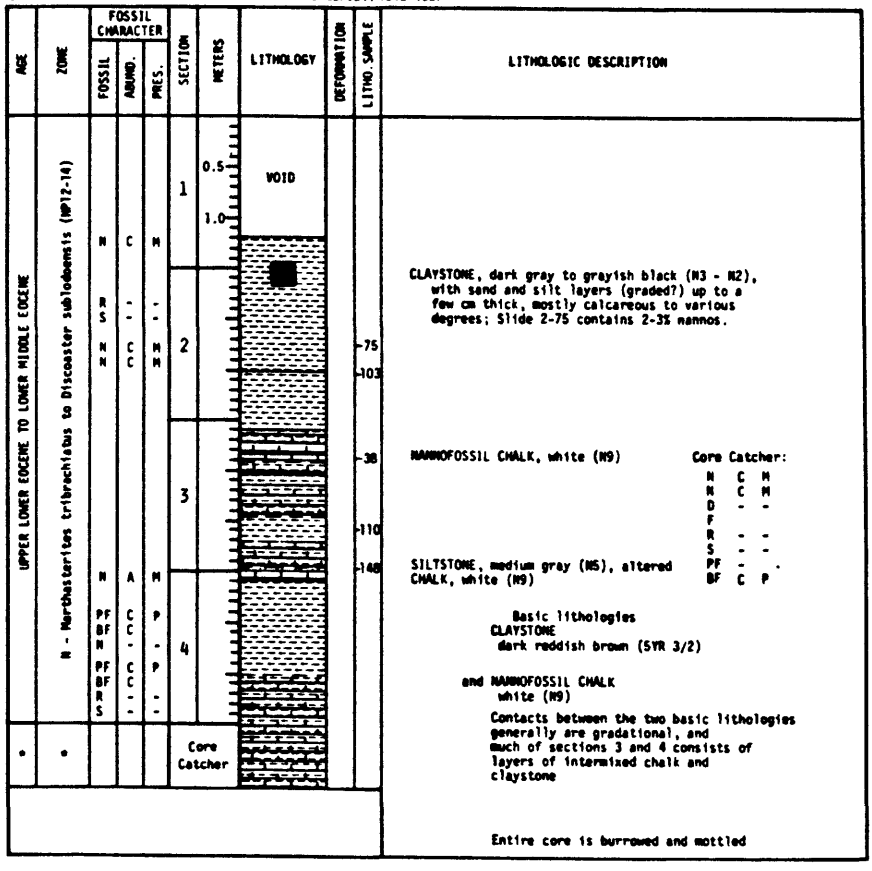

VITRINITE REFLECTANCE

JOB NAME: USGS
SAMPLE NUMBER: KSG6/CGS8322.288
SOURCE: KVENVOLDEN
DEPTH:

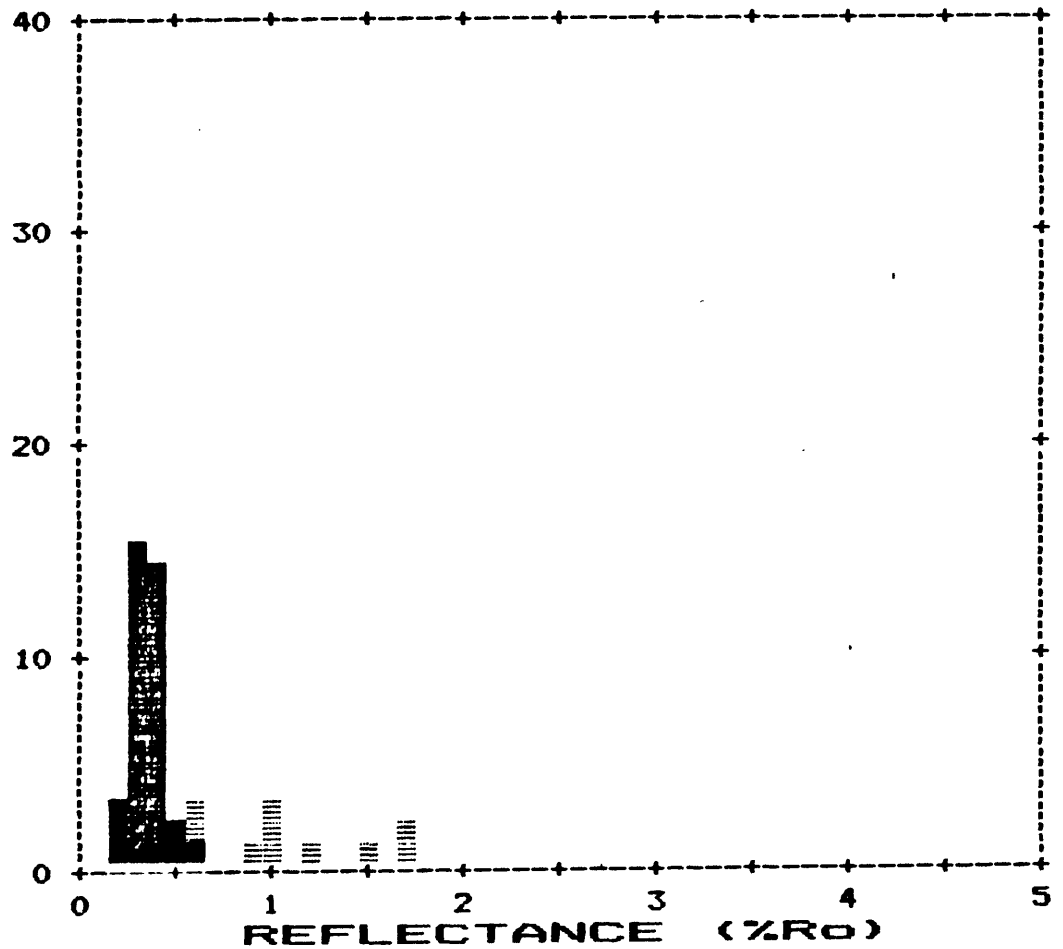

ORDERED READINGS

0.26	0.28	0.29	0.3	0.32
0.34	0.34	0.35	0.35	0.36
0.37	0.37	0.37	0.38	0.38
0.39	0.39	0.39	0.4	0.4
0.4	0.41	0.42	0.42	0.42
0.42	0.42	0.43	0.44	0.45
0.49	0.49	0.5	0.58	0.61
*0.65	*0.68	*0.94	*1.06	*1.07
*1.08	*1.21	*1.55	*1.7	*1.72

MEAN: 0.4 STANDARD DEV.: 0.07
NUMBER: 35 MODE: 0.3
RANGE: 0.26-0.61
* Data not considered in statistical analysis.

VITRINITE REFLECTANCE

JOB NAME: USGS
SAMPLE NUMBER: KSG14/CGS8322.289
SOURCE: KVENVOLDEN
DEPTH:

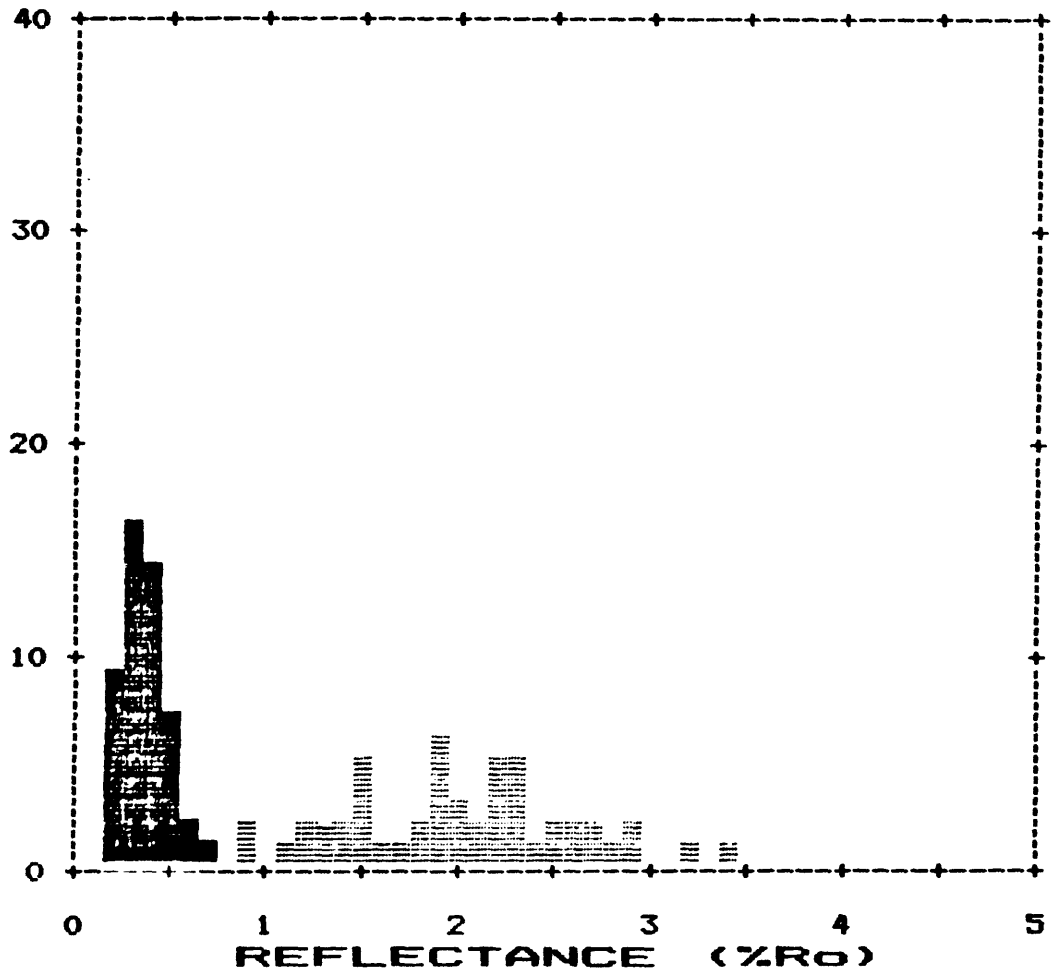

MEAN: 0.4 STANDARD DEV.: 0.11
NUMBER: 49 MODE: 0.3
RANGE: 0.22-0.71
* Data not considered in statistical analysis.

ORDERED READINGS

0.22	0.25	0.26	0.26	0.27
0.27	0.28	0.29	0.29	0.3
0.3	0.31	0.31	0.32	0.33
0.34	0.34	0.35	0.36	0.36
0.36	0.37	0.37	0.37	0.39
0.41	0.41	0.41	0.42	0.42
0.44	0.44	0.45	0.45	0.45
0.47	0.47	0.48	0.48	0.5
0.51	0.54	0.54	0.56	0.58
0.58	0.6	0.64	0.71	*0.92
*0.94	*1.12	*1.21	*1.25	*1.3
*1.32	*1.43	*1.46	*1.51	*1.54
*1.55	*1.56	*1.58	*1.68	*1.77
*1.84	*1.85	*1.94	*1.95	*1.97
*1.98	*1.98	*1.99	*2	*2.01
*2.02	*2.16	*2.17	*2.24	*2.26
*2.27	*2.28	*2.28	*2.33	*2.33
*2.34	*2.35	*2.37	*2.42	*2.52
*2.56	*2.63	*2.68	*2.77	*2.77
*2.8	*2.95	*2.97	*3.26	*3.48

VITRINITE REFLECTANCE

JOB NAME: USGS
SAMPLE NUMBER: KSG16/CGS8322.290
SOURCE: KVENVOLDEN
DEPTH:

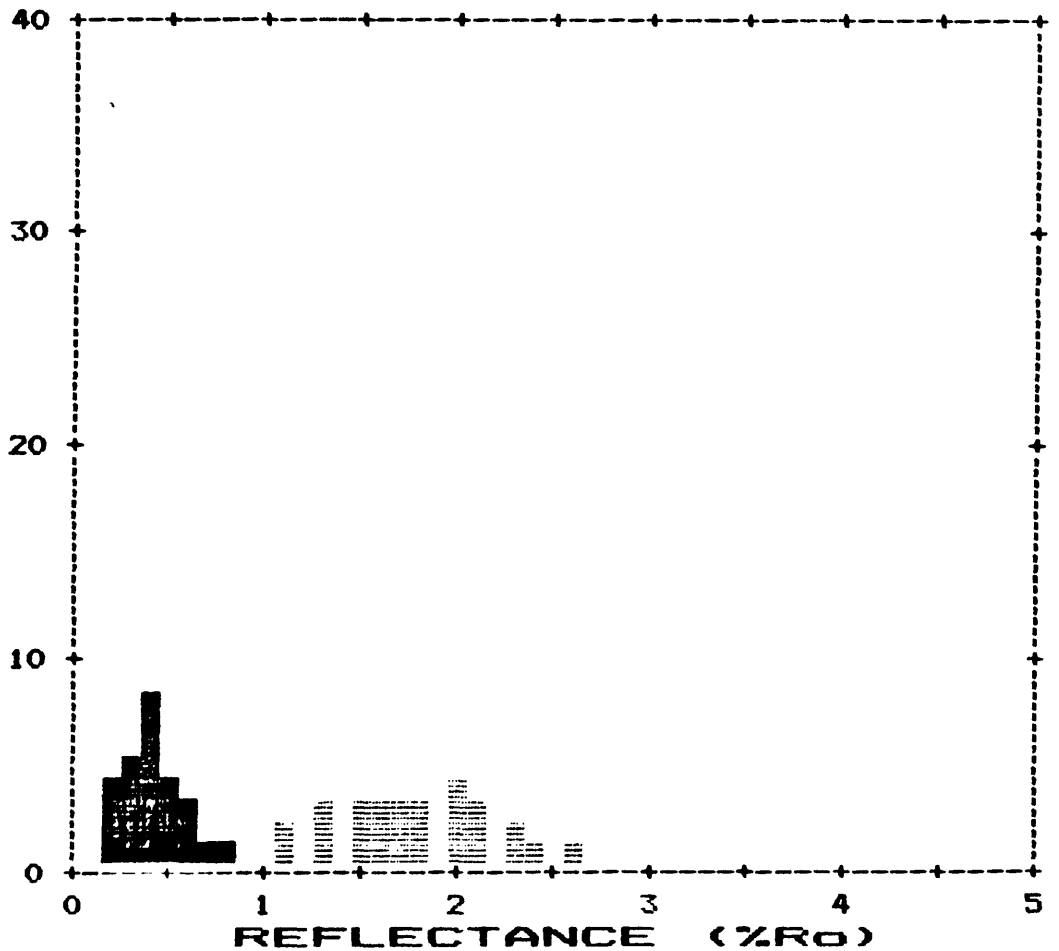

ORDERED READINGS

0.23	0.23	0.25	0.28	0.3
0.3	0.34	0.35	0.39	0.4
0.4	0.41	0.41	0.41	0.42
0.45	0.47	0.52	0.54	0.55
0.59	0.6	0.6	0.67	0.74
0.82	*1.17	*1.17	*1.32	*1.37
*1.38	*1.5	*1.53	*1.56	*1.61
*1.62	*1.68	*1.74	*1.75	*1.77
*1.82	*1.85	*1.88	*2.01	*2.03
*2.03	*2.06	*2.12	*2.16	*2.18
*2.35	*2.36	*2.48	*2.68	

MEAN: 0.45** STANDARD DEV.: 0.15
NUMBER: 26 MODE: 0.4
RANGE: 0.23-0.82
* Data not considered in statistical analysis.
** Statistical analysis may not be significant due to small number of data points.

VITRINITE REFLECTANCE

JOB NAME: USGS
SAMPLE NUMBER: KSG17/CGS8322.291
SOURCE: KVENVOLDEN
DEPTH:

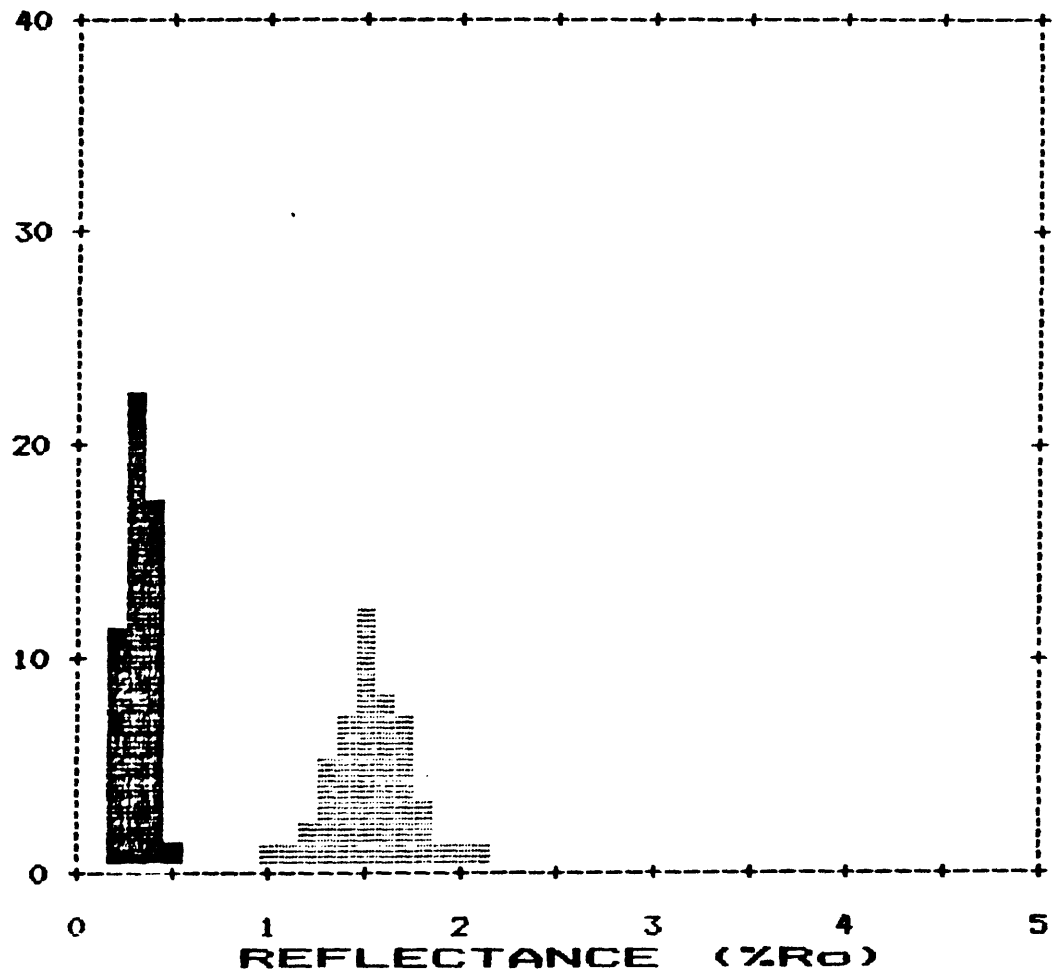

ORDERED READINGS

0.21	0.23	0.23	0.25	0.25
0.26	0.27	0.27	0.28	0.28
0.28	0.3	0.3	0.31	0.31
0.31	0.31	0.32	0.32	0.32
0.32	0.33	0.33	0.35	0.35
0.36	0.36	0.37	0.38	0.38
0.38	0.39	0.39	0.4	0.4
0.4	0.4	0.41	0.42	0.42
0.42	0.43	0.43	0.44	0.44
0.45	0.45	0.46	0.46	0.48
0.57	*1.02	*1.13	*1.27	*1.28
*1.32	*1.33	*1.33	*1.35	*1.35
*1.4	*1.44	*1.46	*1.47	*1.48
*1.48	*1.48	*1.5	*1.52	*1.52
*1.53	*1.53	*1.54	*1.54	*1.54
*1.55	*1.57	*1.58	*1.58	*1.6
*1.62	*1.62	*1.62	*1.64	*1.67
*1.67	*1.68	*1.72	*1.72	*1.72
*1.73	*1.77	*1.78	*1.79	*1.82
*1.85	*1.88	*1.98	*2.06	*2.12

MEAN: 0.36 STANDARD DEV.: 0.08
NUMBER: 51 MODE: 0.3
RANGE: 0.21-0.57
* Data not considered in statistical analysis.

VITRINITE REFLECTANCE

JOB NAME: USGS
SAMPLE NUMBER: KSG19/CGS8322.292
SOURCE: KVENVOLDEN
DEPTH:

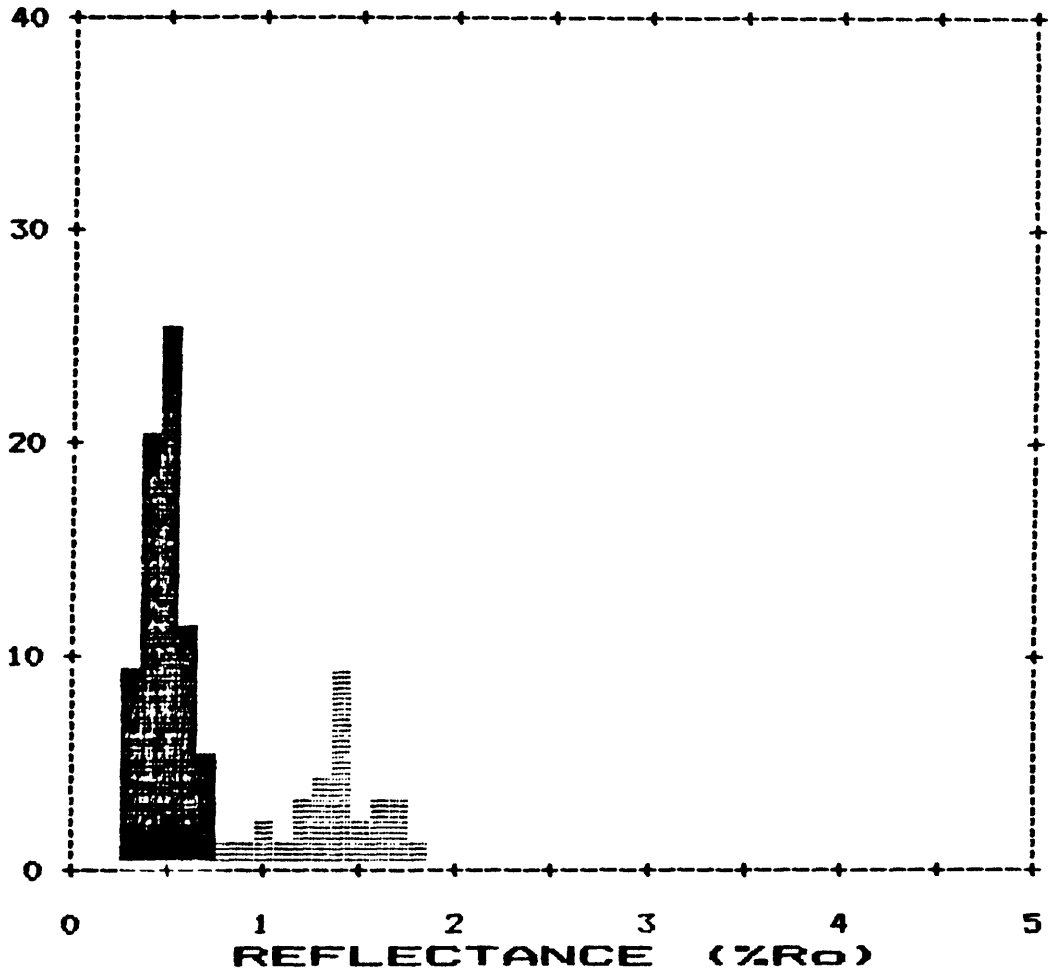

MEAN: 0.52 STANDARD DEV.: 0.11
NUMBER: 70 MODE: 0.5
RANGE: 0.34-0.78
* Data not considered in statistical analysis.

ORDERED READINGS

0.34	0.35	0.35	0.38	0.38
0.38	0.38	0.39	0.39	0.41
0.41	0.42	0.42	0.42	0.43
0.43	0.43	0.44	0.44	0.44
0.44	0.45	0.46	0.46	0.48
0.48	0.48	0.49	0.49	0.5
0.5	0.51	0.51	0.51	0.51
0.52	0.52	0.53	0.54	0.54
0.54	0.55	0.55	0.55	0.55
0.55	0.56	0.56	0.56	0.56
0.57	0.58	0.58	0.58	0.63
0.63	0.63	0.63	0.64	0.65
0.66	0.66	0.66	0.69	0.69
0.7	0.72	0.72	0.76	0.78
*0.87	*0.93	*1.07	*1.08	*1.11
*1.24	*1.24	*1.25	*1.32	*1.32
*1.34	*1.38	*1.4	*1.4	*1.42
*1.43	*1.44	*1.45	*1.47	*1.48
*1.49	*1.52	*1.58	*1.6	*1.62
*1.66	*1.76	*1.77	*1.77	*1.82

VITRINITE REFLECTANCE

JOB NAME: USGS
SAMPLE NUMBER: KSG21/CGS8322.293
SOURCE: KVENVOLDEN
DEPTH:

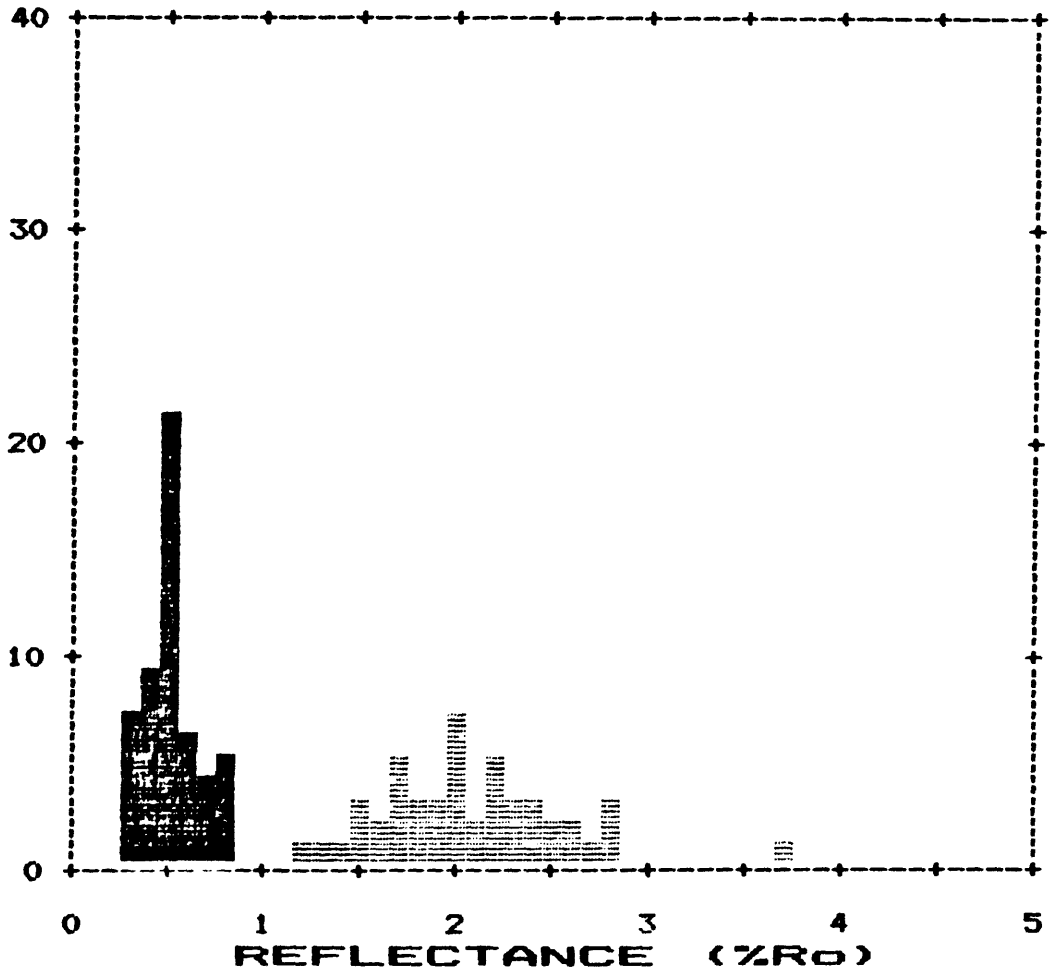

MEAN: 0.56 STANDARD DEV.: 0.14
NUMBER: 52 MODE: 0.5
RANGE: 0.3-0.88
* Data not considered in statistical analysis.

ORDERED READINGS

0.3	0.31	0.33	0.37	0.38
0.38	0.39	0.41	0.41	0.42
0.42	0.44	0.47	0.47	0.48
0.49	0.5	0.5	0.51	0.51
0.52	0.52	0.52	0.52	0.54
0.54	0.54	0.55	0.55	0.56
0.56	0.57	0.57	0.58	0.58
0.58	0.59	0.61	0.62	0.62
0.68	0.68	0.68	0.7	0.7
0.71	0.77	0.82	0.82	0.82
0.88	0.88	*1.27	*1.32	*1.49
*1.54	*1.56	*1.58	*1.62	*1.67
*1.7	*1.72	*1.74	*1.74	*1.79
*1.8	*1.85	*1.88	*1.94	*1.98
*1.98	*2	*2.01	*2.02	*2.02
*2.03	*2.05	*2.08	*2.11	*2.15
*2.24	*2.24	*2.25	*2.27	*2.28
*2.32	*2.35	*2.37	*2.4	*2.45
*2.48	*2.54	*2.57	*2.6	*2.61
*2.77	*2.82	*2.85	*2.88	*3.77

VITRINITE REFLECTANCE

JOB NAME: USGS
SAMPLE NUMBER: KSG27/CGS8322.294
SOURCE: KVENVOLDEN
DEPTH:

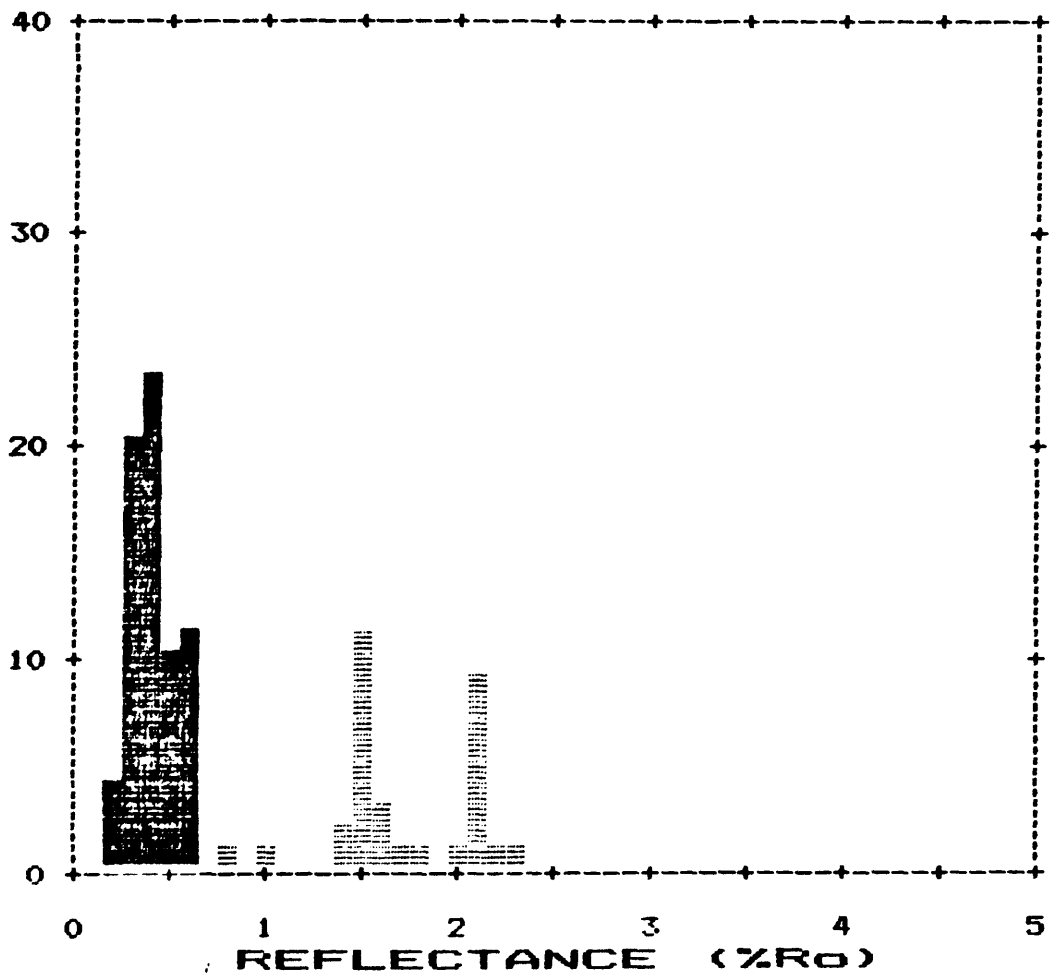

ORDERED READINGS

0.26	0.28	0.29	0.29	0.3
0.32	0.32	0.33	0.33	0.34
0.34	0.35	0.36	0.36	0.36
0.38	0.38	0.38	0.38	0.38
0.38	0.38	0.38	0.39	0.4
0.4	0.4	0.4	0.41	0.41
0.41	0.42	0.42	0.42	0.42
0.43	0.44	0.47	0.47	0.47
0.47	0.47	0.47	0.48	0.48
0.48	0.49	0.5	0.51	0.52
0.53	0.54	0.55	0.57	0.57
0.58	0.59	0.6	0.6	0.62
0.62	0.62	0.62	0.63	0.63
0.64	0.65	0.69	*0.82	*1.01
*1.48	*1.48	*1.5	*1.5	*1.51
*1.51	*1.52	*1.53	*1.54	*1.54
*1.55	*1.55	*1.59	*1.6	*1.62
*1.64	*1.76	*1.88	*2	*2.1
*2.12	*2.15	*2.16	*2.17	*2.17
*2.18	*2.18	*2.19	*2.23	*2.37

MEAN: 0.45 STANDARD DEV.: 0.11
NUMBER: 68 MODE: 0.4
RANGE: 0.26-0.69
* Data not considered in statistical analysis.

VITRINITE REFLECTANCE

JOB NAME: USGS
SAMPLE NUMBER: KS638/CGS8322.295
SOURCE: KVENVOLDEN
DEPTH:

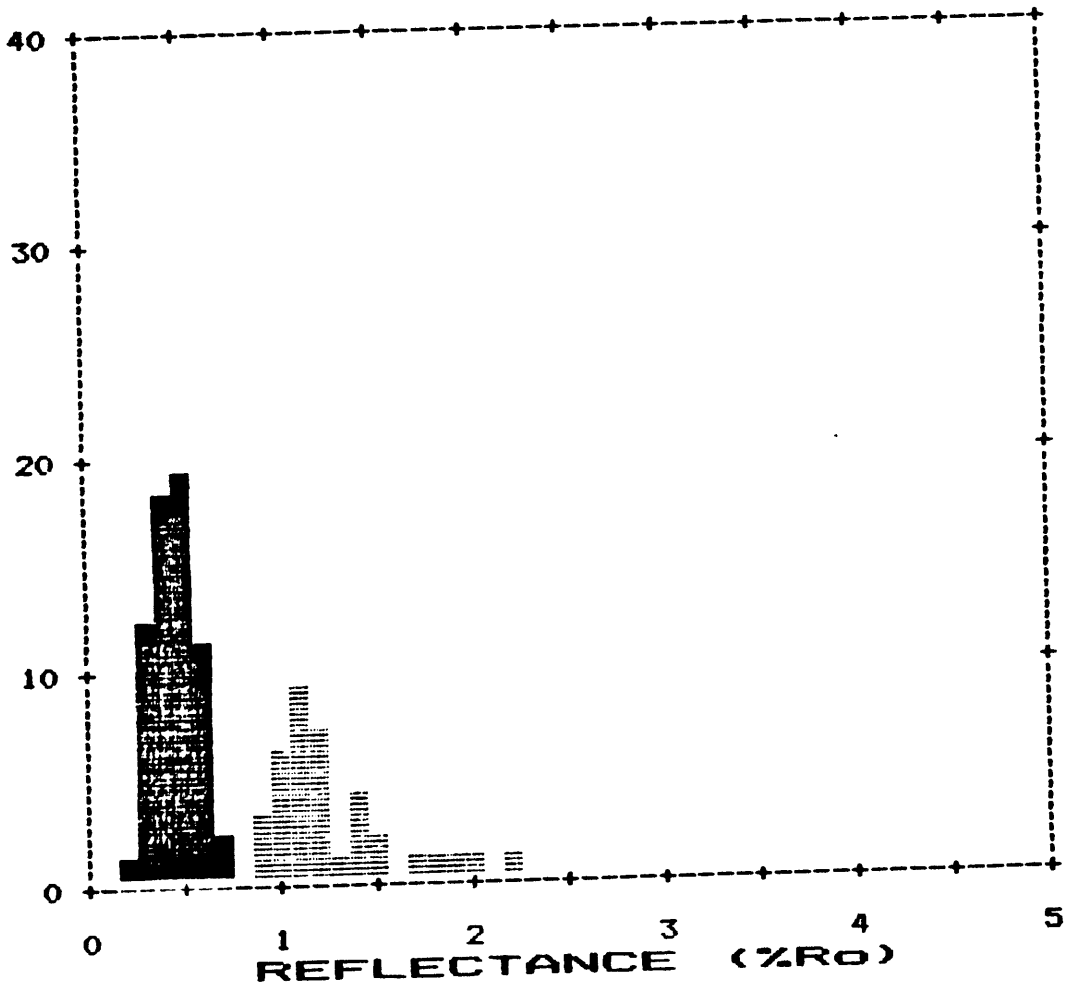

MEAN: 0.5 STANDARD DEV.: 0.11
NUMBER: 63 MODE: 0.5
RANGE: 0.27-0.78
* Data not considered in statistical analysis.

ORDERED READINGS

0.27	0.3	0.32	0.32	0.35
0.35	0.36	0.36	0.37	0.38
0.38	0.38	0.38	0.4	0.41
0.42	0.42	0.42	0.44	0.47
0.47	0.47	0.47	0.47	0.48
0.48	0.48	0.48	0.48	0.49
0.49	0.5	0.5	0.5	0.51
0.51	0.51	0.51	0.52	0.52
0.55	0.55	0.56	0.57	0.58
0.58	0.58	0.58	0.58	0.59
0.62	0.62	0.63	0.64	0.64
0.65	0.65	0.66	0.66	0.68
0.68	0.72	0.78	*0.9	*0.95
*0.95	*1	*1	*1.03	*1.04
*1.05	*1.07	*1.1	*1.12	*1.12
*1.15	*1.17	*1.17	*1.18	*1.18
*1.19	*1.2	*1.2	*1.2	*1.22
*1.25	*1.27	*1.27	*1.31	*1.4
*1.42	*1.44	*1.49	*1.52	*1.58
*1.78	*1.84	*1.9	*2.01	*2.24

VITRINITE REFLECTANCE

JOB NAME: USGS
SAMPLE NUMBER: KSG39/CGS8322.296
SOURCE: KVENVOLDEN
DEPTH:

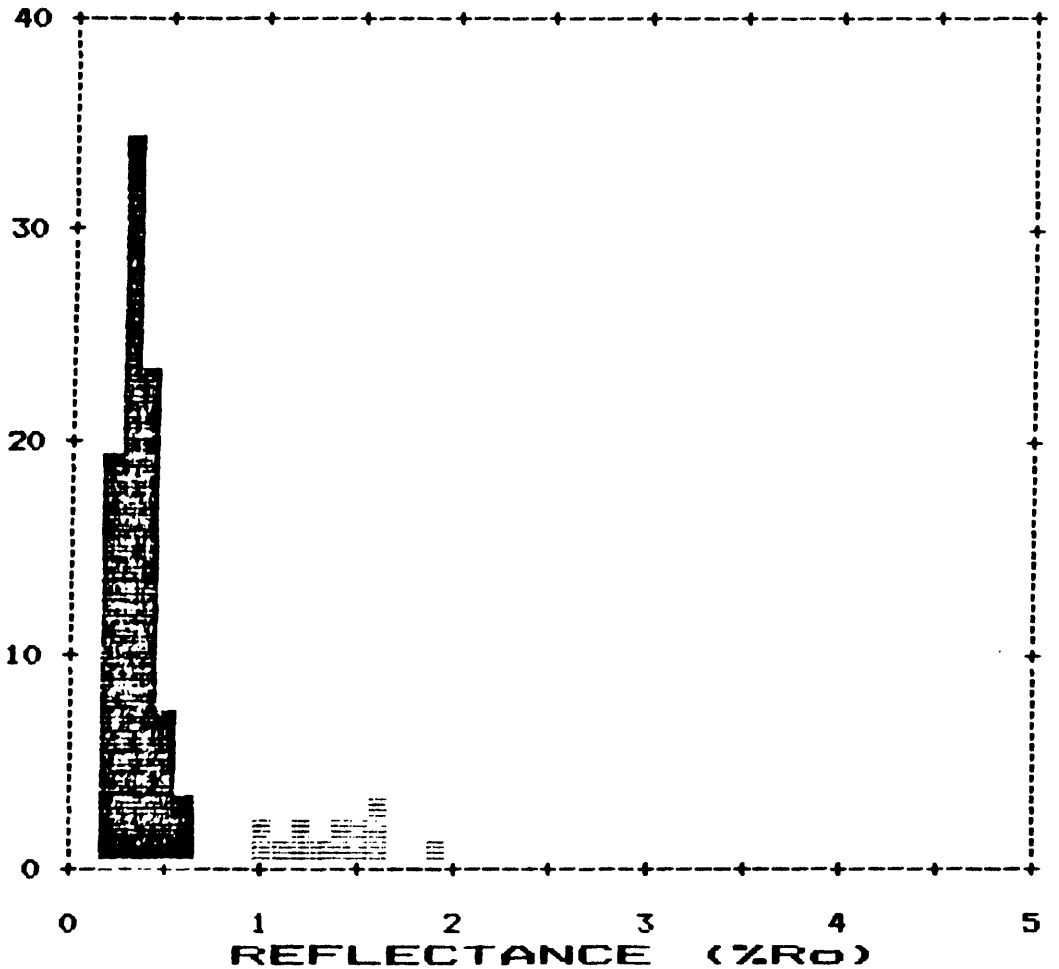

ORDERED READINGS

0.23	0.24	0.25	0.25	0.25
0.25	0.26	0.26	0.27	0.27
0.28	0.28	0.28	0.28	0.28
0.28	0.29	0.29	0.29	0.3
0.3	0.3	0.3	0.3	0.31
0.31	0.31	0.31	0.31	0.31
0.32	0.32	0.33	0.33	0.35
0.35	0.35	0.36	0.36	0.36
0.36	0.36	0.37	0.38	0.38
0.38	0.38	0.38	0.38	0.38
0.38	0.38	0.39	0.4	0.4
0.4	0.4	0.4	0.41	0.41
0.42	0.42	0.42	0.42	0.43
0.44	0.44	0.45	0.45	0.45
0.45	0.46	0.47	0.47	0.47
0.49	0.5	0.51	0.52	0.54
0.55	0.58	0.58	0.6	0.62
0.64	*1.02	*1.07	*1.16	*1.22
*1.26	*1.32	*1.42	*1.42	*1.5
*1.58	*1.61	*1.62	*1.63	*1.93

MEAN: 0.38 STANDARD DEV.: 0.09
NUMBER: 86 MODE: 0.3
RANGE: 0.23-0.64
* Data not considered in statistical analysis.

84-404

Plate 2 Listing of Geochemical Results

Sample No.	API Designation	Leg/ Cruise	Site	Core	Sample	Section	Interval	Latitude	Longitude	Depth of Water (m)	Depth of Sediment (m)	Lithology	Age	wt Orig. Sample (g)	OC (%) est. DSDP	OC (%) TEA/Rock Eval	Total Carbon (%)	Carbonate Carbon (%)	Total Hydrocarbon Yield (%)	"Live Carbon" (%)	Volatile Hydrocarbon (ppm)	Tmax °C TEA/Rock Eval
KSG 1	55-187-90001	1W	17W	5	2	28-34	56°27.38'N	147°07.86W	4218	34.8	Silty clay, md dk gy	Pleistocene	104	0.7	0.62	0.71	0.09	0.05	8	37	475
KSG 2	"	1W	17W	13	3	8-14	"	"	"	108.1	Silty clay, md dk gy	Pleistocene	95	0.5	0.50	0.50	0.0	0.03	6	36	455
KSG 3	"	1W	17W	25	5	31-37	"	"	"	217.3	Silty clay, md dk gy	Late Pliocene	96	0.5	0.35	0.39	0.04	0.03	9	53	494
KSG 4	"	1W	17W	33	3	76-82	"	"	"	319.3	Silty clay, olive gy	Late Pliocene	62	0.4	0.53	0.56	0.03	0.06	11	47	522
KSG 5	"	1W	17W	34	2	64-72	"	"	"	327.2	Silty clay, gn gy, w/diatoms	Late Pliocene	69	0.2	0.23	0.26	0.03	0.05	22	95	422
KSG 6	"	1W	17W	39	3	63-69	"	"	"	395.2	Fine silt & silty clay, md dk gy	Late Pliocene	119	0.4	0.35/0.41	0.49	0.14	0.05	14	32	521/579
KSG 7	"	1W	17W	44	3	75-85	"	"	"	459.8	Silty clay, olive gy	Late Pliocene	73	0.6	0.50	0.52	0.02	0.06	12	47	422
KSG 8	"	1W	17W	47	2	61-67	"	"	"	507.6	Silt & silty clay, dk gn gy	Pliocene	76	0.3	0.33	0.37	0.04	0.04	12	43	437
KSG 9	"	1W	17W	49	1	52-58	"	"	"	591.5	Silt & silty clay, dk gn gy	Pliocene	74	1.0	0.33	0.34	0.01	0.05	15	31	511
KSG 10	"	1W	17W	50	2	132-138	"	"	"	631.8	Diatomite, gn gy	Early Pliocene	65	1.2	0.14	0.17	0.03	0.05	36	86	430
KSG 11	"	1W	17W	53	2	110-116	"	"	"	718.6	Silty clay, olive gy	Middle Pliocene?	63	0.9	0.33	0.34	0.01	0.05	15	38	433
KSG 12	"	1W	17W	54	4	87-93	"	"	"	747.7	Claystone, lt olive gy	Early Miocene	82	0.1	0.06	0.10	0.04	0.03	50	41	442
KSG 13	55-188-90001	1W	180	8	4	40-46	57°21.76'N	147°51.37W	4923	71.4	Clayey silt & silty clay, gy	Late Pleistocene - Holocene	111	0.6	0.67	0.74	0.07	0.07	10	79	448
KSG 14	"	1W	180	15	3	44-50	"	"	"	246.0	Silty clay & clayey silt, gy	Late Pleistocene - Holocene	103	0.7	0.66/0.69	0.73	0.07	0.05	8	76	496/584
KSG 15	"	1W	180	18	2	16-22	"	"	"	272.7	Silty clay & clayey silt, gy	Late Pleistocene - Holocene	108	0.5	0.50	0.59	0.09	0.04	8	67	481
KSG 16	"	1W	180	19	1	30-36	"	"	"	347.3	Silty clay & clayey silt, gy	Late Pleistocene - Holocene	101	0.6	0.59/0.63	0.66	0.07	0.07	12	164	418/574
KSG 17	"	1W	180	24	3	24-30	"	"	"	454.8	Silty clay & clayey silt, gy	Late Pleistocene - Holocene	93	0.8	0.70/0.92	0.83	0.13	0.06	9	60	465/513
KSG 18	55-188-90002	1W	181	2	5	22-28	57°26.30'N	148°27.88W	3086	15.2	Silty clay, olive gy, w/diatoms	Late Pleistocene - Holocene	93	0.5	0.59	0.74	0.15	0.06	10	75	464
KSG 19	"	1W	181	8	4	13-19	"	"	"	71.3	Silty clay, med gy	Late Pleistocene - Holocene	114	0.6	0.63/0.69	0.70	0.07	0.05	8	81	502/581
KSG 20	"	1W	181	15	4	87-93	"	"	"	137.9	Silty clay, med dk gy, w/diatoms	Late Pleistocene - Holocene	112	0.6	0.69	0.73	0.04	0.05	7	90	450
KSG 21	"	1W	181	17	5	21-26	"	"	"	157.7	Silty clay, med dk gy, w/diatoms	Late Pleistocene - Holocene	89	0.8	0.87/1.01	0.90	0.03	0.05	6	73	466/586
KSG 22	"	1W	181	20	1	35-41	"	"	"	177.4	Silty clay, gy bk & gn bk	Pleistocene	102	0.5	0.53	0.56	0.03	0.04	8	56	447
KSG 23	"	1W	181	29	2	42-48	"	"	"	339.5	Silty clay, med dk gy to olive bk	Early Pleistocene?	74	0.4	0.35	0.38	0.03	0.03	8	43	459
KSG 24	55-303-90001	1Y	183	5	4	80-86	52°34.30'N	161°12.33W	4708	35.3	Silty clay, olive gy, w/diatoms	Middle Pleistocene	74	0.5	0.36	0.42	0.06	0.08	22	165	452
KSG 25	"	1Y	183	11	2	106-112	"	"	"	101.6	Silty clay, olive gy, w/diatoms	Late Pliocene	67	0.3	0.29	0.27	0.00	0.05	17	34	458
KSG 26	"	1Y	183	17	3	42-48	"	"	"	167.5	Diatom ooze, lt yel bn	Late Miocene	62	0.1	0.19	0.21	0.01	0.10	52	197	455
KSG 27	"	1Y	183	23	1	25-31	"	"	"	220.3	Clayey silt & clay olive gy & gn gy	Miocene?	83	0.9	0.92/1.04	0.97	0.05	0.07	8	158	428/588
KSG 28	"	1Y	183	31	2	18-24	"	"	"	296.7	Clay, dk gy	Early Oligocene	101	0.3	0.64	0.71	0.07	0.05	8	93	443
KSG 29	"	1Y	183	38	3	114-119	"	"	"	476.2	Clay olive gy to dk gn gy	Middle Eocene?	74	0.7	0.14	0.35	0.01	0.04	12	655	455
KSG 30	55-999-90001	1Y	192	4	5	85-91	53°00.57'N	164°42.81E	3014	25.9	Silty clay, dk gy, w/diatoms	Middle Pleistocene	93	0.3	0.28	0.65	0.37	0.08	14	80	408
KSG 31	"	1Y	192	15	2	100-106	"	"	"	271.5	Clayey diatom ooze, olive gy	Early Pliocene	62	0.4	0.37	0.39	0.02	0.06	16	135	410
KSG 32	"	1Y	192	23	2	42-50	"	"	"	571.0	Silty clay w/diatoms, dk gy	Late Miocene	59	0.2	0.20	0.20	0.00	0.08	20	106	398
KSG 33	"	1Y	192	32	2	53-58	"	"	"	907.0	Claystone, dk gn gy	Miocene?	66	0.1	0.13	0.15	0.02	0.03	23	37	505
KSG 34	"	1Y	192A	4	2	0-6	"	"	3014	1019.5	Claystone, dk gy to gy bk	Middle Eocene	74	0.1	0.05	0.30	0.25	0.04	80	99	473
KSG 35	55-334-90001	S-79-WG	2	9	-	Dredge	53°43.04'N	162°34.25W	1800	Outcrop	Mudstone,volcanic,w/tr ss,pumice	Early to Middle Miocene	120	-	0.45	0.43	0.00	0.03	7	37	440
KSG 36	"		2	10	-	"	"	"	"	"	Dolomite,massive,indurated,pale bn	Middle to Late Eocene	147	-	0.11	9.4	9.1	0.05	15	46	443
KSG 37	"		2	12	-	"	"	"	"	"	Dolomite, clastic, rexl	Early to Middle Miocene	306	-	0.24	9.0	8.8	0.03	13	20	456
KSG 38	"		2	13	-	"	"	"	"	"	Mudstone, mud, indurated, lt gy	Eocene?	183	-	0.66/1.10	0.67	0.01	0.05	8	61	437/409
KSG 39	"		2	16	-	"	"	"	"	"	Mudstone, lt gy	Early to Middle Miocene?	133	-	0.80/0.92	0.77	0.00	0.06	8	94	429/411
KSG 40	55-305-90001	S-79-WG	4	1	-	"	54°30.05'N	159°59.70W	2200	"	Limestone, massive, gy, nodular	Early Pleistocene?	215	-	0.30	6.6	6.3	0.03	10	76	433

84-404

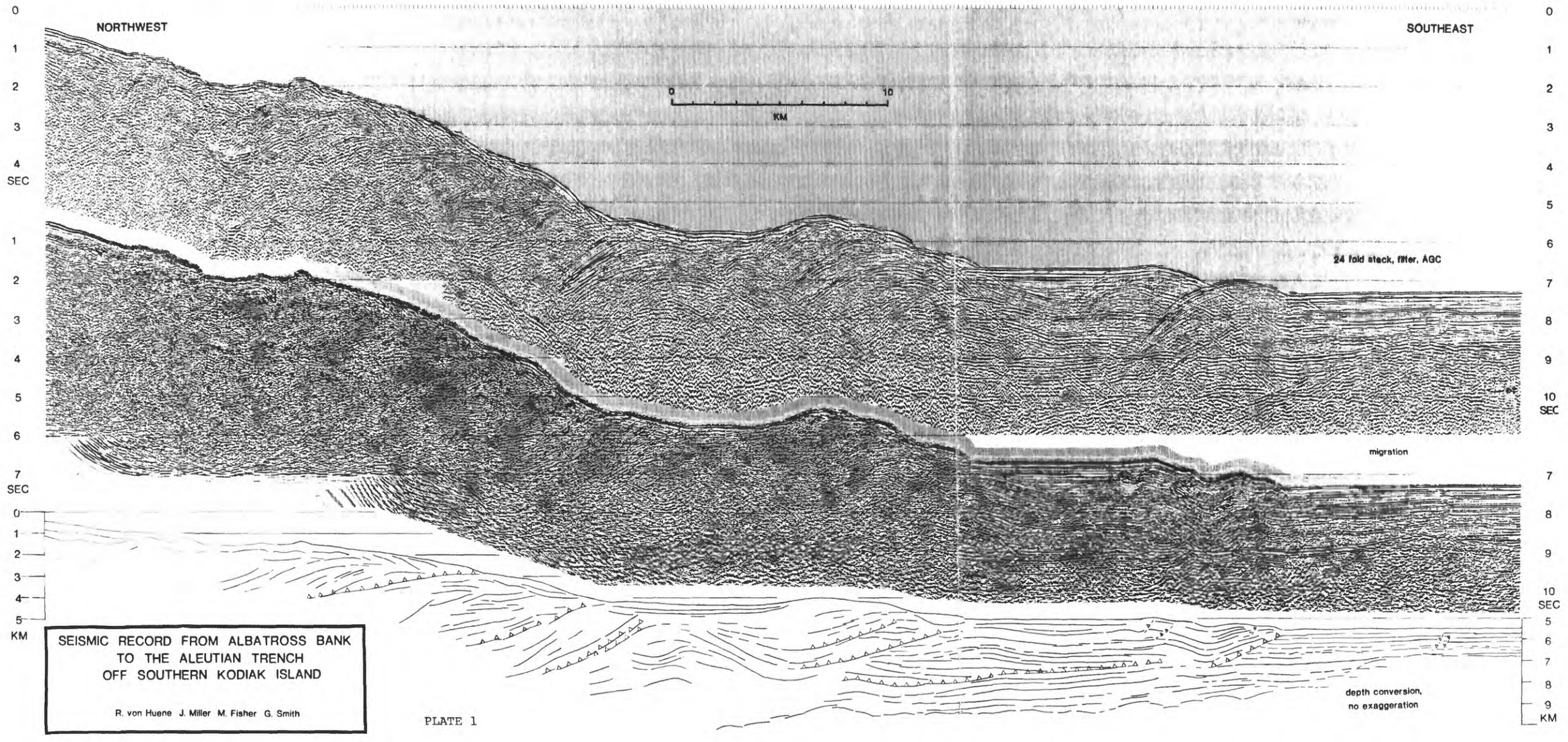

SEISMIC RECORD FROM ALBATROSS BANK
TO THE ALEUTIAN TRENCH
OFF SOUTHERN KODIAK ISLAND

R. von Huene J. Miller M. Fisher G. Smith

PLATE 1